

MINISTÈRE DE L'ENSEIGNEMENT SUPÉRIEUR ET DE LA RECHERCHE SCIENTIFIQUE

UNIVERSITÉ MOHAMED KHIDER - BISKRA

FACULTÉ DES SCIENCES ET DE LA TECHNOLOGIE

DÉPARTEMENT DE GÉNIE ÉLECTRIQUE



Thèse de Doctorat

En vue de l'obtention du diplôme de docteur LMD en électrotechnique

Contribution à la commande des systèmes non linéaires : application à la machine synchrone à réluctance variable

Réalisé par: **Anouar BOUKHLOUF**

Soutenue publiquement le: 15/06/2023

Devant le jury composé de:

Abdenacer TITAOUINE	professeur	Université de Biskra	Président
Mohamed Yacine HAMMOUDI	Maître de conférences	Université de Biskra	Rapporteur
Mohamed SAHRAOUI	professeur	Université de Biskra	Examineur
Laid ZELLOUMA	professeur	Université d'El-Oued	Examineur

Année Universitaire 2022/2023

State estimation of nonlinear system modelled by
multiple models: application to the synchronous
reluctance machine

Anouar BOUKHLOUF

June 15, 2023

Dedication

I dedicate this work to my beloved parents, who have made the greatest sacrifices for our education. May Allah protect them,

To my cherished grandparents,

To my dear wife and daughters,

To my brothers, Abd Rahmen and Abd Elhak,

To my sisters and their children,

And to all my friends, both in my social and academic life.

Acknowledgments



First and foremost, I am profoundly grateful to Allah, the Most Gracious and Merciful, who has blessed me with knowledge and imbued me with strength, courage, patience, and serenity throughout my years of study. I humbly express my deepest gratitude for His infinite mercy and grace, which have been pivotal in enabling me to complete this work. His benevolence has been the guiding light on this journey, for which I will forever be thankful.

My profound gratitude and appreciation extend to my thesis director, Dr. Hammoudi Mohamed Yacine, a member of the LMSE Laboratory at the University of Biskra. His availability, unwavering support, and, most importantly, patience were key factors in the success of my thesis.

I wish to express my sincerest appreciation to Mr. Boumehraz Mohamed, the head of the Laboratory of Energy Systems Modeling (LMSE), as well as Mrs. Batka, the laboratory engineer, for providing an ideal environment for research and experimental work. The completion of this work would not have been possible without their assistance and the support of all members of the LMSE.

I extend my sincere thanks to the esteemed members of my jury: Professor Abdenacer Titaouine, from the University of Biskra, who did me the honor of chairing my thesis; Professor Mohamed Sahraoui, also from the University of Biskra; and Professor Laid Zellouma, from the University of Eloued, for their gracious agreement to be part of my jury.

Undoubtedly, I cannot conclude without expressing heartfelt thanks to my parents, my grandparents, my wife, and my brothers, Abd Rahmen and Abd Elhak. My deepest appreciation is also extended to my sisters and friends for their boundless love and support, which have undoubtedly eased the difficulties encountered along this journey.

To everyone who offered help without exception through a smile, words of encouragement, or provision of information; to all who showed confidence in me and provided the energy I needed to persevere and achieve success, I offer my sincerest thanks.

List of Publications

Journal Publications

- **Boukhlof, A.**, Hammoudi, M. Y., Saadi, R., & Benbouzid, M. E. H. (2023). Hardware-in-the-loop implementation of an unknown input observer for synchronous reluctance motor. *ISA transactions*, 133, 485-494.
- Mimoune, K., Hammoudi, M. Y., Saadi, R., Benbouzid, M., & **Boukhlof, A.** (2023). Real-Time Implementation of Non Linear Observer Based State Feedback Controller for Induction Motor Using Mean Value Theorem. *Journal of Electrical Engineering & Technology*, 18(1), 615-628.

International Conferences

- **Boukhlof, A.**, Hammoudi, M.Y., Saadi R. , Mimoune, K., & Ayad, M. Y. State and unknown inputs estimation of polytopic system by convex optimization. In 2020 International Conference on Emerging and Renewable Energy Generation and Automation (ICEREGA 20)
- Hammoudi, M. Y., Kraa, O., Saadi, R., Ayad, M. Y., Bacha, S., & **Boukhlof , A.** (2018, October). Non linear control of a Fuel Cell Interleaved Boost Converter using Weighted Mixed Sensitivity H_∞ . In 2018 International Conference on Electrical Sciences and Technologies in Maghreb (CISTEM) (pp. 1-5). IEEE.

ملخص

تتطلب العديد من المشكلات الهندسية تقدير حالة النظام عبر مراقب. ومع ذلك ، فإن النمذجة والتوليف للمراقب تصبح مهام صعبة للأنظمة غير الخطية. في مواجهة هذه الصعوبات، يمكن استخدام نهج متعدد النماذج.

يركز العمل البحثي المقدم في هذه الأطروحة على تقدير الحالة للأنظمة غير الخطية الممثلة بنماذج متعددة ضبابية من نوع Takagi-Sugeno المقترن. يتم الحصول على هذا التمثيل بفضل استخدام التحلل في القطاعات غير الخطية مما يسمح لنا بإعادة كتابة النظام الجديد في شكل polytopes دون فقدان المعلومات. هذا النموذج مفيد بعد ذلك لتركيب مراقب قوي فيما يتعلق بالمدخلات غير المعروفة من أجل إعادة بناء حالات النظام والمدخلات غير المعروفة.

بعد مقدمة موجزة للنهج متعدد النماذج ، تتم معالجة مشكلة تقدير الحالة للأنظمة غير الخطية الموصوفة بواسطة نماذج متعددة غامضة مقترنة. بعد ذلك ، تقدم خوارزميات لتجميع مراقبي الحالة الأقوياء ضد المدخلات غير المعروفة. استخدمنا نوعين من المكاسب النسبية المتكاملة ومراقبين المكاسب المتعددة. أخيراً ، نطبق هذه الأساليب على نموذج الآلة المتزامنة ذات الممانعة المتغيرة.

الكلمات المفتاحية : النظام غير الخطي ، نموذج متعدد تاكاجي-سوجينو ، محرك ممانعة متزامن ، تقدير الحالة ، عدم مساواة المصفوفة الخطية.

Abstract

Several problems require the state estimation of system via an observer. However, modeling and synthesizing the observer become challenging tasks for non-linear systems. In response to these difficulties, a multi-model approach can be utilized.

The research presented in this thesis focuses on the state estimation of non-linear systems represented by coupled Takagi-Sugeno fuzzy multi-models. This representation is achieved through the use of non-linear sector decomposition, which allows us to rewrite the new system in the form of polytopes without loss of information. This form is then useful for synthesizing a robust observer with respect to unknown inputs in order to reconstruct the system's states and unknown inputs.

After a brief introduction to the multi-model approach, the problem of state estimation for non-linear systems described by coupled fuzzy multi-models is addressed. We then present algorithms to synthesize a robust unknown input observers. We have used two types of observers such as proportional-integral gains and multi-integral gains. Finally, we apply these approaches to the model of a variable reluctance synchronous machine.

Key words: Non-linear system, Takagi-Sugeno multi model, Synchronous reluctance motor, state estimation, Linear Matrix Inequality, unknown inputs.

Résumé

Nombreux sont les problèmes en ingénierie nécessitant l'estimation de l'état d'un système via un observateur. Cependant, la modélisation et la synthèse de l'observateur deviennent des tâches difficiles pour des systèmes non linéaires. Face à ces difficultés, l'approche multimodèle peut être mise à profit.

Les travaux de recherche présentés dans cette thèse portent sur l'estimation d'état des systèmes non linéaires représentés par des multimodèles flous de type Takagi-Sugeno couplé. Cette représentation est obtenue grâce à l'utilisation de la décomposition en secteurs non linéaire qui nous permettant de réécrire le nouveau système sous forme de polytopes sans perte d'information. Cette forme est ensuite utile pour la synthèse d'un observateur robuste vis-à-vis des entrées inconnues afin de reconstruire les états du système et les entrées inconnues.

Après une brève introduction à l'approche multimodèle, le problème de l'estimation d'état des systèmes non linéaires décrits par les multimodèles flous couplés est abordé. Ensuite, nous présentons des algorithmes pour synthétiser des observateurs d'état robustes face à des entrées inconnues. Nous avons utilisé deux types d'observateurs à gains proportionnel-intégral et à gains multi-intégral. Finalement, nous appliquons ces approches au modèle d'une machine synchrone à réluctance variable.

Mots-Clés: Système non linéaire, multi-modèle de Takagi-Sugeno, estimation de l'état, moteur synchrone à réluctance variable, inégalités matricielles linéaire, entrées inconnues.

Table of Contents

<i>General Introduction</i>	4
1 <i>State of the Art for Synchronous Reluctance Motor (SynRM)</i>	8
1.1 Introduction	9
1.2 Electric machines	9
1.2.1 DC Machine	10
1.2.2 Induction machine (IM)	11
1.2.3 Switched Reluctance Machine (SRM)	12
1.2.4 Permanent Magnet Synchronous Machine (PMSM)	13
1.2.5 Synchronous reluctance Machine (SynRM)	14
1.3 A comparative analysis of SynRM and other electrical machine types	15
1.4 History of the development of (SynRM)	17
1.5 Operating principle	18
1.5.1 Reluctance Concept	18
1.5.2 Functioning	19
1.6 Impact of the L_d/L_q parameter on machine performance	20
1.7 Types of rotor geometry	23
1.7.1 Solid rotor	24
1.7.2 Segmented rotor	24
1.7.3 Axially laminated anisotropic rotor (ALA)	25
1.7.4 Transversally laminated anisotropic (TLA) rotor	26
1.7.5 Permanent magnet assisted rotor	27
1.7.6 Rotor with superconductor assistance	28
1.8 Rotor types comparison	29
1.9 Dynamical model of synchronous reluctance motor	31
1.9.1 Simplifying Assumptions	31

1.9.2	Electrical equations of the synchronous reluctance machine in the abc frame	32
1.9.3	Electrical equations of the SynRM in the frame $d - q$	33
1.9.4	Mechanical equations	35
1.10	Voltage inverter modelling	36
1.11	Conclusion	38
2	<i>State of the Art for Takagi-Sugeno Multi-Model</i>	40
2.1	Introduction	41
2.2	Modelling by multi-model approach	41
2.2.1	Operating space	43
2.2.2	Operating zone	43
2.2.3	Sub-model	44
2.2.4	Premise variable	44
2.2.5	Activation function	45
2.2.6	Multi-model	45
2.3	Different multi-model structures	46
2.3.1	Coupled structure	46
2.3.2	Decoupled structure	49
2.3.3	Hierarchical structure	50
2.4	Methods for obtaining multi-models	51
2.4.1	Multiple model construction by identification	51
2.4.2	Multiple model construction by linearisation	52
2.4.3	Multiple model construction by neural approach	53
2.4.4	Multiple model construction by sector non linearity approach	53
2.5	Stability analysis of dynamic systems	57
2.5.1	Stability in the sense of Lyapunov	57
2.5.2	Types of Lyapunov functions	59
2.6	Stability of Takagi-Sugeno fuzzy systems	63
2.6.1	Quadratic Stability of Takagi-Sugeno fuzzy Models	63
2.6.2	Alternative Approaches to Stability Analysis in Takagi-Sugeno fuzzy Models	64
2.7	Conclusion	65

3	<i>State Estimation of TS Multi-Model</i>	66
3.1	Introduction	66
3.1.1	The different types of observers of non-linear systems	68
3.2	Takagi-Sugeno multi-model State Observer	69
3.2.1	Measurable premise variables (<i>MPV</i>)	70
3.2.2	Non-measurable premise variables (<i>NMPV</i>)	71
3.3	Structure of state multi gain observer based on the Lipschitz approach	72
3.4	State and unknown input observer	75
3.4.1	Structure of robust proportional integral (PI) observer	75
3.4.2	Structure of the proportional multi integral (PMI) observer	81
3.5	Conclusion	85
4	<i>State and Unknown Estimation of the Synchronous Reluctance Machine (SynRM)</i>	87
4.1	Introduction	87
4.2	Application to synchronous reluctance motor	88
4.2.1	TS model design of SynRM	89
4.2.2	Syntax code in MATLAB	90
4.3	Simulation results and comparative analysis	92
4.4	Hardware-in-the-loop validation	97
4.5	Conclusions	108
	<i>General Conclusion</i>	109
	<i>Annexe</i>	111

List of Figures

1.1	Classification of radial flux motor types	10
1.2	History of SynRM development[TRU16].	18
1.3	Two objects in a magnetic field Ψ a) isotopic geometry b) anisotropic geometry [Tag15].	19
1.4	Vector diagram of SynRM in steady-state	21
1.5	Stator current position in $(d - q)$ axis.	22
1.6	Power factor as a function of the saliency ratio L_d/L_q	23
1.7	Different types of solid rotor	24
1.8	Segmented rotor	25
1.9	Transversally laminated anisotropic rotor	26
1.10	Transversally laminated anisotropic rotor	26
1.11	permanent magnet assisted synchronous reluctance motor	28
1.12	Mounting the magnets to the rotor	28
1.13	Rotor with superconductor assistance	29
1.14	Diagram of a three-phase voltage inverter - synchronous reluctance machine association.	37
2.1	Complexity and precision of the representation of non-linear systems	42
2.2	Multiple model structure	43
2.3	Schematic diagram of the multi-model approach a)- Non-linear system , b - c)- Multi-models representation	44
2.4	Architecture of TS multi-model	47
2.5	Architecture of a decoupled multi-model	50
2.6	Architecture of a hierarchical multi-model	51
2.7	Non-linear sectors	54
4.1	Rotor speed and its estimation via (LO - MGO - PIO).	93
4.2	Error of the rotor speed.	93

4.3	The d-axis stator current and its estimation via (LO - MGO - PIO).	94
4.4	Error of the d-axis stator current.	94
4.5	The q-axis stator current and its estimation via (LO - MGO - PIO).	95
4.6	Error of the q-axis stator current.	95
4.7	The Unknown load torque and its estimation via PIO.	96
4.8	Test bench.	98
4.9	Overall architecture of the HIL test system.	99
4.10	Rotor speed and its estimation case 1.	101
4.11	Error speed case 1.	102
4.12	d-axis stator current and its estimation case 1.	102
4.13	q-axis stator current and its estimation case 1.	103
4.14	Rotor speed and its estimation case 2.	103
4.15	Error speed case 2.	104
4.16	d-axis stator current and its estimation case 2.	104
4.17	q-axis stator current and its estimation case 2.	105
4.18	Unknown load torque and its estimation case 2.	105
4.19	Rotor speed and its estimation case 3.	106
4.20	Error speed case 3.	106
4.21	d-axis stator current and its estimation case 3.	107
4.22	q-axis stator current and its estimation case 3.	107
4.23	Unknown load torque and its estimation case 3.	108

Nomenclature

Abbreviation

SynRM	Synchronous reluctance motor
FOC	Field Oriented Control
LPV	Linear Parameter Varying
TS	Takagi-Sugeno
LMI	Linear Matrix Inequality
BMI	Bilinear Matrix Inequality
MM	Multi-modèles
MGO	Multi-gain observer
PIO	Proportional integral observe
PMI	Proportional multi integral observe
UI	Unknown inputs
HIL	Hardware-in-the-loop

Abbreviation

V_d, V_q	Direct and quadrature axis stator voltage components
i_d, i_q	Direct and quadrature axis stator current components
L_d, L_q	Direct and quadrature axis stator inductance components
Ω	Rotor speed
R_s	Stator winding resistance
n_p	Number of pole pairs
J	Inertia moment
f	Friction coefficient
T_e, T_L	Electromagnetic and load torque
i_f	The direct current at the input of the inverter
ξ_i	Premise variables
F_i	Membership functions
h_i	Weighting functions

General Introduction

General presentation

In control theory, modeling a process proves to be an indispensable and fundamental task. A physical system can be described according to two types of representations, the first is called implicit, and the second, most often used, is called explicit. These representations, which should aim to resemble reality as closely as possible, link output and input variables through a state vector describing the evolution of the system.

Real processes are often of a nonlinear nature, this nonlinearity is due either to the complexity of the phenomena described, or to the nature of the feedback loops used. The complexity of these systems thus leads to the development of representation approaches suited to linear models, among these techniques, the Takagi-Sugeno (*TS*) fuzzy multi-model representation. This is based on obtaining a set of polytopes interconnected by nonlinear functions, verifying the convex sum property. Each sub-model describes the behaviour of the nonlinear system in a particular operating zone. Two major families of TS fuzzy models are widely used in the literature, the first is known as coupled TS models, this is obtained by four methods, the first one is the identification approach [BMR99], [Gas00], which is used in cases where there is a difficulty in describing the nonlinear system using an analytical model, the second method is based on the linearisation of the system around different operating points [MSH98], and the third technique is based on the convex polytopic transformation of the system's nonlinear terms, is called also the sectors nonlinearities transformation [KTIT92],[TW04], [Bez13], it allows to obtain a representation to the nonlinear model without any information losses compared to the other two approaches. Note that this last approach will be used in this thesis. The last one is based on the neural approach [EDBB10],[CB12]. The second family is known as heterogeneous TS fuzzy multi-models [Fil91], this representation is dedicated to complex systems presenting structural changes induced by their operating mode, each sub-model has its own state space in which it evolves independently, this type of model introduces

a certain flexibility in the identification problems. The activation functions (nonlinear functions) depend on variables known as decision variables or premise variables, these can be measurable (VDM) or non-measurable (VDNM).

After the modeling phase, the estimation of the state variables of the system is an essential step for the synthesis of control laws or for the diagnosis of industrial processes. This estimation is carried out through a dynamic system, often called a state estimator or observer. The observer is an auxiliary system that dynamically reconstructs the internal state of the system. Its inputs are the measured (input-output) variables of the system, and its outputs are the estimated state variables. When a part (or all) of the inputs is not available, the observer is said to have unknown inputs. The problem to be solved then becomes more complex, as it involves estimating the system's state, despite the presence of inputs that effectively intervene in the system's dynamics but cannot be included in the observer's dynamics, or estimating both the state and the unknown inputs. The design of unknown input observers is a major subject in two fields: robust systems control, where disturbances can degrade the performance of control systems [ZZOL19, LLYL19, KPS18], and fault detection based on an analytical model, which transforms fault detection into an estimation problem [YCKW17, KPS18, ALA20].

One of the most successful approaches in the estimation of unknown inputs is the use of a proportional integral observer (PIO). This approach allows for the simultaneous estimation of states and unknown inputs [YCKW17]. Furthermore, it exhibits strong robustness to disturbances, sensitivity to noise, and favorable real-time performance [YIO⁺14, IMRM09].

The great interest to the synchronous reluctance motor (SynRM) is linked to its advantage such as, robust structure, fast dynamic response, and high reliability. The absence of permanent magnetic material in SynRM makes it suitable for high speed applications, low cost compared to similar sized permanent magnet synchronous motor and operates in high temperature environments [LCC11, AKK⁺15]. The magnet-free rotor eliminate copper losses, for this reason the SynRM produces higher torque and efficiency compared to similar sized induction motors [AKNM17]. All this make the SynRM looked as a serious alternative to permanent magnet synchronous motor and inductance motor [AKK⁺15].

Contributions

The main contribution of this thesis is to propose an extension of the conventional tools of nominal estimation to the robust estimation of systems described by Takagi-Sugeno multi-models, particularly those with non-measurable decision variables. Our approach is exclusively based on Lyapunov's second method and its formulation around Linear Matrix Inequalities (LMI). The interest in LMI-based methods stems from the fact that they can be resolved using convex programming. With this approach, we are no longer confined to problems with an analytical solution. By solving these inequalities, we obtain a domain of feasible solutions, that is, solutions satisfying these LMIs, which is larger than that generated by seeking analytical solutions. This is due to the fact that an inequality possesses more solutions than an equality. The problem of state estimation in the presence of unknown inputs is addressed for the synchronous reluctance machine.

Generally, we have directed our work in several directions, which have resulted in the following contributions:

- We presented the model of the synchronous reluctance machine using the Takagi-Sugeno multi-model, which was obtained through the transformation of the nonlinear sector.
- We focused on the problem of robust estimation for nonlinear systems described by the TS multi-model, within the context of both academic examples and practical applications such as the SynRM machine.
- Preliminary results on the robust state estimation of the SynRM machine have been validated in real-time using the Hardware-in-the-Loop platform.

Organization of the thesis

This thesis is organized into four primary chapters, each discussing a different aspect of the research topic.

Chapter 1 delves into the concept of the Synchronous Reluctance Machine (SynRM), comparing it with other types of electrical machines. This chapter explores the history of SynRM development, its operating principles, and the impact of the L_d/L_q parameter on machine performance. It further examines different types of rotor geometry. A comparison

of various rotor types is undertaken, followed by an extensive discussion on the dynamic model of the synchronous reluctance motor, which includes its electrical and mechanical equations. The chapter concludes with a brief exploration of voltage inverter modeling.

Chapter 2 focuses on modeling using a multi-model approach, introducing key concepts such as operating space and zone, sub-model, premise variable, activation function, and multi-model. Various multi-model structures, such as coupled structure and decoupled structure, are discussed in detail. This chapter also explains different methods for obtaining multi-models and provides a thorough analysis of the stability of dynamic systems. The chapter wraps up by discussing the stability of Takagi-Sugeno fuzzy systems.

Chapter 3 begins with an introduction and then delves into the state of the art on the observability of non-linear systems. It looks at different types of observers of non-linear systems and specifically discusses the Takagi-Sugeno multi-model State Observer. The chapter discusses state reconstruction with unmeasurable decision variables and presents the structure of the proportional integral (PI) observer and the proportional multi integral (PMI) observer.

Chapter 4 applies the knowledge from the previous chapters to the synchronous reluctance motor. The TS model design of SynRM is discussed, and Hardware-in-the-loop validation is performed. The chapter discusses the multi gain observer and PI observer for the SynRM and concludes with a comparative analysis and final remarks.

State of the Art for Synchronous Reluctance Motor (SynRM)

1.1	Introduction	9
1.2	Electric machines	9
1.2.1	DC Machine	10
1.2.2	Induction machine (IM)	11
1.2.3	Switched Reluctance Machine (SRM)	12
1.2.4	Permanent Magnet Synchronous Machine (PMSM)	13
1.2.5	Synchronous reluctance Machine (SynRM)	14
1.3	A comparative analysis of SynRM and other electrical machine types	15
1.4	History of the development of (SynRM)	17
1.5	Operating principle	18
1.5.1	Reluctance Concept	18
1.5.2	Functioning	19
1.6	Impact of the L_d/L_q parameter on machine performance	20
1.7	Types of rotor geometry	23
1.7.1	Solid rotor	24
1.7.2	Segmented rotor	24
1.7.3	Axially laminated anisotropic rotor (ALA)	25
1.7.4	Transversally laminated anisotropic (TLA) rotor	26
1.7.5	Permanent magnet assisted rotor	27
1.7.6	Rotor with superconductor assistance	28
1.8	Rotor types comparison	29
1.9	Dynamical model of synchronous reluctance motor	31
1.9.1	Simplifying Assumptions	31

1.9.2	Electrical equations of the synchronous reluctance machine in the abc frame	32
1.9.3	Electrical equations of the SynRM in the frame $d - q$	33
1.9.4	Mechanical equations	35
1.10	Voltage inverter modelling	36
1.11	Conclusion	38

1.1 Introduction

In recent years, the demand for energy-efficient and cost-effective electric machines has increased significantly due to growing environmental concerns and the need for sustainable energy solutions. This chapter aims to provide an overview of various electric machines, focusing on the Synchronous Reluctance Machine (SynRM) and its comparison to other electrical machine types. The chapter begins with a brief introduction to different types of electric machines, including DC Machines, Induction Machines (IM), Switched Reluctance Machines (SRM), and Permanent Magnet Synchronous Machines (PMSM). It then delves into the history, operating principles, and rotor geometry types of SynRMs. The impact of the L_d/L_q parameter on machine performance is discussed, followed by a comparison of rotor types. A dynamical model of synchronous reluctance motors is presented, along with voltage inverter modelling. The chapter concludes with a summary of the key points and the potential future developments in the field of electric machines.

1.2 Electric machines

Electric machines, essential in converting electrical energy to mechanical energy and vice versa, are categorized into several types, including Induction Machines (IM), Permanent Magnet Synchronous Machines (PMSM), Switched Reluctance Machines (SRM), and Synchronous Reluctance Machines (SynRM). Figure 1.1 illustrates the classification of electric machines based on their rotor and stator configurations. The primary classifications of electric machines are DC machines, induction machines, and synchronous

machines. Understanding their distinctions is vital for choosing the most appropriate machine for a given application.

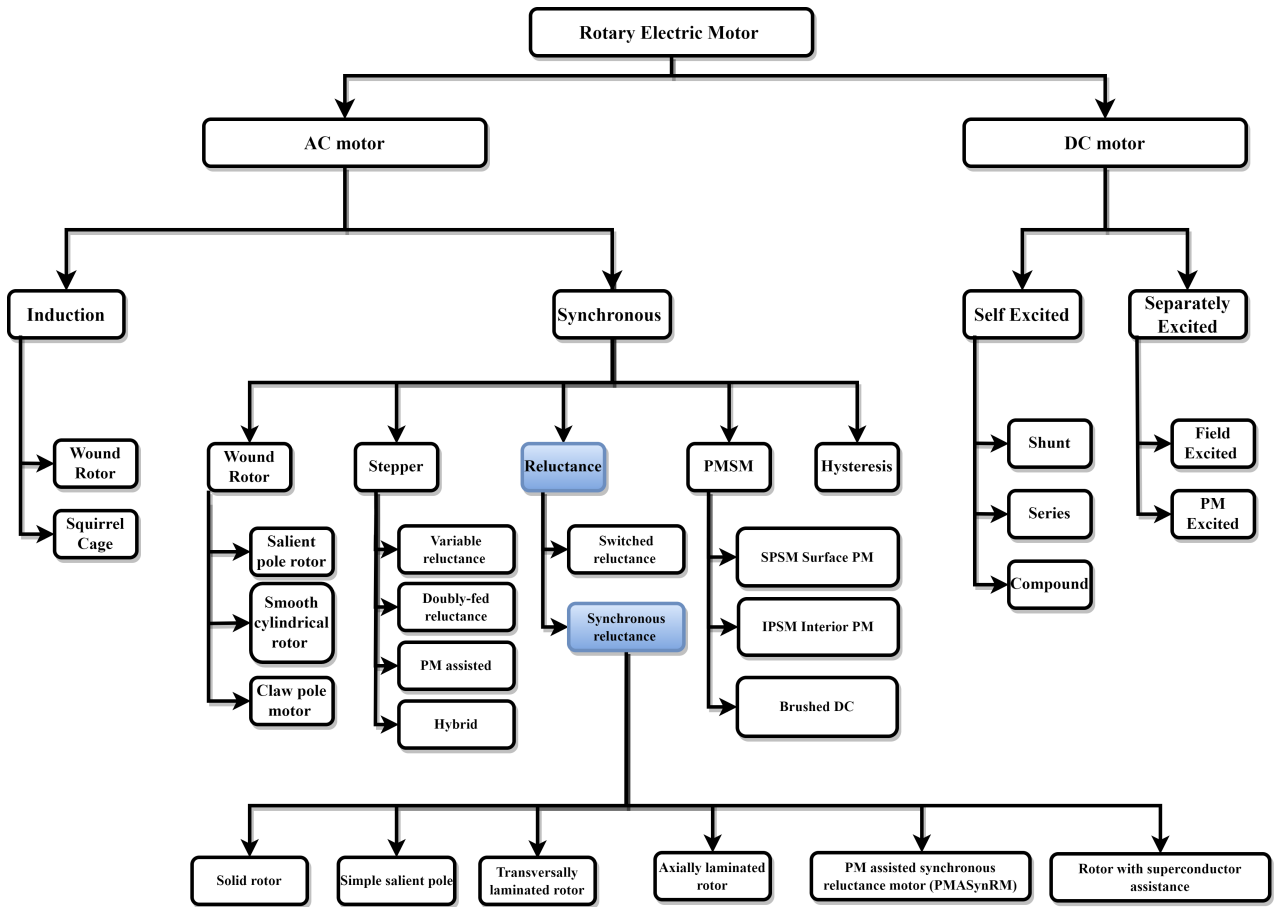


Fig 1.1: Classification of radial flux motor types

1.2.1 DC Machine

DC machines, which have been utilized for various applications since their inception, are well-known for their simplicity and versatility. They are an attractive choice for adjustable speed applications due to their mature properties, such as control simplicity, good speed regulation, frequent starting ability, simple braking and reversing, and proper torque-speed characteristics.

The operating principle of a DC machine is straightforward, relying on the interaction between the armature flux, which is determined by the input voltage and back electromotive force (EMF), and the field flux created by field current or magnetic material. There are four types of wound-field DC motors based on the interconnection between the field and armature windings: separately excited, shunt excited, series excited, and compound

excited.

Separately excited DC machines controlled by a DC-DC chopper are commonly used in traction applications, offering several advantages such as control flexibility of the armature and field voltage, higher efficiency, fast dynamic response, and small size. However, the presence of a commutator in the armature structure is a significant drawback. It leads to increased operating costs due to regular maintenance and reduced machine reliability.

Despite the limitations associated with the commutator-brush assembly, which requires additional maintenance and is less suited for medium power applications, DC machines continue to be employed in various low power applications. One such example is shutter actuators that regulate the air flow in various systems. The power converter for these machines, an H-bridge, is simple to develop, further highlighting the benefits of using DC machines in certain applications [Tag15, Rod15].

In conclusion, DC machines provide a mature, simple, and versatile solution for various applications that require adjustable speed and reliable performance. However, the presence of a commutator necessitates regular maintenance, making it less suitable for higher power applications and limiting its overall efficiency and reliability.

1.2.2 Induction machine (IM)

Induction machines (IM) have become a popular choice in various industries due to their numerous advantages over conventional DC commutator drives. These benefits, which are particularly important for a wide range of applications, include high efficiency, low cost, high power density, robustness, ruggedness, and the ability to operate in hostile environments.

As an AC machine with an asynchronous topology, the induction machine features a stator and rotor field rotating at different speeds. The slip, which is generally small, influences the output power and the torque developed by the machine. Induction machines can be divided into squirrel cage and wound rotor types. The squirrel cage rotor is the most common type used in traction applications, while the wound rotor type is less popular due to its higher cost and maintenance requirements.

Asynchronous machines, such as cage induction machines, are widely produced and available in an extensive power range. They require minimal maintenance and have a very low failure rate. These machines are employed in various applications, including inertial

energy storage systems. One notable advantage of asynchronous machines is their wide speed variation range for a constant power regime, with a ratio of maximum to minimum speed of about 1 to 5.

Double-fed asynchronous machines, which are wound-rotor asynchronous machines with a stator coupled to a transformer and a rotor connected to a static converter, have also been used in variable-speed wind energy production. While they have some disadvantages, such as power dissipation in resistive elements and reduced robustness due to the presence of the ring and brush system, their variable speed operation offers sufficient benefits to be utilized by various manufacturers [Tag15, Bel08].

1.2.3 Switched Reluctance Machine (SRM)

Switched Reluctance Machines (SRMs) are a type of permanent magnet-free motor that has gained interest for various applications. SRMs have a unique stator design, utilizing step-by-step control to generate torque, resulting in high specific power and high-speed capabilities. Their robust structure, consisting of steel in the rotor, adds to their appeal [Yam15].

SRMs are double salient single excited motors, featuring simple concentric windings on the stator and a rotor without windings, magnets, commutators, or brushes. Their low rotor moment of inertia allows for fast dynamic response and rapid acceleration. Additionally, SRMs have a high starting torque and high torque to inertia ratio. Some of the benefits of SRMs include low cost, a wide speed range, high efficiency, simple and rugged structure, simplicity in control, high-speed operation capability, reliability, fault-tolerant operation, and easy cooling with insensitivity to high temperatures.

However, there are several drawbacks to SRMs that may limit their adoption in certain applications. These technical issues include high torque ripple, acoustic noise generation, significant DC bus current ripple, electromagnetic interference (EMI) noise generation, the need for a special converter topology, and complexity in design. Furthermore, SRMs require non-standard inverters for operation and control, which may pose challenges [Tag15, MC17].

1.2.4 Permanent Magnet Synchronous Machine (PMSM)

Permanent Magnet Synchronous Machines (PMSMs) have gained significant attention in various applications due to their high efficiency, high power density, and low maintenance requirements. There are different types of PMSMs, such as machines with radial magnetization, discoidal generators with axial field, and those with external rotors.

PMSMs can be classified into two main configurations based on the location of the permanent magnets: Interior Permanent Magnet (IPM) and Surface-mounted Permanent Magnet (SPM). IPMs offer better overload capability and mechanical robustness, while SPMs usually have less complex structures. Additionally, PMSMs can be categorized based on the shape of the produced electromotive force (back-emf) as Sinusoidal Permanent Magnet Synchronous Machines and Brushless DC (BLDC) machines [Tag15].

The advantages of PMSMs include high efficiency, wide speed range, low noise, absence of Joule losses in the rotor, compactness, fast torque response, and low maintenance. However, these machines also have some drawbacks. The PMSMs have a more limited constant power speed range, with the maximum speed typically twice the base speed. Any increase in speed above the base speed is accompanied by a weakening of the permanent magnet flux, leading to reduced machine efficiency. The presence of permanent magnets, especially in the rotor, makes them highly sensitive to temperature changes, which can lead to decreased performance and potential demagnetization at high temperatures. The cost of high-temperature permanent magnets, such as Sm-Co, remains high. Furthermore, the mechanical complexity associated with certain structures is increased due to the fragility of permanent magnets [Bel08, YM22].

Rare Earth PMSMs offer high-intensity fields in the air gap without the need for excitation, providing a high power density. However, they are temperature-sensitive and vulnerable to demagnetization at high temperatures. Non-Rare Earth PMSMs, which use materials with lower remanent field densities, can serve as a more cost-effective alternative, but this technology is not yet widely used [Yam15].

Externally Excited Synchronous Machines (EESMs) do not contain permanent magnets and require additional DC/DC conversion for rotor excitation. While these machines have a robust structure and can achieve high speeds, they also have higher Joule losses in the rotor windings, which need to be dissipated [Yam15].

1.2.5 Synchronous reluctance Machine (SynRM)

Synchronous Reluctance Machines (SynRMs) are an alternative motor technology that operates based on the reluctance concept to create motion and torque. Similar to Switched Reluctance Machines (SRMs), SynRMs do not contain permanent magnets and are fed by sinusoidal currents to generate a rotating magnetic field. They have a robust structure with a stator resembling that of an induction motor and a rotor without magnets or copper windings. These machines have the potential to be a low-cost solution for various applications.

Advantages of SynRMs include:

- Low cost.
- High efficiency due to the absence of Joule losses in the rotor.
- High torque per ampere capability.
- Insensitivity to operating temperature.
- Simplicity in control and easy field weakening capability.
- Identical topology for stator and inverter power circuits to induction motors.
- Short time overload capability.
- Simple and rugged structure.
- Reliability.

However, SynRMs also have some drawbacks:

- Low power factor.
- Limited speed range.
- Torque ripple.

The rotor geometry plays a crucial role in the design and optimization of synchronous reluctance machines for various applications. Despite the drawbacks, the interest in SynRMs is rapidly increasing due to their potential to provide similar performance characteristics as induction motors and brushless DC motors but at a lower cost [Tag15, Yam15].

1.3 A comparative analysis of SynRM and other electrical machine types

In this section, we provide a detailed comparison of various electrical machines, focusing on their performance, efficiency, and manufacturing aspects. The analysis includes Induction Machines (IM), Permanent Magnet Synchronous Machines (PMSM), Switched Reluctance Machines (SRM), and Synchronous Reluctance Machines (SynRM), highlighting their advantages and disadvantages in different applications.

1. **Induction Machines (IM)** Induction Machines are the most common type of electrical machine, mainly due to their simplicity, robustness, and low cost. They are widely used in many industrial applications [Yam15, BP08].

Advantages:

- Easy starting and open-loop speed regulation
- Low torque ripple
- Simple and robust construction
- Lower cost compared to other machine types

Disadvantages:

- Higher rotor losses, leading to lower efficiency in some applications
- Low power factor at high speeds
- Slip-dependent operation, which can result in lower performance compared to synchronous machines

2. **Permanent Magnet Synchronous Machines (PMSM)** Permanent Magnet Synchronous Machines are increasingly used in applications requiring high efficiency and compact size, such as electric vehicles and robotics [TRU16].

Advantages:

- High power-to-volume ratio
- High efficiency due to the absence of rotor losses

- Excellent torque and speed control capabilities
- Low maintenance and longer lifespan due to the absence of brushes

Disadvantages:

- High cost due to the use of rare earth permanent magnets
- Complex rotor construction, which may lead to manufacturing challenges
- Demagnetization risk under high temperatures or strong external magnetic fields

3. **Switched Reluctance Machines (SRM)** Switched Reluctance Machines are gaining attention for their unique characteristics, such as a simple construction and the absence of magnets or windings on the rotor [VL18].

Advantages:

- Competitive specific power and high torque density
- Robust construction without permanent magnets
- High fault tolerance due to the independent phase windings
- Potential for lower cost compared to PMSM machines

Disadvantages:

- Noisy operation due to the high torque ripple
- Complex design and control requirements
- Lower efficiency compared to PMSM machines due to higher copper losses

4. **Synchronous Reluctance Machines (SynRM)** Synchronous Reluctance Machines are emerging as an alternative to traditional electrical machines, offering a balance between performance, efficiency, and cost [Yam15, BP08].

Advantages:

- Competitive performance compared to other machine types
- Easy to manufacture and use of standard materials
- Good efficiency and high reliability

- Cost reduction due to the absence of permanent magnets
- 10-15% higher rated torque and 1.5% higher efficiency than IMs

Disadvantages:

- Reduced torque density compared to PM motors
- Less robust rotor compared to solid rotor or switched reluctance machines
- Requires more sophisticated control strategies for optimal performance

In Conclusion based on the detailed comparison of Induction Machines (IM), Permanent Magnet Synchronous Machines (PMSM), Switched Reluctance Machines (SRM), and Synchronous Reluctance Machines (SynRM), it is clear that each type of electrical machine has its own advantages and disadvantages, depending on the specific application and requirements.

Synchronous Reluctance Machines (SynRM) stand out as a promising alternative due to their competitive performance, ease of manufacturing, and cost-effectiveness. While they may not offer the highest torque density or power-to-volume ratio, their absence of rotor losses, use of standard materials, and good efficiency make them a suitable choice for a wide range of applications. Further research and development into SynRM technology can potentially lead to even more enhanced performance and efficiency, making them an even more attractive option for various industries.

1.4 History of the development of (SynRM)

The development of synchronous reluctance motors (SynRM) can be traced back to the 1930s, when researchers began studying "unexcited salient pole synchronous motors" (variable reluctance synchronous motors) for applications requiring precise and constant speed along with autonomous startup. These early motors had limited use due to their low power factor and efficiency [SMW93, Lub03]. In the 1960s, interest in these motors was renewed, particularly in England, leading to the emergence of segmented rotor, flux barrier, and axially laminated rotor designs, which aimed to increase the saliency ratio and improve performance. At the same time in France, the Vernier reluctance motor with a large number of teeth and high torque density became popular for low-speed direct drive applications. The term "Switched Reluctance Motor" was introduced in 1969, and

in the 1990s, electronic-controlled double saliency reluctance machines gained traction in academia and industry, with companies like Allenwest Ltd. in the UK and Sime-Motori in Italy commercializing them. In recent years, SynRM has garnered interest due to its simple structure, high efficiency, low manufacturing cost, and robust operation. However, challenges remain in reducing noise and increasing efficiency, prompting the need for ongoing research and optimization in design and control methods. Current applications of SynRM include the textile industry, machine tools, high-speed applications, and more recently, electric vehicles, pumping, and ventilation systems[TRU16, TP15].

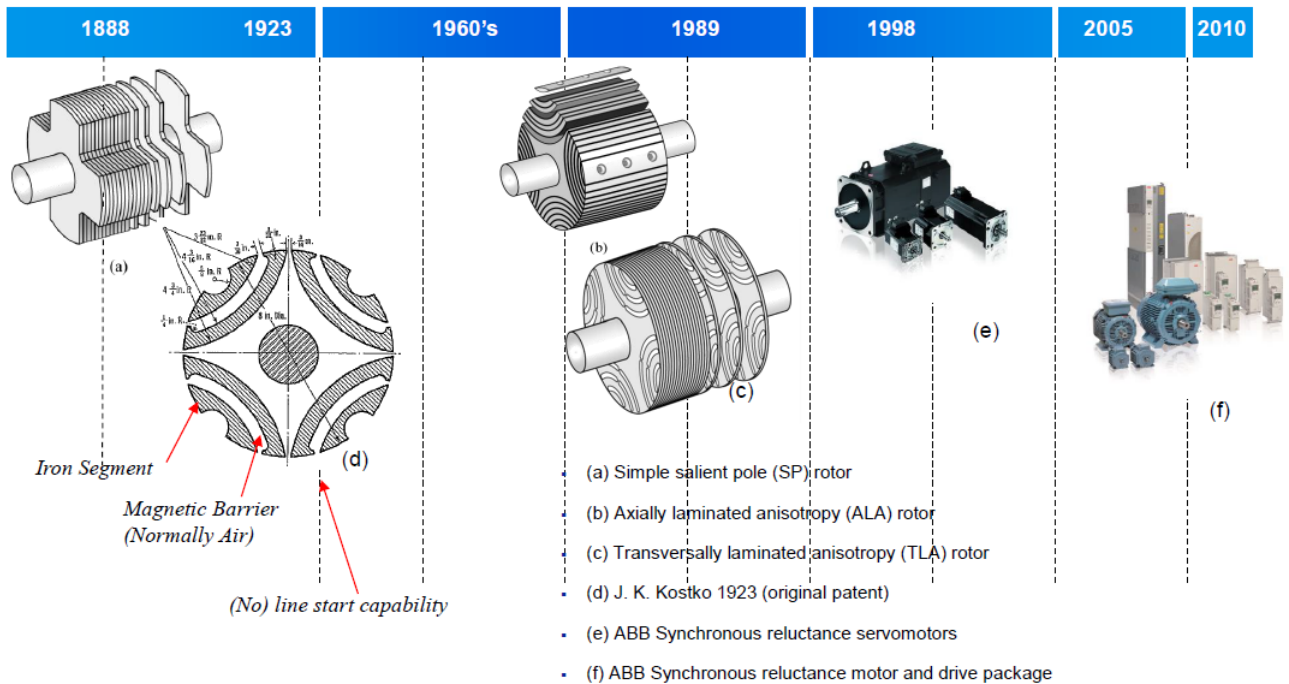


Fig 1.2: History of SynRM development[TRU16].

1.5 Operating principle

1.5.1 Reluctance Concept

The operating principle of SynRM is based on two main concepts:

- the reluctance effect.
- The application of a rotating sinusoidal magneto-motrice force generated by the stator of a three-phase induction type machine.

The main idea of the variable reluctance concept is shown in figure (1.3). Objects (a) and (b) are made by isotropic magnetic material and are exposed to a magnetic field Ψ . Object (a) does not generate a couple since it has the same geometric dimensions in all directions and hence the same reluctances in the d -axis and q -axis. This is called an isotropic object, whereas object (b) has different geometric dimensions in the d and q -axis which refer to different reluctances; this is called an anisotropic object. If the d -axis of the object has a misalignment angle of ε with the magnetic field, this will introduce a field distortion that is aligned with the q -axis and will increase the reluctance in the d -axis; see the field solution in Figure (1.3) (right). As a result, an electromagnetic potential energy is created that can develop an electromechanical torque to force the object to be aligned with the minimum reluctance at the field direction (d -axis) of the object (b) [RM11, Tag15].

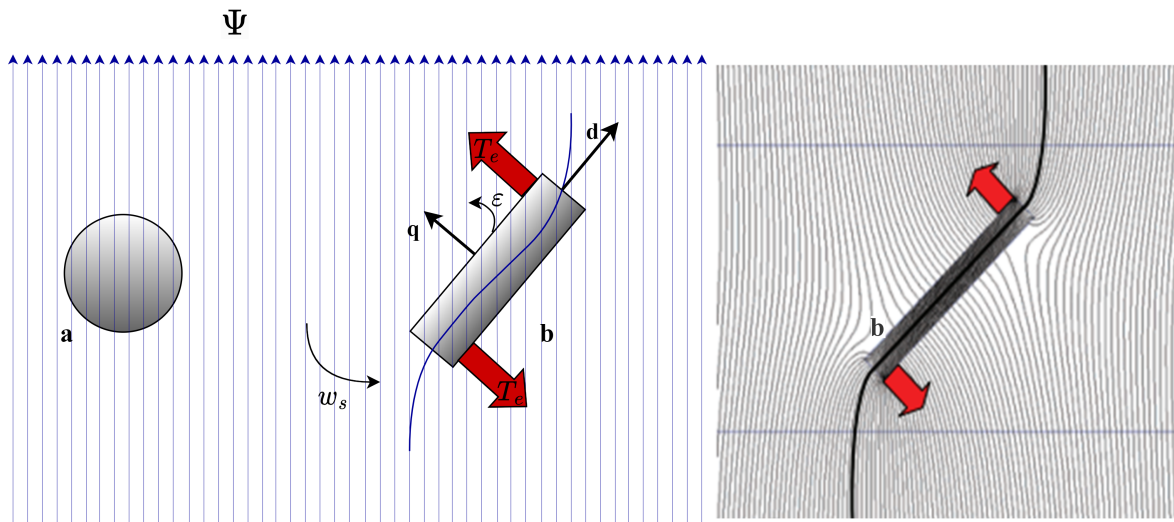


Fig 1.3: Two objects in a magnetic field Ψ a) isotropic geometry b) anisotropic geometry [Tag15].

In the case of SynRM, this same principle of reluctance variation will create the couple. The rotor will try to align with the magnetic field created by the stator coils. As the stator has a rotating magneto-mortice force, the rotor will also rotate generating the movement [Mar16].

1.5.2 Functioning

The SynRM (Synchronous Reluctance Motor) is a type of electric motor that operates on the principle of reluctance torque. It has a stator with windings that produce a rotating

magnetic field, similar to that of an induction motor. It consists of a three-phase winding with p pairs of poles, which is fed by a balanced three-phase current system of pulsating currents w_s , and distributed to create a rotating magneto-motive force (mmf) that is as sinusoidal as possible. However, unlike a conventional salient-pole synchronous motor, the SynRM does not have an excitation winding in the rotor. The rotor is constructed solely of salient poles using air gaps and steel segments and is designed with a special shape to induce torque through reluctance. This geometric anisotropy of the rotor causes it to continuously follow the rotating field in a steady state, resulting in a highly efficient motor that provides high torque and precise control at low speeds. SynRM technology is becoming increasingly popular in various industrial applications such as compressors, pumps, and fans due to its high efficiency, low maintenance, and reliable performance [Tag15, Ram06, Mar16].

1.6 Impact of the L_d/L_q parameter on machine performance

One of the most critical parameters for assessing the performance of a SynRM is the saliency ratio, given by equation (1.1). To design a high-performance SynRM, the primary objective is to achieve a high L_d value and a low L_q value, resulting in maximum flux in the d -axis and minimum flux in the q -axis.

$$\zeta = \frac{L_d}{L_q} \quad (1.1)$$

The vector diagram is a vital tool for visualizing and comprehending the SynRM's operational principles and performance characteristics. The d -axis and q -axis components of the rotor's magnetic flux are distinguished in the vector diagram, with the d -axis representing the high reluctance path and the q -axis corresponding to the low reluctance path. Torque is generated by altering the reluctance between these axes. In the vector diagram, the stator current vector is decomposed into its d -axis and q -axis components, which play a crucial role in determining the motor's torque production and overall performance.

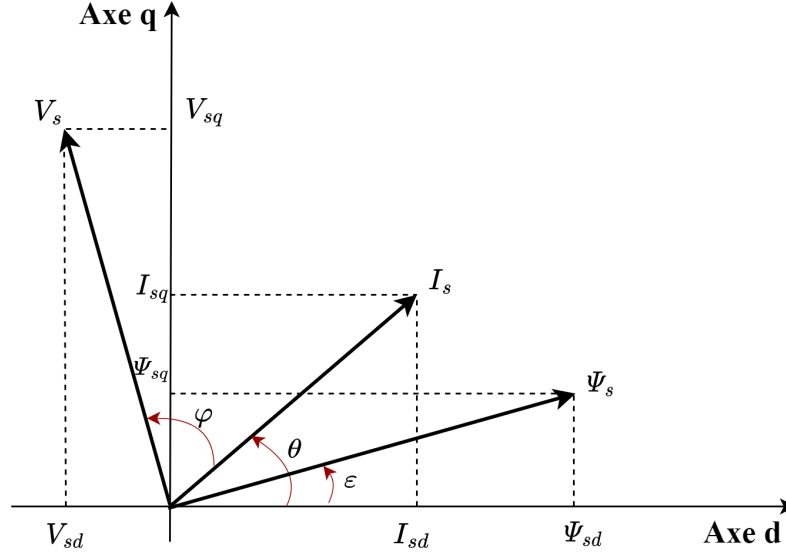


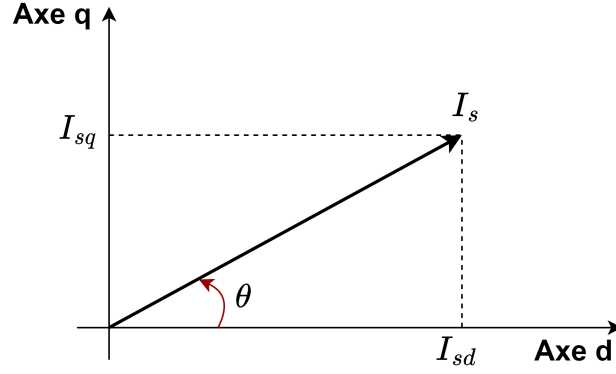
Fig 1.4: Vector diagram of SynRM in steady-state

The electromagnetic torque produced by this machine in steady-state is expressed as:

$$T_e = n_p \cdot (L_d - L_q) \cdot I_{sq} \cdot I_{sd} \quad (1.2)$$

In equation (1.2), n_p denotes the number of pole pairs, while I_{sd} and I_{sq} represent the stator current components in the $d - q$ frame linked to the rotor. The inductances of the d -axis and q -axis stator are represented by L_d and L_q , respectively. To increase the torque without altering the current value, the difference between the direct-axis inductance (L_d) and the quadrature-axis inductance (L_q) must be increased. In other words, to boost torque, the saliency ratio (ζ) must be increased [Ham09].

The angle θ , which identifies the stator current vector's position (I_s) in relation to the d -axis (current angle), is depicted in figure (1.5). The stator current vector remains fixed in a steady state.


 Fig 1.5: Stator current position in $(d - q)$ axis.

The stator current's magnitude is determined by the following equation:

$$I_s = \sqrt{I_{sq}^2 + I_{sd}^2} \quad (1.3)$$

The electromagnetic torque can be expressed in terms of θ and the stator current I_s :

$$T_e = \frac{1}{2} n_p \cdot (L_d - L_q) I_s^2 \cdot \sin 2\theta \quad (1.4)$$

From the previous relations, it can be shown that when the stator current is set to a specific value, the maximum torque is achieved at $\theta = \pi/4$, corresponding to $I_{sd} = I_{sq} T_e$, a mode of operation associated with a particular control strategy. By setting $\theta = \pi/4$ in equation (1.4), equation (1.5) is obtained, revealing the saliency ratio ζ .

$$T_e = \frac{1}{2} n_p \cdot L_d \cdot I_s^2 \cdot \left(1 - \frac{1}{\zeta}\right) \quad (1.5)$$

The synchronous reluctance machine is an AC machine intended to be powered by three-phase sinusoidal currents in a steady state. The power factor of the machine, defined as the phase difference between the fundamental of the line current and the corresponding phase-to-neutral voltage, can be determined. This factor also represents the ratio between the active power and the apparent power absorbed by the machine. It is crucial for this ratio to be as close as possible to 1 to limit the electrical power of the source supplying the machine. By neglecting the losses in the machine model, we can obtain a simple expression for the power factor:

$$\cos \varphi = \frac{(\zeta - 1) \cdot \sin \theta}{\sqrt{(\zeta)^2 + \tan^2 \theta}} \quad (1.6)$$

By employing a specific control strategy (imposing $\tan \theta = \sqrt{\zeta}$), the power factor is maximized and depends only on the L_d/L_q ratio. The power factor's expression is then given by the following relation [BLJ⁺93, Lub03]:

$$\left(\cos \varphi \right)_{max} = \frac{\zeta - 1}{\zeta + 1} \quad (1.7)$$

Figure (1.6) illustrates the variations in the power factor as a function of the saliency ratio L_d/L_q . It can be observed that the power factor becomes more significant for saliency ratios exceeding 8. According to Equations (1.5) and (1.7), to optimize the performance of the machine, the rotor structure should be designed to achieve the maximum possible L_d value and the largest feasible L_d/L_q ratio [Lub03].

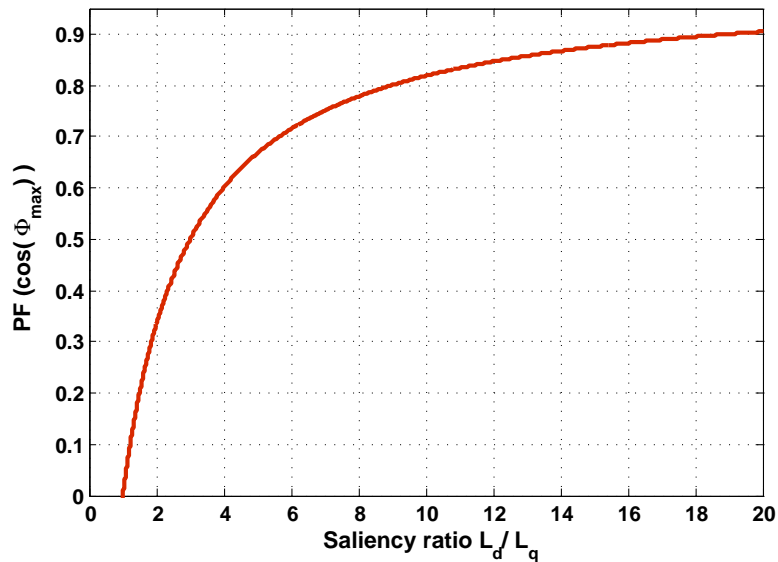


Fig 1.6: Power factor as a function of the saliency ratio L_d/L_q

1.7 Types of rotor geometry

In this section, rotor architectures that allow for a higher salience ratio have been mentioned. We will introduce various structural types identified in the literature, compare them, and highlight their primary benefits and drawbacks.

1.7.1 Solid rotor

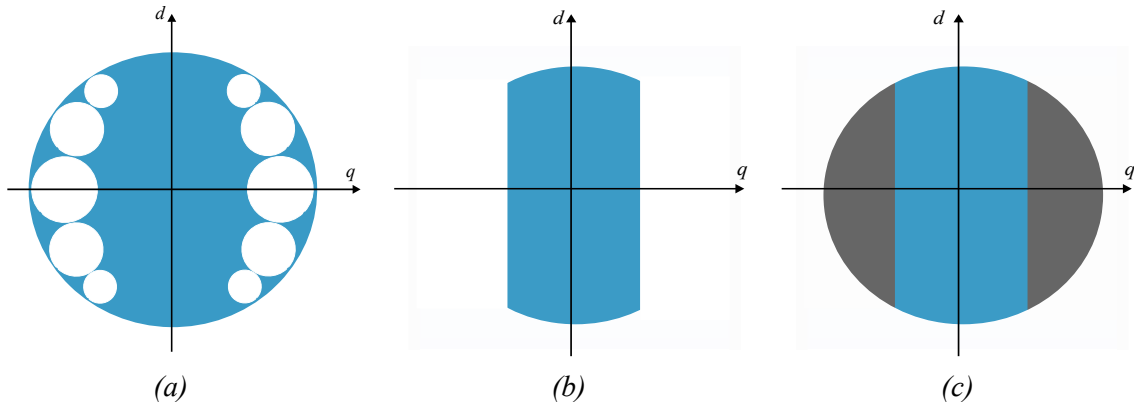


Fig 1.7: Different types of solid rotor

The solid rotor, also known as the simple saliency rotor, is a solid block of ferromagnetic material with cut-outs made to create protrusions on the rotor. This structure is the simplest and most economical to manufacture, and also the most robust since it consists of a single, unassembled block. It is ideal for high-speed operation due to its mechanical sturdiness. Additionally, the rotor can be slightly saturated as the passage section of the d -axis flux is wide enough. During asynchronous regime, eddy currents can circulate axially in the rotor, eliminating the need for a starting cage. To reduce aerodynamic losses, the rotor can be shrouded by non-magnetic material or perforated, as shown in Figure 1.7. However, the main drawback of this rotor type is the relatively weak saliency ratio (L_d/L_q), which is around 4.5, and a power factor that is less than 0.65 [Mar16].

1.7.2 Segmented rotor

These structures consist of segmented iron components assembled onto a non-magnetic section, making them suited for compact motor applications (small motor sizes). Figure 1.8 presents a cross-sectional representation of this machine's model, along with an axial view of a prototype. Due to the insertion of pole pieces, the rotor's mechanical strength is not as robust as that of a solid rotor. Nevertheless, this design attains a maximum saliency ratio of 5.1, offering performance benefits for the motor [Rod15].

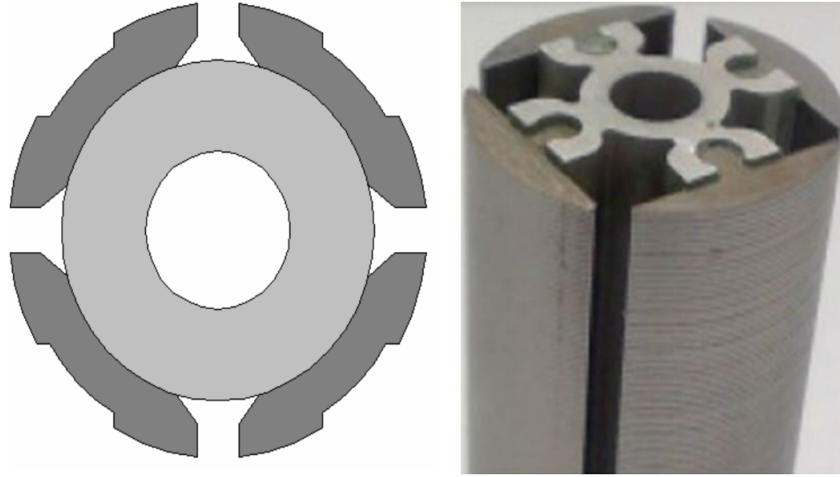


Fig 1.8: Segmented rotor

1.7.3 Axially laminated anisotropic rotor (ALA)

The Axially Laminated Anisotropic (ALA) rotor design is used in Synchronous Reluctance Motors (SynRM) to improve their performance and efficiency. Unlike the Transversally Laminated Anisotropic (TLA) rotor design, the ALA rotor uses non-laminated massive blocks held together by a screw. The rotor's laminations are arranged axially to reduce eddy current losses, and its anisotropic nature is achieved by stacking ferromagnetic and non-magnetic sheets together. The thickness of these sheets can be adjusted to create a preferred direction of magnetic flux, leading to increased torque density.

Research has demonstrated that the ALA rotor design can significantly enhance the performance of SynRM motors. For example, Monsieur Boldea [BFN94] successfully designed a high-efficiency motor with a power factor of 0.91 and an efficiency of 84 % using an ALA rotor with a saliency ratio of 16. However, the ALA rotor design has a low mechanical strength, which limits its use to low-speed and low-power applications. Despite this limitation, the ALA rotor design can achieve a high saliency ratio of up to 20 in a two-pole motor and 10 in a four-pole motor, making it a promising solution for specific applications. Nevertheless, there are two challenges associated with the ALA rotor design. Firstly, the structure is complex, requiring the stacking of axial lamination layers and axial insulation layers alternately. Secondly, the industrial manufacturing and assembly costs are high, making mass production in the industry challenging.

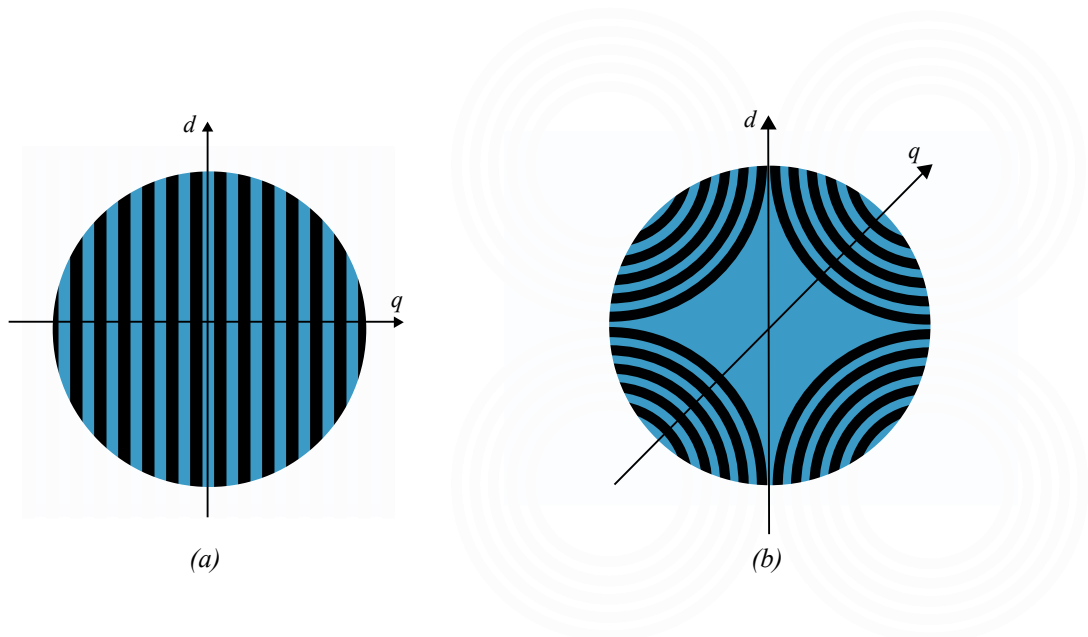


Fig 1.9: Transversally laminated anisotropic rotor

In conclusion, the ALA rotor design is a viable option for improving the performance and efficiency of SynRM motors. Its axial laminations and anisotropic design minimize eddy current losses and increase the motor's torque density. However, the ALA rotor's low mechanical strength must be taken into account when choosing the appropriate rotor design for a given application. Despite this limitation, the ALA rotor design can still achieve a high saliency ratio, making it a suitable option for specific low-speed and low-power applications [Rod15, Mar16, Tag15, Yam15].

1.7.4 Transversally laminated anisotropic (TLA) rotor

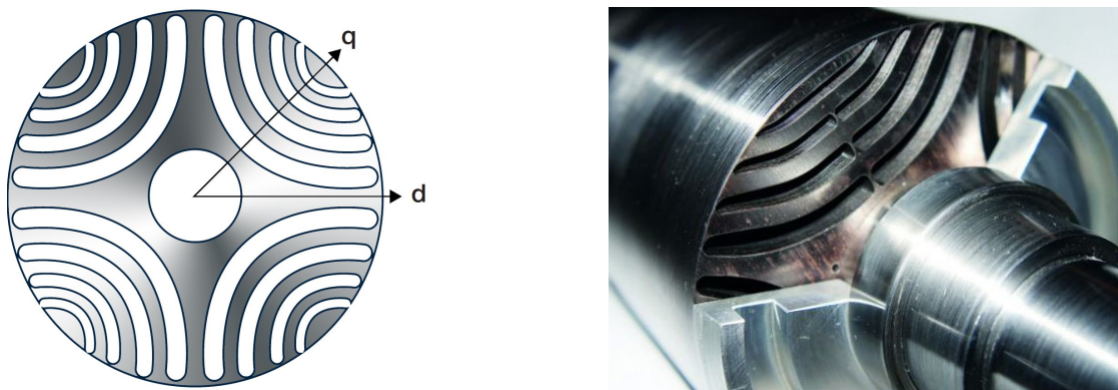


Fig 1.10: Transversally laminated anisotropic rotor

The transversely laminated (TLA) rotor, also known as the multiple-flux barrier rotor, is a next-generation rotor design for SynRM. This design features multiple flux barriers per pole, which limit the circulation of flux in the q-axis without hindering the circulation in the d-axis. The rotor lamination is transversely oriented and connected by thin ribs that act as magnetic short circuits. As a result, the TLA rotor design ensures the mechanical feasibility and strength of the rotor, even for large rotor diameters or high-speed applications. Moreover, the TLA rotor design is easy and cheap to manufacture, and it is suitable for rotor skewing. Proper shaping of the flux barriers and their access points at the air-gap can also optimize the TLA rotor to minimize airgap harmonics and their effect on torque ripple [RM11]. However, the TLA rotor design does have some drawbacks, including the need for bridges to ensure mechanical strength, which can decrease the machine's performance. Studies have been conducted to improve the TLA rotor's performance by selecting the appropriate number of flux barriers relative to the number of stator slots to reduce torque ripple [Rod15]. Nevertheless, the TLA rotor design remains the most adopted topology in the construction of SynRMs, offering a promising solution for future motor design improvements. The TLA rotor design can increase the saliency ratio of a SynRM to up to approximately 13 in a two-pole motor, making it a valuable option for high-performance applications [Ram06, HS00].

1.7.5 Permanent magnet assisted rotor

The Permanent Magnet Assisted Rotor of Synchronous Reluctance Motors (PM-SynRM) is an innovative rotor design that aims to enhance the motor's performance by incorporating permanent magnets into the flux barriers. This design increases the saliency ratio and overall torque production, resulting in a higher efficiency, improved power density, and a wider constant power speed range compared to traditional SynRM motors. The use of permanent magnets in the rotor structure, such as rare-earth or ferrite-type magnets, also increases the power factor, addressing a common issue in standard synchronous reluctance motor designs [Rod15, Mar16]. However, the incorporation of permanent magnets adds to the manufacturing cost and can lead to dependence on rare-earth materials and potential demagnetization issues. Despite these challenges, PM-SynRM motors have garnered significant interest in various applications, particularly in the automotive and industrial sectors, due to their enhanced performance and efficiency

[Mar16, LK22].

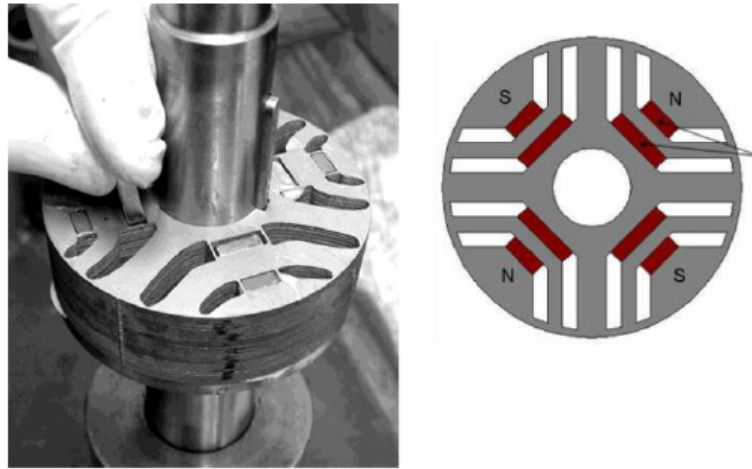


Fig 1.11: permanent magnet assisted synchronous reluctance motor

The magnets in the Permanent Magnet Assisted Rotor of Synchronous Reluctance Motors (PMSynRM) consistently prevent the circulation of flux in the q -axis while minimally affecting the flux in the d -axis. This characteristic leads to an increase in power, efficiency, and torque for the motor. Figure (1.12) illustrates the principle of operation for the magnets positioned within the rotor.

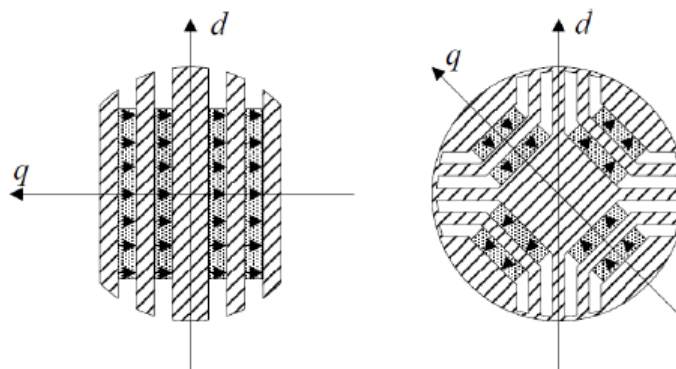


Fig 1.12: Mounting the magnets to the rotor

1.7.6 Rotor with superconductor assistance

Also to prevent the passage of flux in the q axis, superconducting materials were used. This type of machine makes it possible to conserve the inductance of the d axis and to considerably reduce the inductance in the q axis. The results are very impressive; the

$d-q$ axes inductance difference $L_d - L_q$ and saliency ratio L_d/L_q have increased, and as a consequence, the torque and power factor have increased quite well. The superconducting material acts as a real magnetic insulator, which means that this type of motor can still work in both directions. The main disadvantages of this machine are the price and the complexity of implementing the cooling of the superconducting material [CT05, Mar16].

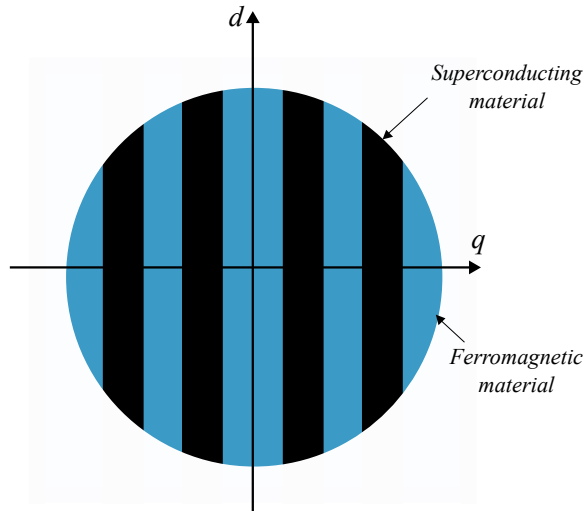


Fig 1.13: Rotor with superconductor assistance

1.8 Rotor types comparison

The table below compares various types of synchronous reluctance motor (SynRM) rotors based on several important factors: cost, saliency ratio, torque ripple, mechanical strength, manufacturing complexity, iron losses, and efficiency.

1. **Solid rotor:** This rotor performs well in terms of cost, mechanical strength, and manufacturing complexity. However, it has a lower saliency ratio, higher torque ripple, and higher iron losses compared to some other rotor types.
2. **Segmented rotor:** The segmented rotor offers a good balance between cost, saliency ratio, torque ripple, mechanical strength, and manufacturing complexity. It has moderate iron losses and efficiency compared to the other rotor types.
3. **Axially Laminated Anisotropic (ALA) rotor:** This rotor type boasts the highest saliency ratio among the options and offers good performance in terms of torque

ripple and mechanical strength. However, it has a higher cost and more manufacturing complexity, as well as moderate iron losses.

4. **Transversally Laminated Anisotropic (TLA) rotor:** This rotor type provides a good balance in cost, saliency ratio, torque ripple, and mechanical strength. Its manufacturing complexity is relatively low, making the production process easier compared to other rotor types. This rotor has the lowest iron losses and excellent efficiency among all rotor types.
5. **Permanent magnet assisted rotor:** This rotor type has the highest saliency ratio and good performance in torque ripple and mechanical strength. It has moderate cost and manufacturing complexity, but it also has higher iron losses compared to the TLA rotor, although its efficiency is still excellent.
6. **Rotor with superconductor assistance:** Although this rotor type has a higher cost, it achieves the highest saliency ratio, good torque ripple, and moderate mechanical strength. Its manufacturing complexity is also higher, and it has higher iron losses compared to the TLA rotor, but it still boasts the best efficiency among all rotor types.

In summary, the table provides an overview of various SynRM rotor types, highlighting their respective strengths and weaknesses based on key parameters, including iron losses as a negative aspect. This information can be helpful in deciding which rotor type is best suited for a specific application or design.

Table 1.1

SynRM	Cost	Saliency ratio	Torque ripple	Mechanics straight	Manufacturing complicating	Iron losses	Efficiency
Solid rotor	✓✓✓✓	✓	✓	✓✓✓	✓✓✓✓	✓	✓
Segmented rotor	✓✓✓	✓✓	✓✓	✓✓	✓✓	✓✓✓	✓✓
Axially laminated anisotropic rotor (ALA)	✓	✓✓✓✓	✓✓	✓✓	✓	✓✓	✓✓✓✓
Transversally laminated anisotropic (TLA) rotor	✓✓✓	✓✓✓	✓✓✓	✓✓✓	✓✓✓	✓✓✓✓	✓✓✓
Permanent magnet assisted rotor	✓✓	✓✓✓✓	✓✓	✓✓✓	✓✓	✓✓✓	✓✓✓✓
Rotor with superconductor assistance	✓	✓✓✓✓	✓✓	✓	✓	✓✓✓✓	✓✓✓✓

1.9 Dynamical model of synchronous reluctance motor

A three-phase synchronous reluctance motor with symmetrically distributed stator windings has been modelled in the synchronous reference frame. The validity of the model is presented in several papers [SOK⁺20] [LCC11].

1.9.1 Simplifying Assumptions

To develop the equivalent electrical model of the machine, certain assumptions need to be made. In the case of SynRM, the modelling relies on the following simplifying assumptions:

- The hysteresis in the magnetic parts as well as the iron losses are neglected.
- Assuming the magnetic circuit is unsaturated.
- Not considering notch and gap harmonics.
- Assuming the spatial distribution of the magneto-motive forces in the air gap is sinusoidal.
- Neglecting the effect of temperature on the resistance values.

1.9.2 Electrical equations of the synchronous reluctance machine in the abc frame

The electrical equations governing the operation of a SynRM machine in a fixed frame linked to the stator are written in the following form[Ngu15]:

$$[V_{abc}] = [R_s] \cdot [I_{abc}] + \frac{d}{dt} [\Psi_{abc}] \quad (1.8)$$

$$\text{with } [V_{abc}] = \begin{bmatrix} v_a \\ v_b \\ v_c \end{bmatrix}; [I_{abc}] = \begin{bmatrix} i_a \\ i_b \\ i_c \end{bmatrix}; [\Psi_{abc}] = \begin{bmatrix} \Psi_a \\ \Psi_b \\ \Psi_c \end{bmatrix}; [R_s] = \begin{bmatrix} R_s & 0 & 0 \\ 0 & R_s & 0 \\ 0 & 0 & R_s \end{bmatrix}$$

The totalized fluxes of the stator phases are written in the reference linked to the stator in the following matrix form:

$$[\Psi_{abc}] = [L] \cdot [I_{abc}] \quad (1.9)$$

where $[L]$ is the inductance matrix which depends on the angle θ

$$[L] = \begin{bmatrix} L_a(\theta) & M_{ab}(\theta) & M_{ac}(\theta) \\ M_{ba}(\theta) & L_b(\theta) & M_{bc}(\theta) \\ M_{ca}(\theta) & M_{cb}(\theta) & L_c(\theta) \end{bmatrix} \quad (1.10)$$

With the hypothesis of the first space harmonic, the terms of (1.10) are written:

$$\begin{cases} L_a(\theta) = L_f + L_0 + L_2 \cos(2\theta) \\ L_b(\theta) = L_f + L_0 + L_2 \cos(2\theta + 2\pi/3) \\ L_c(\theta) = L_f + L_0 + L_2 \cos(2\theta - 2\pi/3) \\ M_{ab}(\theta) = M_{ba} = M_0 + M_2 \cos(2\theta - 2\pi/3) \\ M_{ac}(\theta) = M_{ca} = M_0 + M_2 \cos(2\theta + 2\pi/3) \\ M_{bc}(\theta) = M_{cb} = M_0 + M_2 \cos(2\theta) \end{cases}$$

L_f is the leakage inductance of a phase. In the same framework of assumptions, we have the following relations:

$$M_0 = -\frac{1}{2}L_0 \quad \text{et} \quad M_2 = L_2 \quad (1.11)$$

1.9.3 Electrical equations of the SynRM in the frame $d - q$

The system of electrical equations (1.9) represents a system with parameters that vary periodically over time. Solving this system requires inverting the inductance matrix at each calculation step, which can be cumbersome. Furthermore, this inconvenience hinders the synthesis of control laws. Therefore, there is a need to search for an equivalent model with constant parameters. The Park transformation addresses this issue.

The Park matrix is [Ngu15, Ham09]:

$$[P] = \frac{2}{3} \begin{bmatrix} \cos\theta & \cos(\theta - \frac{2\pi}{3}) & \cos(\theta + \frac{2\pi}{3}) \\ -\sin\theta & -\sin(\theta - \frac{2\pi}{3}) & -\sin(\theta + \frac{2\pi}{3}) \\ \frac{1}{\sqrt{2}} & \frac{1}{\sqrt{2}} & \frac{1}{\sqrt{2}} \end{bmatrix} \quad (1.12)$$

The calculation of the inverse of $[P]$ is immediate, it comes:

$$[P]^{-1} = \begin{bmatrix} \cos\theta & -\sin\theta & 1 \\ \cos(\theta - \frac{2\pi}{3}) & -\sin(\theta - \frac{2\pi}{3}) & 1 \\ \cos(\theta + \frac{2\pi}{3}) & -\sin(\theta + \frac{2\pi}{3}) & 1 \end{bmatrix} \quad (1.13)$$

If we project all the quantities into the reference frame $d - q$ linked to the rotor using the Park transformation, we then write, in the general case:

$$\begin{bmatrix} x_a \\ x_b \\ x_c \end{bmatrix} = [P]^{-1} \begin{bmatrix} x_d \\ x_q \\ x_h \end{bmatrix} \quad (1.14)$$

The equation (1.8) becomes:

$$[P]^{-1}[V_{dqh}] = [R_s][P]^{-1}[I_{dqh}] + [P]^{-1}\frac{d[\Psi_{dqh}]}{dt} + \frac{d[P]^{-1}}{dt}[\Psi_{dqh}] \quad (1.15)$$

where $[Xdqh]$ designates any vector of quantities expressed in the frame of reference linked to the rotor.

The multiplication of the two members of (1.15) by $[P]$ gives us:

$$[V_{dqh}] = [R_s][I_{dqh}] + \frac{d[\Psi_{dqh}]}{dt} + n_p\Omega[P]\frac{d[P]^{-1}}{d\theta}[\Psi_{dqh}] \quad (1.16)$$

$$\text{with } [P]\frac{d[P]^{-1}}{d\theta} = \begin{bmatrix} 0 & -1 & 0 \\ 1 & 0 & 0 \\ 0 & 0 & 0 \end{bmatrix}$$

We finally arrive at the following equations:

$$[V_{dqh}] = [R_s][I_{dqh}] + \begin{bmatrix} L_d & 0 & 0 \\ 0 & L_q & 0 \\ 0 & 0 & L_h \end{bmatrix} \frac{d[I_{dqh}]}{dt} + n_p\Omega \begin{bmatrix} 0 & -L_q & 0 \\ L_d & 0 & 0 \\ 0 & 0 & 0 \end{bmatrix} [I_{dqh}] \quad (1.17)$$

with

$$\begin{bmatrix} L_d & 0 & 0 \\ 0 & L_q & 0 \\ 0 & 0 & L_h \end{bmatrix} = [P] [L] [P]^{-1} \quad (1.18)$$

where

$$\begin{cases} L_d = L_f + \frac{3}{2}(L_0 + L_2) \\ L_q = L_f + \frac{3}{2}(L_0 - L_2) \\ L_h = L_f \end{cases}$$

The neutral of the machine being isolated, which naturally implies $i_h = 0$, we can write:

$$\begin{bmatrix} V_d \\ V_q \end{bmatrix} = \begin{bmatrix} R_s & -n_p\Omega L_q \\ n_p\Omega L_d & R_s \end{bmatrix} \begin{bmatrix} i_d \\ i_q \end{bmatrix} + \begin{bmatrix} L_d & 0 \\ 0 & L_q \end{bmatrix} \frac{d}{dt} \begin{bmatrix} i_d \\ i_q \end{bmatrix} \quad (1.19)$$

The stator voltage equations of the SynRM can be described in rotational $d - q$ reference frames as follows:

$$\begin{cases} V_d = R_s i_d - \Omega n_p L_q i_q + L_d \frac{di_d}{dt} \\ V_q = R_s i_q + \Omega n_p L_d i_d + L_q \frac{di_q}{dt} \end{cases} \quad (1.20)$$

Or, in the form of state equations:

$$\frac{d}{dt} \begin{bmatrix} i_d \\ i_q \end{bmatrix} = \begin{bmatrix} -\frac{R_s}{L_d} & \frac{n_p \Omega L_q}{L_d} \\ -\frac{n_p \Omega L_d}{L_q} & -\frac{R_s}{L_q} \end{bmatrix} \begin{bmatrix} i_d \\ i_q \end{bmatrix} + \begin{bmatrix} \frac{1}{L_d} & 0 \\ 0 & \frac{1}{L_q} \end{bmatrix} \begin{bmatrix} V_d \\ V_q \end{bmatrix} \quad (1.21)$$

1.9.4 Mechanical equations

The electromagnetic torque calculation of the machine is based on knowledge of the total instantaneous power $P_t(t)$, i.e. [Ngu15]:

$$P_t = \frac{3}{2} R_s (i_d^2 + i_q^2) + \frac{3}{2} \left(\frac{d\Psi_d}{dt} i_d + \frac{d\Psi_q}{dt} i_q \right) + \frac{3}{2} n_p \Omega (\Psi_d i_q + \Psi_q i_d) \quad (1.22)$$

Such as:

$$P_j = \frac{3}{2} R_s (i_d^2 + i_q^2)$$

represents the Joule effect losses in the stator windings;

$$P_w = \frac{3}{2} \left(\frac{d\Psi_d}{dt} i_d + \frac{d\Psi_q}{dt} i_q \right)$$

represents the variations of the magnetic energy stored in the machine;

$$P_e = \frac{3}{2} n_p \Omega (\Psi_d i_q + \Psi_q i_d)$$

represents the electrical power transformed into mechanical power inside the machine or electromagnetic power. The electromagnetic power results from the interaction of a flux term and a current term.

The electromagnetic torque is stated as:

$$T_e = \frac{3}{2} n_p (L_d - L_q) i_d i_q \quad (1.23)$$

and

$$T_e = \frac{3}{2} n_p (\Psi_d i_q - \Psi_q i_d) \quad (1.24)$$

The electromagnetic torque is stated as:

$$T_e = \frac{3}{2} n_p (L_d - L_q) i_d i_q \quad (1.25)$$

The motor dynamic equation is expressed by:

$$T_e = J \frac{d\Omega}{dt} + f \Omega + T_L \quad (1.26)$$

Combining equations (1.20-1.26) the mathematical dynamic model of the SynRM can be described by the differential equation (1.27) [SOK⁺20]:

$$\begin{cases} L_d \frac{di_d}{dt} = V_d - R_s i_d + \Omega n_p L_q i_q \\ L_q \frac{di_q}{dt} = V_q - R_s i_q - \Omega n_p L_d i_d \\ J \frac{d\Omega}{dt} = \frac{3}{2} n_p (L_d - L_q) i_d i_q - f \Omega - T_L \end{cases} \quad (1.27)$$

The systems shown in equation (1.27) can be written as a linear parameter-varying (LPV):

$$\begin{cases} \dot{x}(t) = A(x(t)).x(t) + B.u(t) + E.\delta(t) \\ y(t) = C.x(t) \end{cases} \quad (1.28)$$

where

$$\begin{aligned} x(t) &= [i_d, i_q, \Omega]^T, \quad u(t) = [u_d, u_q]^T, \quad \delta(t) = T_L, \quad y(t) = [i_d, i_q]^T, \\ A(x(t)) &= \begin{bmatrix} \frac{-R_s}{L_d} & 0 & \frac{L_q i_q n_p}{L_d} \\ -\frac{L_d}{L_q} \Omega n_p & \frac{-R_s}{L_d} & 0 \\ \frac{3}{2.J} n_p (L_d - L_q) i_q & 0 & -\frac{f}{J} \end{bmatrix}, \quad B = \begin{bmatrix} \frac{1}{L_d} & 0 \\ 0 & \frac{1}{L_q} \\ 0 & 0 \end{bmatrix}, \\ C &= \begin{bmatrix} 1 & 0 & 0 \\ 0 & 1 & 0 \\ 0 & 0 & 1 \end{bmatrix}, \quad E = \begin{bmatrix} 0 \\ 0 \\ -\frac{1}{J} \end{bmatrix}. \end{aligned}$$

1.10 Voltage inverter modelling

The voltage inverter is a static converter ensuring the transformation of a DC voltage E_{bus} into an AC voltage. It is made up of three arms, each comprising two switching cells mounted in series, generally at *IGBT* or *MOSFET* for low and medium powers and *GTO* for high powers, equipped with an anti-parallel according to the power to be transmitted.

The states of the switches are imposed by the command *PWM*. The figure (1.14) illustrates the structure of a three-phase inverter - synchronous reluctance machine association.

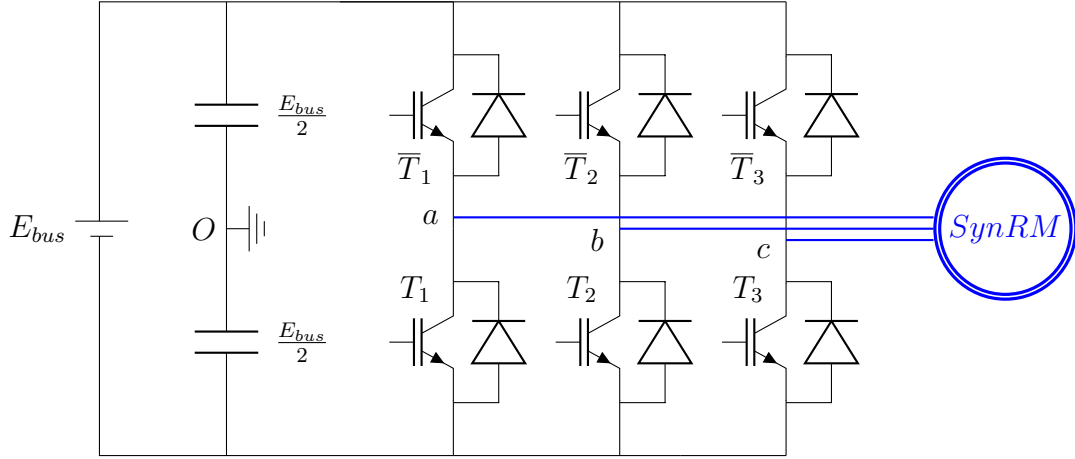


Fig 1.14: Diagram of a three-phase voltage inverter - synchronous reluctance machine association.

Assumptions or choices are made in order to model the voltage inverter, such as:

- The DC voltage source is modelled as an ideal source, without losses and of constant value.
- The output voltages of the inverter are referenced with respect to a midpoint of a fictive bridge divider input O .
- The neutral of the machine is not connected to the middle point O of the inverter.
- The dead times necessary to avoid short circuits are neglected.

The voltage supplied by the three-phase inverter, instantaneously varies from zero to the value of the DC bus voltage and vice versa, making it non-linear from the instantaneous point of view.

The expression of the output voltages in terms of the stator voltages and the neutral potential V_{N0} is given by:

$$\begin{cases} V_{an} = V_{ao} - V_{no} \\ V_{bn} = V_{bo} - V_{no} \\ V_{cn} = V_{co} - V_{no} \end{cases} \quad (1.29)$$

Where V_{no} represents the fictitious voltage between the neutral of the load and the fictitious point O .

For a balanced system:

$$V_{no} = \frac{1}{3}(V_{ao} + V_{bo} + V_{co}) \quad (1.30)$$

The phase-neutral point voltages N can be written as following form:

$$\begin{cases} V_{an} = \frac{2}{3}V_{ao} - \frac{1}{3}V_{bo} - \frac{1}{3}V_{co} \\ V_{bn} = -\frac{1}{3}V_{ao} + \frac{2}{3}V_{bo} - \frac{1}{3}V_{co} \\ V_{cn} = -\frac{1}{3}V_{ao} - \frac{1}{3}V_{bo} + \frac{2}{3}V_{co} \end{cases} \quad (1.31)$$

The switches T_i, \bar{T}_i $i \in \{1, 2, 3\}$ are complementary, and the logic control pulses S_a, S_b, S_c are transmitted to the triggers of the static switches of the three inverter arm [Kou08]. The determination of $S_i (i = a, b, c)$ depends on the control strategy used.

In this work we will choose the voltage inverter controlled by the technique of Pulse Width Modulation (*PWM*), the sine-delta modulation was chosen for the generation of the supply voltages of the synchronous reluctance machine .

The state $s_i = 1$ represents the passing mode of the switch T_i , and the state $s_i = 0$ it is the blocked mode of T_i :

$$\begin{cases} 1 & Si T_i \text{ est fermé} \\ 0 & Si T_i \text{ est ouvert} \end{cases}$$

If the neutral of the machine is isolated, the phase-to-neutral stator voltages are deduced by:

$$\begin{bmatrix} v_a \\ v_b \\ v_c \end{bmatrix} = \frac{E_{bus}}{3} \begin{bmatrix} 2 & -1 & -1 \\ -1 & 2 & -1 \\ -1 & -1 & 2 \end{bmatrix} \begin{bmatrix} S_a \\ S_b \\ S_c \end{bmatrix} \quad (1.32)$$

The direct current at the input of the inverter will have the expression:

$$i_f = S_a i_a + S_b i_b + S_c i_c \quad (1.33)$$

1.11 Conclusion

Throughout this chapter, we have explored the characteristics and functionality of various electric machines, with a particular focus on Synchronous Reluctance Machines (SynRM). The SynRM has emerged as a promising technology due to its energy efficiency, low cost, and simple structure. Despite some drawbacks, such as torque ripple and low power factor, the SynRM's advantages make it a viable alternative to other electric machines, such as Induction Motors and Permanent Magnet Synchronous Machines.

We have also discussed the importance of rotor geometry and the L_d/L_q parameter in the design and optimization of SynRMs for various applications. The development of advanced rotor geometries, such as axially and transversally laminated anisotropic rotors, has led to improved machine performance. Voltage inverter modeling is essential for the effective control of SynRMs, which is crucial for their successful implementation in real-world applications.

In conclusion, the Synchronous Reluctance Machine has the potential to play a significant role in the future of electric machines, offering energy-efficient and cost-effective solutions for a wide range of applications. Further research and development in this area will undoubtedly lead to improved performance, novel rotor designs, and expanded application possibilities, contributing to a more sustainable and environmentally friendly future for electric machines.

State of the Art for Takagi-Sugeno

Multi-Model

2.1	Introduction	41
2.2	Modelling by multi-model approach	41
2.2.1	Operating space	43
2.2.2	Operating zone	43
2.2.3	Sub-model	44
2.2.4	Premise variable	44
2.2.5	Activation function	45
2.2.6	Multi-model	45
2.3	Different multi-model structures	46
2.3.1	Coupled structure	46
2.3.2	Decoupled structure	49
2.3.3	Hierarchical structure	50
2.4	Methods for obtaining multi-models	51
2.4.1	Multiple model construction by identification	51
2.4.2	Multiple model construction by linearisation	52
2.4.3	Multiple model construction by neural approach	53
2.4.4	Multiple model construction by sector non linearity approach	53
2.5	Stability analysis of dynamic systems	57
2.5.1	Stability in the sense of Lyapunov	57
2.5.2	Types of Lyapunov functions	59
2.6	Stability of Takagi-Sugeno fuzzy systems	63
2.6.1	Quadratic Stability of Takagi-Sugeno fuzzy Models	63

2.6.2 Alternative Approaches to Stability Analysis in Takagi-Sugeno fuzzy Models	64
2.7 Conclusion	65

2.1 Introduction

This chapter focuses on the multi-model approach for modelling non-linear systems. The multi-model approach involves developing multiple models, each representing the behaviour of the system in a specific operating zone. These models are then combined to create a comprehensive model that can accurately represent the non-linear system. The chapter covers different multi-model structures, including coupled, decoupled, and hierarchical structures. The methods for obtaining multi-models are also discussed, including identification, linearisation, neural approach, and sector non-linearity approach. Additionally, the chapter covers stability analysis of dynamic systems, with a specific focus on the stability of Takagi-Sugeno fuzzy systems.

2.2 Modelling by multi-model approach

Control and observation of a process are generally based on a good model of the system; the latter becomes more delicate when it comes to complex and highly non-linear systems. This is why there are two situations: either using simplifying assumptions, in which case the model obtained does not take into account all the complexity of the system, or else obtaining a very complex model, which sometimes makes it unusable for the control. Indeed, the multi-model representation is a practical and alternative approach to apprehending the behaviour of a process in different operating zones [Ham15]. There are currently two methods for representing a system using a multi-model structure [Nag10]: direct construction of the multi-model form, which has the disadvantage of losing information due to system linearisation, or the sector non-linearity approach [TW04], which is the most commonly used.

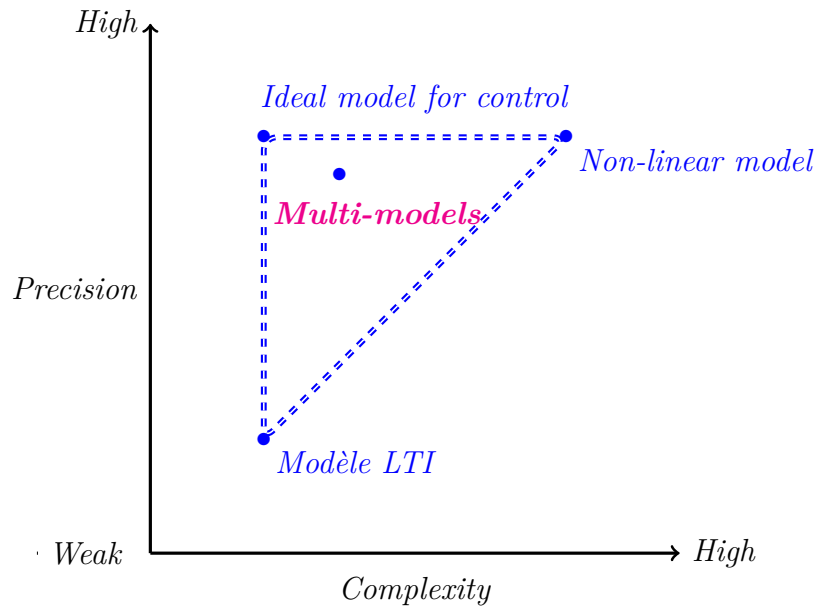


Fig 2.1: Complexity and precision of the representation of non-linear systems

Currently, the multi-model (MM) approach is a widely used tool for modelling non-linear systems. In the literature, several terminologies, which are equivalent, are used to define this type of model, as shown in figure 2.2: the multi-model [MSJ], the fuzzy Takagi-Sugeno model [TS85], the polytopic linear model [Ang01], etc. The main idea of this approach is based on the contribution of sub-models to the global model of the system; this contribution, which is quantified by a weighting function (activation function), is a convex combination of the sub-systems.

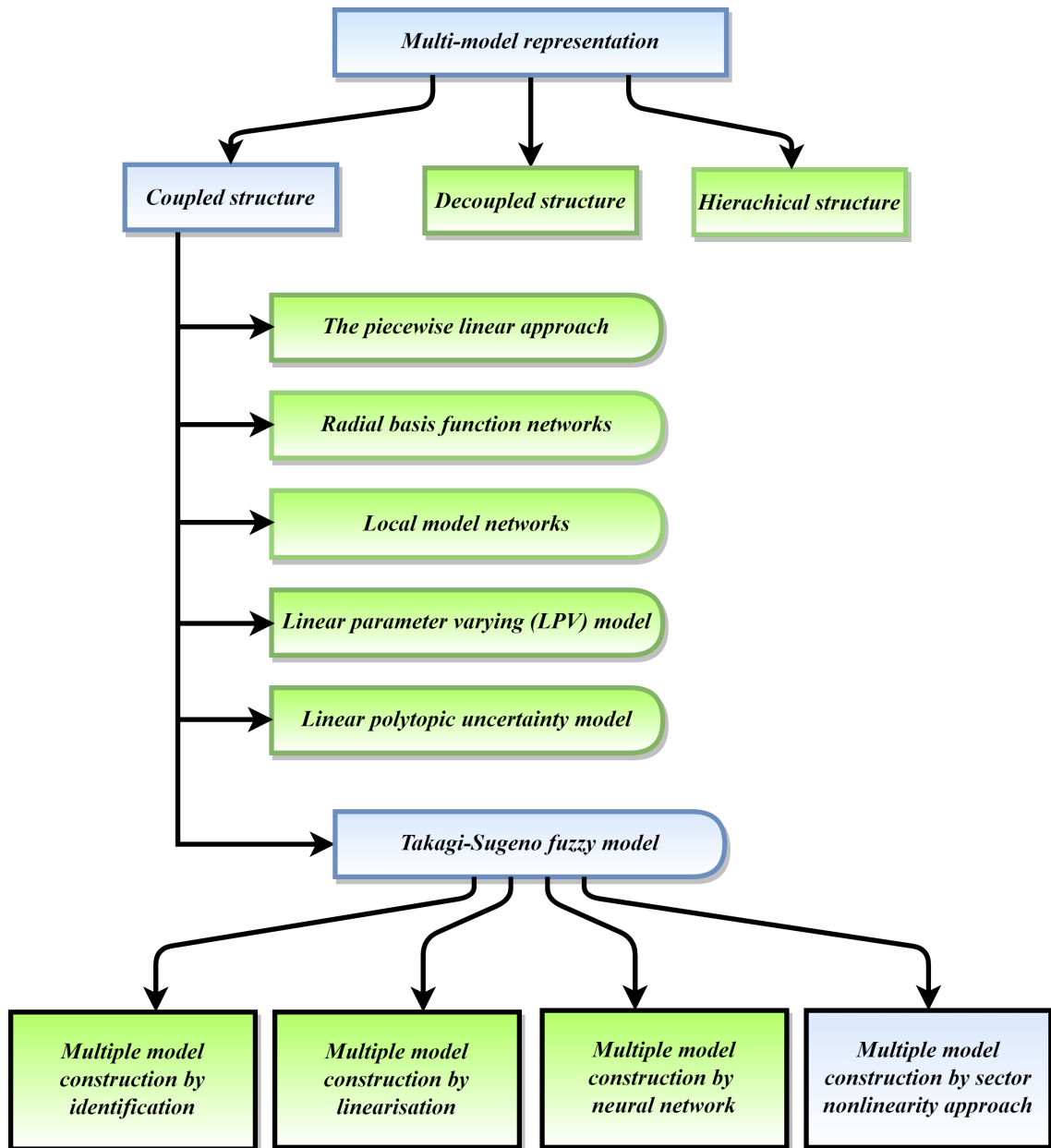


Fig 2.2: Multiple model structure

2.2.1 Operating space

It is a vector space inside which the variables of the system evolve.

2.2.2 Operating zone

The operating zones represent the domains of validity of the local models; each domain is defined around an operating point [Kso99]. These domains can be of disjoint validity or overlap, as indicated in figure (2.3).

In the case where the domain is of disjoint validity, the activation functions can only

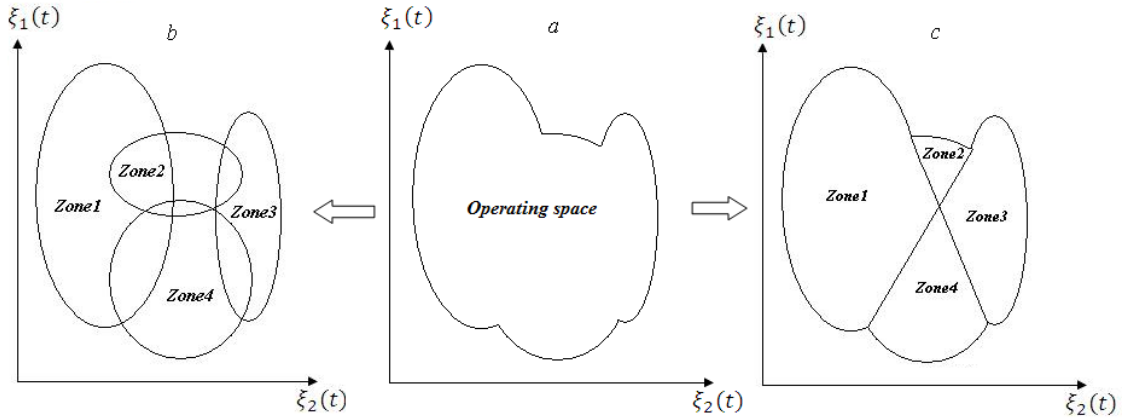


Fig 2.3: Schematic diagram of the multi-model approach
 a)- Non-linear system , b – c)- Multi-models representation

take values of 0 or 1, and at any given moment, there is only one valid model, and the others are zero. This type of partitioning is frequent in the case of systems with multiple configurations or with several operating modes; the model obtained is called Piecewise Affine [SSPP23, Ham12]. The other situation that can also be encountered in a multi-model description is the case where the domains of validity overlap or have common areas; this overlap is due to the substitution of the activation functions with a stretched front by functions with a gentle slope. In this case, these functions become continuous derivative functions whose slope determines the speed of transition from one model to another [Ham15, Ham12].

2.2.3 Sub-model

It is the model that represents the behaviour of the non-linear system in a specific operating zone.

2.2.4 Premise variable

Also known as a decision variable. $\xi(t)$ is a system vector variable that intervenes in the weighting functions $\mu(t)$. This variable can include one or more internal or external variables of the system. These variables can be either accessible to measurement as measurable state variables or system input signals or inaccessible to measurement.

2.2.5 Activation function

It is a function that determines the degree of activation of the associated local sub-model. Depending on the zone where the system evolves, this function indicates the more or less important contribution of the corresponding local model to the global model. It ensures a gradual transition from this model to neighbouring local models. These functions depend on the decision variables.

The weighting functions represent a normalisation of the laws $\mu_i(\xi(t))$ which are the weighting weights of the local models. These functions depend on the internal and/or external variables of the non-linear system (decision variables).

$$h_i(\xi(t)) = \frac{\mu_i(\xi(t))}{\sum_{i=1}^r \mu_i(\xi(t))} \quad (2.1)$$

These functions are generally chosen in order to verify the properties of the convex sum:

$$\begin{cases} 0 \leq h_i(\xi(t)) \leq 1 \\ \sum_{i=1}^r h_i(\xi(t)) = 1 \end{cases}$$

These functions have been constructed in various ways over time. They can be chosen as Boolean types with discontinuous derivatives (triangular functions) or functions with continuous derivatives (sigmoidal or Gaussian functions). In the continuous case, the exponential law is often used and applies to the different premise variables [ACMR04] [Nag10]. The weighting functions can also be constructed by using the bounds of the decision variables.

The multi-model representation of a non-linear system can be obtained from different structures. These structures are distributed according to the dimension of the state space and the nature of the coupling between the local models associated with the operating zones [Ham12].

2.2.6 Multi-model

The multi-model is based on the decomposition of the dynamic behaviour of the system into several operating zones, each zone being characterised by a subsystem. Depending on the area where the system evolves, each subsystem contributes more or less to the

approximation of the global behaviour of the system. In general, the system presents a homogeneous dynamic behaviour inside an operating zone. Thus, the contribution of each subsystem to the global model, which is a convex combination of the subsystems, is defined by a weighting function [Nag10].

2.3 Different multi-model structures

The multi-model representation of a non-linear system can be obtained from different structures. A state representation of the sub-models makes it easy to highlight them. This multi-model state representation has the advantage of being compact, simple, and more general than a presentation in the form of an input/output regression equation. Moreover, the synthesis of a control law or the construction of non-linear observers often require such a description of the system [Orj08]. The multi-model representation of a non-linear system can be obtained from different structures depending on whether the segmentation is done on the input or the output (i.e., on the measurable state variables) and also according to the nature of the coupling between the local models associated with the zones of functioning. However, three multi-model structures exist:

- coupled structure
- decoupled structure
- hierarchical structure

2.3.1 Coupled structure

2.3.1.1 Takagi-Sugeno fuzzy model

The Takagi-Sugeno fuzzy model approach proposed by [TS85], it's allows for the representation of the non-linear system in a compact set with a convex combination of different linear subsystems. The fuzzy multi-model structure is described by fuzzy IF-THEN rules: The i^{th} rule of the Takagi-Sugeno multi-model is of the following form:

Plant Rule i

$$\begin{array}{l}
 \text{IF} \quad \xi_1(t) \text{ is } F_{i,1} \text{ and } \xi_2(t) \text{ is } F_{i,2} \dots \xi_r(t) \text{ is } F_{i,r} , \\
 \text{THEN} \quad \left\{ \begin{array}{l} \dot{x}_i(t) = A_i x(t) + B_i u(t) \\ y_i(t) = C_i x(t) + E_i u(t) \end{array} \right. \quad i = 1, 2, \dots, r
 \end{array} \tag{2.2}$$

where the premises are obtained from the linguistic propositions, allowing the evaluation of the weighting functions μ_i and where the consequences correspond to the sub-models. One of the multiple interests of this model is that it allows the introduction of a priori knowledge about the systems in the modelling stage by providing an initial fuzzy partition of the operating space. This model has been widely studied since its appearance, having been the subject of many developments and extensions of classic tools, from automatic control to fuzzy models. The system (2.2) can be represented as a global fuzzy multi-model by using the non linear sector transformation (see figure 2.4) [IMRM09]:

$$\begin{cases} \dot{x}(t) = \sum_{i=1}^r h_i(\xi(x(t))) (A_i x(t) + B_i u(t)) \\ y(t) = C_i x(t) + E_i u(t) \end{cases} \quad (2.3)$$

Where $A_i \in \mathfrak{R}^{n \times n}$, $B_i \in \mathfrak{R}^{n \times n_u}$, $E_i \in \mathfrak{R}^{n \times n_\delta}$, are the state, input, and the influence matrices respectively, $C_i \in \mathfrak{R}^{n_y \times n}$ and $E_i \in \mathfrak{R}^{n_y \times n}$ are the output matrix.

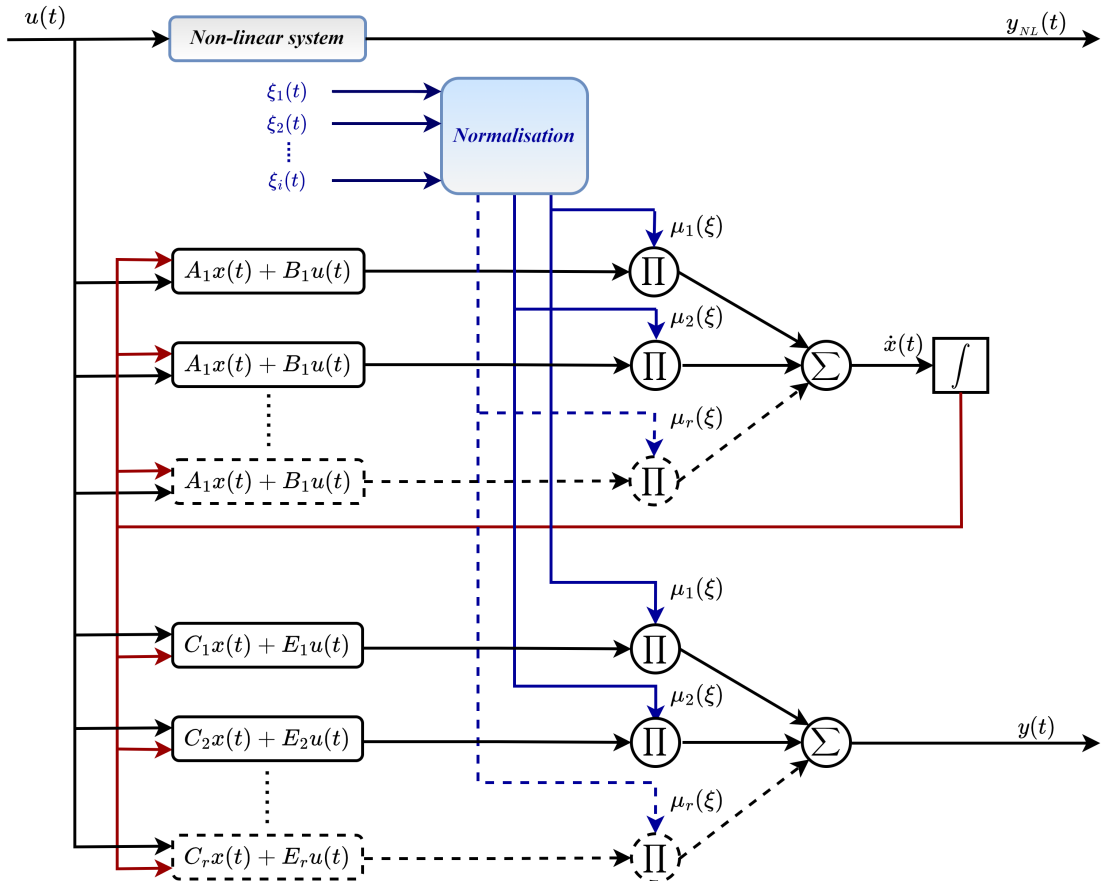


Fig 2.4: Architecture of TS multi-model

Many non-linear system modelling techniques share the same structure (2.2). The choice of the structure of the sub-models and the weighting functions is at the root of

their differences. It is possible to cite different models based on this structure.

2.3.1.2 The piecewise linear approach

This type of model is constructed by considering linear sub-models and Boolean weighting functions [Son81]. This selection of weighting functions is a result of the separation of the operating space into completely separate operating zones. In the switching phases, this results in a discontinuous approximation of the non-linear system. This discontinuity may prove undesirable in certain applications [Orj08].

2.3.1.3 Radial basis function networks

It has been shown that, under certain restrictions, radial basis function networks are equivalent to the TS multi-model [JS93]. Indeed, the equivalence between the models is guaranteed if the weighting functions employed are of the Gaussian type and if the sub-models are reduced to a constant F_i (sub-models of order 0). This type of model also possesses the property of universal approximation, as it is capable of representing any non-linear system. This method has two significant drawbacks, namely the large number of sub-models required to obtain a satisfactory approximation of a non-linear system and the sensitivity of the model obtained [Orj08].

2.3.1.4 Local model networks

Since the publication of [MSJ97] work, multi-models have become a prominent tool in the modelling of systems in the presence of multiple operating regimes. The multi-model and the Takagi-Sugeno fuzzy model cover very similar notions. Indeed, if the number of rules is equal to the number of sub-models then these two approaches are identical. Only the means used to obtain the weighting functions $\mu_i(\cdot)$ and the interpretation given to them distinguish them. For fuzzy models, the partitioning of the operating space of the system often calls on the knowledge of experts in order to obtain linguistic proposals leading to fuzzy subsets. For multi-models, the partitioning of the system operating space is carried out using optimization techniques [Nag10].

2.3.1.5 Linear parameter varying (LPV) model

Many systems can be described by linear systems whose parameters vary over time (LPV) [DIA19]. In the classic LPV modelling approach, weighting functions are not used: it is the decision variables $\xi(t)$ that are used to describe the operating conditions of the system. The variable $\xi(t)$ is an exogenous or endogenous variable of the system, accessible by measurement, and varying within a compact set of known bounds. If $\xi(t)$ is a signal endogenous to the system, the output, for example, then we speak of quasi-LPV systems. In practice, however, LPV and quasi-LPV systems are analysed similarly. The structure 2.3 is a particular form of the LPV model where the weighting functions deliver the evolution laws of the parameters [Orj08, Nag10].

2.3.1.6 Linear polytopic uncertainty model

In this context, the matrices representing the system are not completely known but fall within a range of known limits. Vertex matrices are a collection of matrices that represent the various modelling errors of the system. Modelling errors are represented by a collection of vertex matrices that define a polytope, and system behaviour is expressed as a barycentric combination of these matrices. If the vertex matrices are regarded as sub-model matrices, then the relationship to an MM structure is evident [DTH20, Nag10].

2.3.2 Decoupled structure

The decoupled structure, or local multi-models, is proposed by [Fil91] where there are several state vectors. It assumes that the process is composed of decoupled local models and admits independent state vectors, and can be seen as the parallel connection of r affine models weighted by their weights [Ham12]. It should be emphasized that the outputs $y_i(t)$ of the sub-models represent artificial modelling signals, used only to describe the non-linear behaviour of the real system. These signals are not accessible for measurement and have no physical meaning [Ham15]. This structure can be very interesting [Orj08] in the context of parameter identification because it allows for adjusting the dimensions of the sub-models to the complexity of the different behaviours of a process.

$$\begin{cases} \dot{x}_i(t) = \sum_{i=1}^r h_i(\xi(t))(A_i x_i(t) + B_i u(t)) \\ y_i(t) = C_i x_i(t) + E_i u(t) \\ y(t) = \sum_{i=1}^r h_i(\xi(t)) y_i(t) \end{cases} \quad (2.4)$$

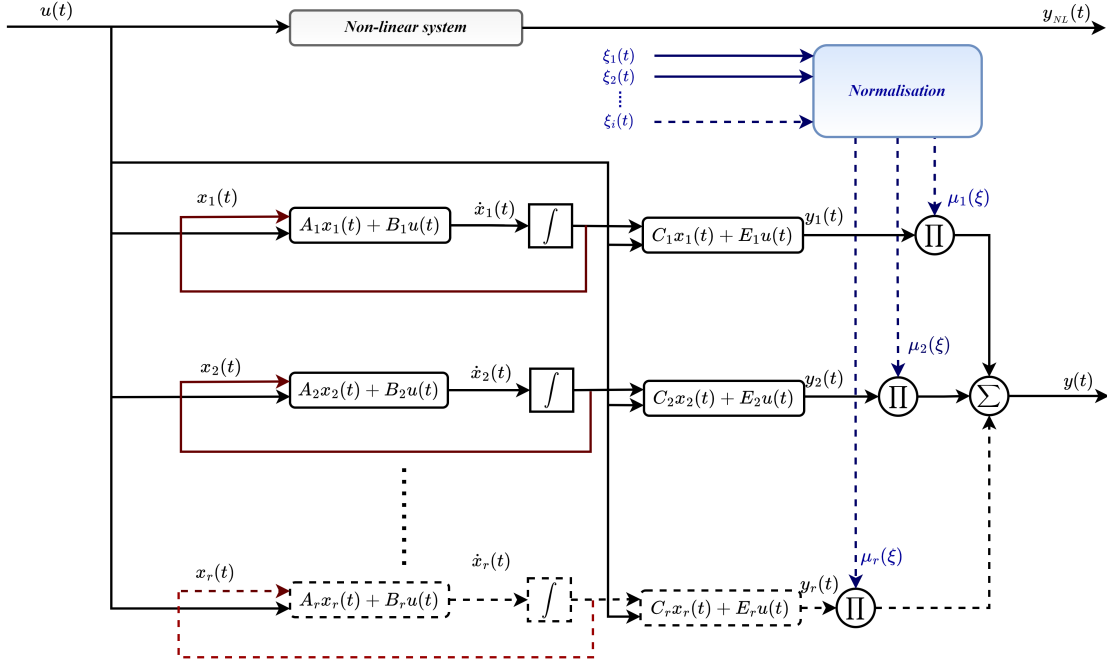


Fig 2.5: Architecture of a decoupled multi-model

2.3.3 Hierarchical structure

Although the multi-model approach has been very successful in many fields (control, diagnosis, etc.), its application is limited to systems with few variables (small size). The number of local models increases exponentially with the increase in the number of variables. A multi-model with r variables and m activation functions defined for each variable, for instance, is comprised of m^r local models [Akh04]. To overcome this problem, Raju et al [RZK91] proposed a hierarchical structure multi-model. The latter is distinguished by a linear increase in the number of rules as the number of entries increases. Nonetheless, according to Kikuchi et al. [HAS98], this structure is not capable of producing a precise expression for any non-linear function. Furthermore, Wang [Li-98] demonstrates that the hierarchical MM can approximate any function very closely [Nag10]. Figure 2.6 shows a typical example of a hierarchical multi-model that has r inputs and $r - 1$ outputs. In this

structure, the local models have two inputs each, and the global model is then composed of r local models.

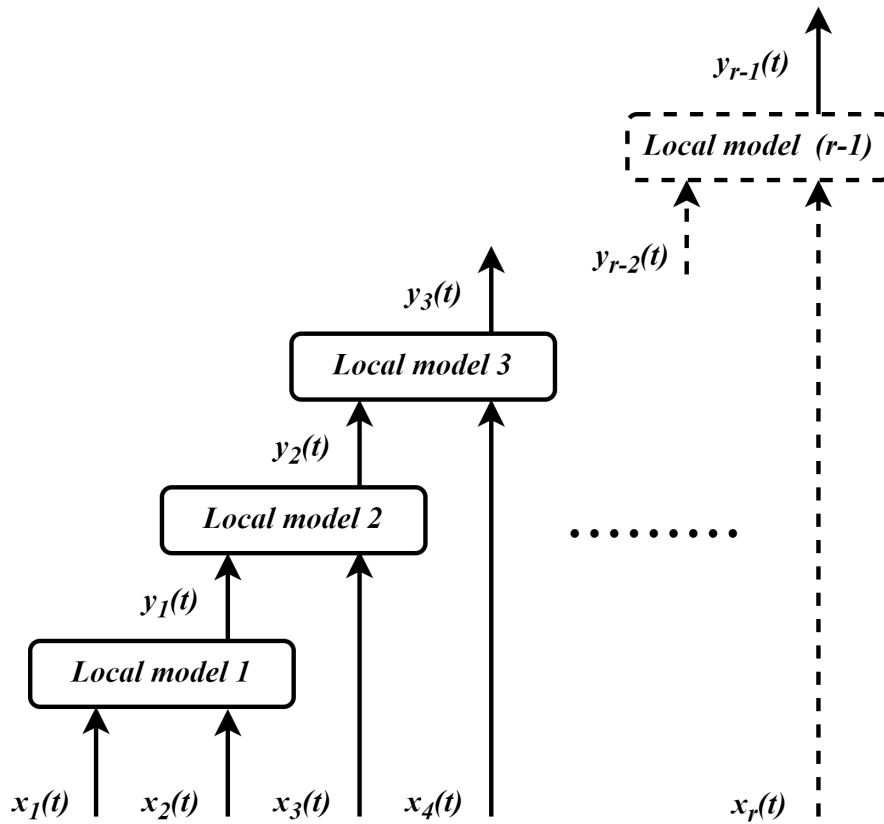


Fig 2.6: Architecture of a hierarchical multi-model

2.4 Methods for obtaining multi-models

In this section, we describe the three methods for obtaining a coupled multi-model structure from a non-linear model.

2.4.1 Multiple model construction by identification

The identification approach to fuzzy modelling is suitable for plants that are unable or too difficult to be represented by analytical and/or physical models (black box) [TW04]. In general, identification methods for unknown parameters are based on the minimization of a functional of the difference between the estimated output of the multiple model $y_m(t)$ and the measured output of the system $y(t)$. The criterion commonly used is the minimization of the quadratic error. By using digital optimization techniques, the identification of the parameters of the local models around the various operating points previously defined

becomes possible. The problem of identifying non-linear systems is reduced by representing them in multi-model form and allowing the identification of subsystems defined by local linear models and activation functions [CB12], [Ham15].

2.4.2 Multiple model construction by linearisation

The principle of this method consists in linearising the non-linear system around a finite set of judiciously chosen operating points, leading to a defined number of LTI models. Obtaining a T-S representative in this case is achieved by interconnecting these LTI models using carefully chosen non-linear membership functions (Gaussian, triangular, trapezoidal, etc.) [Bou09]. Consider the non-linear system described by:

$$\begin{cases} \dot{x}(t) = f(x(t), u(t)) \\ y(t) = g(x(t), u(t)) \end{cases} \quad (2.5)$$

Where $x(t) \in \mathfrak{R}^{n_x}$, $u(t) \in \mathfrak{R}^{n_u}$, and $y \in \mathfrak{R}^{n_y}$ are the state, the input, and the output measurement vectors respectively, and $(f, g) \in \mathbb{R}^{2n}$ are continuous non linear functions. The non linear system (2.5) will then be represented by a multi-model composed of several local linear or affine models obtained by linearising the non linear system around an arbitrary operating point. $(x_i, u_i) \in \mathbb{R}^n \times \mathbb{R}^m$, [Gas00], [Oud08]:

$$\begin{cases} \dot{x}_m(t) = \sum_{i=1}^r h_i(\xi(t))(A_i x_m(t) + B_i u(t) + D_i) \\ y_m(t) = \sum_{i=1}^r h_i(\xi(t))(C_i x_m(t) + E_i u(t) + N_i) \end{cases} \quad (2.6)$$

with

$$\begin{aligned} A_i &= \frac{\partial f(x, u)}{\partial x} \Big|_{(x,u)=(x_i,u_i)} , \quad B_i = \frac{\partial f(x, u)}{\partial u} \Big|_{(x,u)=(x_i,u_i)} \\ C_i &= \frac{\partial h(x, u)}{\partial x} \Big|_{(x,u)=(x_i,u_i)} , \quad E_i = \frac{\partial h(x, u)}{\partial u} \Big|_{(x,u)=(x_i,u_i)} \\ D_i &= f(x_i, u_i) - A_i x - B_i u , \quad N_i = h(x_i, u_i) - C_i x - E_i u \end{aligned}$$

Note that in this case, the number of local models (r) depends on the desired modelling accuracy, the complexity of the non linear system, and the choice of the activation function structure.

2.4.3 Multiple model construction by neural approach

Multiple model representation using the neural approach When there is no general starting model available, it often becomes difficult to create a multiple model representation of a process, and particularly to define a priori the base number of models to choose. In this respect, it is tempting to create a multiple model representation directly during the identification phase by using a neural approach. There are four steps to this approach [EDBB10] ,[CB12]:

- When input- output signals are considered to be sufficiently strong, to distribute this data into classes using a rival penalized competitive learning neural classification technique, this approach enables us to define the required number of models.
- To use the result of this classification in order to refine it from Kohonen self-adaptive networks and from the fuzzy K-means method.
- To associate a model, mostly linear, i.e. to each data set.
- To determine at each operating point the validity or coefficient relevant to each type of model.

2.4.4 Multiple model construction by sector non linearity approach

The modelling of Takagi-Sugeno fuzzy systems by the non-linear sector approach was first introduced in the works of [KTIT92], and subsequently extended by [TW04]. This approach consists of representing the non-linear system exactly in a compact space of state variables. In this context, sometimes it is difficult to find a global sector for the non-linear system; for this reason, we consider a local non-linear sector, as shown in Figure (2.7) [Ham15].

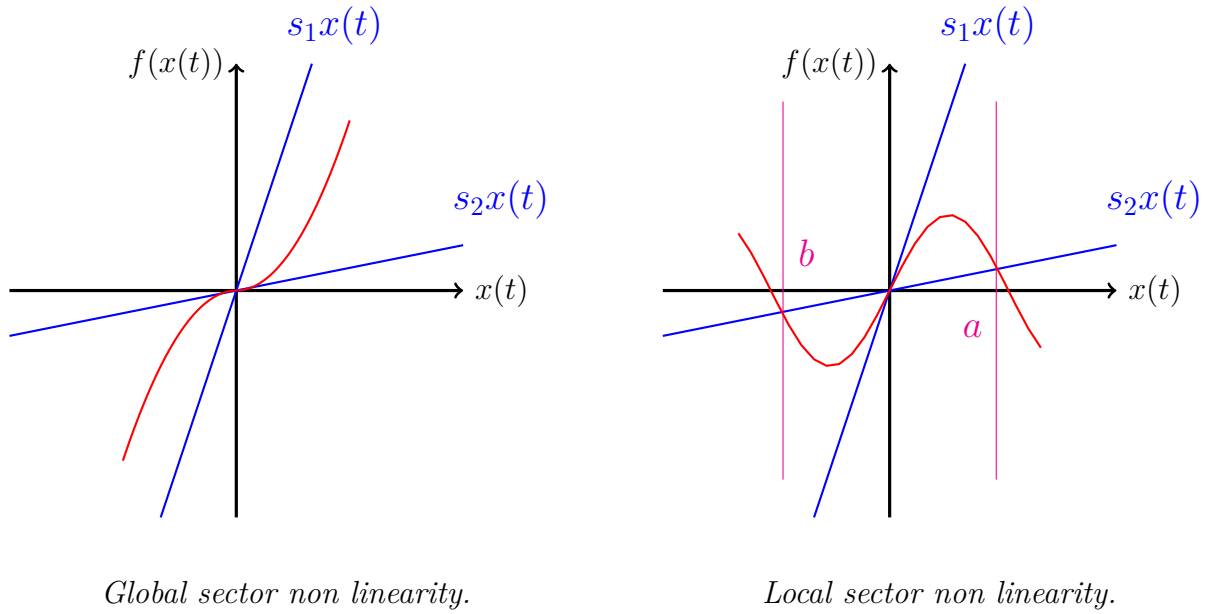


Fig 2.7: Non-linear sectors

We can write the system (2.5) in LPV form:

$$\begin{cases} \dot{x}(t) = A(\xi(t))x(t) + B(\xi(t))u(t) \\ y(t) = C(\xi(t))x(t) + E(\xi(t))u(t) \end{cases} \quad (2.7)$$

Let k be the number of non linear functions present in the system (2.7). These functions appear in state matrices $A(\cdot)$, $B(\cdot)$, $C(\cdot)$, and $E(\cdot)$; they generally depend on the state x and the command u and are denoted $\xi_i(t)$, $i = 1, \dots, k$. Suppose there is a compact C of the variables $\xi(t)$ where the non linearity are bounded, in this case the ξ_i verify [Bez13]:

$$\xi_i(t) \in [\xi_{i,2}, \xi_{i,1}], \text{ for } i = 1, \dots, k \quad (2.8)$$

The non-linearity ξ_i can then be written in the following form:

$$\xi(t) = F_{i,1}(\xi_i(t))\xi_{i,1} + F_{i,2}(\xi_i(t))\xi_{i,2} \quad (2.9)$$

where

$$\begin{cases} \xi_{i,1} = \max\{\xi_i(t)\} \\ \xi_{i,2} = \min\{\xi_i(t)\} \\ F_{i,1}(\xi_i(t)) = \frac{\xi_i(t) - \xi_{i,2}}{\xi_{i,1} - \xi_{i,2}} \\ F_{i,2}(\xi_i(t)) = \frac{\xi_{i,1} - \xi_i(t)}{\xi_{i,1} - \xi_{i,2}} \end{cases} \quad (2.10)$$

The activation functions $\mu_i(\xi(t))$ are obtained from the functions $F_{i,1}(\xi(t))$ and $F_{i,2}(\xi_i(t))$ by:

$$\mu_r(\xi(t)) = \prod_{i=1}^{2^k} F_{i,\sigma_r^i}(\xi_i(t)) \quad (2.11)$$

The number of sub-models is $r = 2^k$. The indices σ_r^i ($r = 1, \dots, 2^k$ and $i = 1, \dots, k$) are equal to 1 or 2 and indicate which partition of the sub-model i ($F_{i,1}$ Where $F_{i,2}$) is used to define the sub-model r . The relationship between the sub-model number i and the indices σ_r^i is given by the following equation:

$$i = 2^{n-1}\sigma_i^1 + 2^{n-2}\sigma_i^2 + \dots + 2^0\sigma_i^n - (2^1 + 2^2 + \dots + 2^{n-1}) \quad (2.12)$$

The matrices A_i , B_i , and C_i are obtained by replacing $\xi_i(t)$ by ξ_{i,σ_r^i} in $A(\xi(t))$, $B(\xi(t))$, $C(\xi(t))$ and in (2.7). We thus obtain the following T-S system:

$$\begin{cases} \dot{x}(t) = \sum_{i=1}^{r=2^k} h_i(\xi(t))(A_i x(t) + B_i u(t)) \\ y(t) = \sum_{i=1}^{r=2^k} h_i(\xi(t))C_i x(t) \end{cases} \quad (2.13)$$

This multi-model structure is linked to the number of non-linear terms in the original system. The drawback of this method remains in the number of local models as well as the accessibility of the decision variables of the weighting functions. However, from a structural point of view, all the sub-models constituting this multi-model have the same dimension; a single state vector is being employed. The complexity of the sub-models is therefore constant, regardless of the complexity of the system in the different operating zones. The multi-model thus obtained then risks being over-parametrized and its complexity unnecessarily increased [Ham12].

Example:

Consider the following non-linear system:

$$\begin{pmatrix} \dot{x}_1(t) \\ \dot{x}_2(t) \end{pmatrix} = \begin{pmatrix} -x_1(t) + x_1(t)x_2^3(t) \\ -x_2(t) + (3 + x_2(t))x_1^3(t) \end{pmatrix} \quad (2.14)$$

We suppose that $x_1(t) \in [-1, 1]$ et $x_2(t) \in [-1, 1]$. The previous system can be written in the form:

$$\dot{x}(t) = \begin{bmatrix} -1 & x_1(t)x_2^2(t) \\ (3 + x_2(t))x_1^2(t) & -1 \end{bmatrix} x(t)$$

with $x(t) = [x_1(t), x_2(t)]^T$ and $x_1(t)x_2^2(t)$ and $(3 + x_2(t))x_1^2(t)$ are non-linear terms, for this reason we will assign the following choice:

$$\xi_1(t) = x_1(t)x_2^2(t) \text{ and } \xi_2(t) = (3 + x_2(t))x_1^2(t)$$

then:

$$\dot{x}(t) = \begin{bmatrix} -1 & \xi_1(t) \\ \xi_2(t) & -1 \end{bmatrix} x(t)$$

Then, we calculate the minimum and maximum values of $\xi_1(t)$ and $\xi_2(t)$ for $x_1(t) \in [-1, 1]$ and $x_2(t) \in [-1, 1]$.

$$\xi_{1max} = \xi_1(t)|_{max\{x_1(t), x_2(t)\}} = 1$$

$$\xi_{1min} = \xi_1(t)|_{min\{x_1(t), x_2(t)\}} = -1$$

$$\xi_{2max} = \xi_2(t)|_{max\{x_1(t), x_2(t)\}} = 4$$

$$\xi_{2min} = \xi_2(t)|_{min\{x_1(t), x_2(t)\}} = 0$$

$\xi_1(t)$ and $\xi_2(t)$ can be represented by:

$$\xi_1(t) = x_1(t)x_2^2(t) = M_1(\xi_1(t)) \cdot \xi_{1max} + M_2(\xi_1(t)) \cdot \xi_{1min}$$

$$\xi_2(t) = (3 + x_2(t))x_1^2(t) = N_1(\xi_2(t)) \cdot \xi_{2max} + N_2(\xi_2(t)) \cdot \xi_{2min}$$

$$M_1(\xi_1(t)) + M_2(\xi_1(t)) = 1.$$

$$N_1(\xi_2(t)) + N_2(\xi_2(t)) = 1.$$

The membership functions are then:

$$M_1(\xi_1(t)) = \frac{\xi_1(t) - \xi_{1min}}{\xi_{1max} - \xi_{1min}} = \frac{\xi_1(t) + 1}{2}, M_2(\xi_1(t)) = \frac{\xi_{1max} - \xi_1(t)}{\xi_{1max} - \xi_{1min}} = \frac{1 - \xi_1(t)}{2}$$

$$N_1(\xi_2(t)) = \frac{\xi_2(t) - \xi_{2min}}{\xi_{2max} - \xi_{2min}} = \frac{\xi_2(t)}{4}, N_2(\xi_2(t)) = \frac{\xi_{2max} - \xi_2(t)}{\xi_{2max} - \xi_{2min}} = \frac{4 - \xi_2(t)}{4}$$

These membership functions are called "Positive", "Negative", "Big" and "Small" respectively. Then the previous linear system can be represented by the fuzzy model of Takagi-Sugeno following:

- Rule 1: If $\xi_1(t)$ is "Positive" and $\xi_2(t)$ is "Big" Then $\dot{x}(t) = A_1x(t)$.
- Rule 2: If $\xi_1(t)$ is "Positive" and $\xi_2(t)$ is "Small" Then $\dot{x}(t) = A_2x(t)$.
- Rule 3: If $\xi_1(t)$ is "Negative" and $\xi_2(t)$ is "Big" Then $\dot{x}(t) = A_3x(t)$.
- Rule 4: If $\xi_1(t)$ is "Negative" and $\xi_2(t)$ is "Small" Then $\dot{x}(t) = A_4x(t)$.

with

$$A_1 = \begin{bmatrix} -1 & 1 \\ 4 & -1 \end{bmatrix}, A_2 = \begin{bmatrix} -1 & 1 \\ 0 & -1 \end{bmatrix}, A_3 = \begin{bmatrix} -1 & -1 \\ 4 & -1 \end{bmatrix}, A_4 = \begin{bmatrix} -1 & -1 \\ 0 & -1 \end{bmatrix}$$

The non-linear system is represented by the following fuzzy Takagi-Sugeno model:

$$\dot{x}(t) = \sum_{i=1}^4 h_i(\xi(t))A_i x(t)$$

with

$$h_1(\xi(t)) = M_1(\xi_1(t)) \times N_1(\xi_2(t)), h_2(\xi(t)) = M_1(\xi_1(t)) \times N_2(\xi_2(t)),$$

$$h_3(\xi(t)) = M_2(\xi_1(t)) \times N_1(\xi_2(t)), h_4(\xi(t)) = M_2(\xi_1(t)) \times N_2(\xi_2(t))$$

This fuzzy model represents in an exact way the previous non-linear system in the region $[-1, 1] \times [-1, 1]$ of the state space.

2.5 Stability analysis of dynamic systems

2.5.1 Stability in the sense of Lyapunov

This section reviews stability in continuous-time dynamical systems. Stability is defined as the behaviour of a system's trajectories near points of equilibrium. Studying stability helps to examine how a system's trajectory evolves when the initial state is close to an equilibrium point. The theory of stability in the sense of Lyapunov is applicable to any differential equation and means that the solution of the equation, when initialized near an equilibrium point, stays close to it [Zer11].

The non-linear system (2.5) With initial condition $x(t_0) = x_0$, it is assumed that the system has an equilibrium point \bar{x}

Stable equilibrium The point \bar{x} is a stable equilibrium point of the system (2.5) if for every $\varepsilon > 0$, there exists a $\delta > 0$ such that, for every initial condition x_0 satisfying $|x_0 - \bar{x}| < \delta$, the solution $x(t)$ of the system (2.5) satisfies $|x(t) - \bar{x}| < \varepsilon$ for all $t \geq 0$.

In other words, a point \bar{x} is a stable equilibrium of the system if, given a small enough initial deviation from \bar{x} , the solution remains arbitrarily close to \bar{x} for all future times.

Attractor equilibrium The point \bar{x} is an attractor equilibrium point of the system (2.5) if for every $\varepsilon > 0$, there exists a $\delta > 0$ such that, for every initial condition x_0 satisfying $|x_0 - \bar{x}| < \delta$, the solution $x(t)$ of the system (2.5) converges to \bar{x} as $t \rightarrow \infty$, i.e., $\lim_{t \rightarrow \infty} |x(t) - \bar{x}| = 0$. In other words, an attractor equilibrium is a stable equilibrium to which the solutions of the system converge as time goes on, regardless of the initial conditions. It acts as a "attractor" for nearby solutions, pulling them towards it as time progresses. An attractor equilibrium is a stronger concept of stability, as it implies not only that the solution remains arbitrarily close to the equilibrium for all future times, but also that the solution approaches the equilibrium as time goes on.

Asymptotically stable equilibrium The point \bar{x} is considered an asymptotically stable equilibrium for the system (2.5) if it is both stable and attractive. If all initial states x_0 converge towards the asymptotically stable equilibrium, it is referred to as the basin of attraction. Asymptotic stability is a desirable property in practice, but it does not specify the rate at which the trajectory $x(t)$ approaches equilibrium. To address this, the concept of exponential stability is introduced.

Exponential stability The point \bar{x} is an exponentially stable equilibrium point if there exist positive real numbers $\varepsilon, \alpha, \beta$, and δ such that for any initial value x_0 satisfying $|x_0 - \bar{x}| < \delta$, the solution of the system satisfies $|x(t) - \bar{x}| \leq \alpha|x_0 - \bar{x}|e^{-\beta t}$ for all $t \leq t_0$, where t_0 is a fixed time. It is clear that exponential stability implies asymptotic stability, but the reverse is not necessarily true. In the following, we will consider stability around the origin, i.e., when $\bar{x} = 0$.

2.5.1.1 Lyapunov first method

The Lyapunov First Method, also known as the Indirect Method, assesses stability of a system by examining the linearisation of the system around the equilibrium point \bar{x} . This involves evaluating the eigenvalues $\lambda_i(A)$ of the Jacobian matrix A at the equilibrium, i.e.

$$A = \frac{\partial f}{\partial x} \bar{x}$$

The indirect method of Lyapunov is a method for determining the stability of an equilibrium point $\bar{x} = 0$ in a dynamical system. If all the eigenvalues of the Jacobian

matrix have a negative real part, meaning their real parts are less than zero $Re(\lambda_i(A)) < 0$, then the equilibrium point $\bar{x} = 0$ is considered to be exponentially stable. If at least one eigenvalue has a positive real part $Re(\lambda_i(A)) > 0$, the equilibrium $\bar{x} = 0$ is considered unstable. While the indirect method is simple to implement, it only provides a partial analysis of stability and does not indicate the size of the basins of attraction [Zer11].

2.5.1.2 Lyapunov second method

Lyapunov's second method, also known as the direct method, involves the use of a positive definite function (usually denoted $V(x(t))$) called Lyapunov's function to assess the stability of an equilibrium point. The function must decrease along the system's trajectories and be positive definite within the attraction basin. While more general than the indirect method, it is also more challenging to implement [Zer11, Cha02].

Local stability and asymptotic stability For the system (2.5) to be considered locally stable, there must be a continuous and differentiable function, $V(x(t))$, and a vicinity, V_0 , such that:

- $\forall x \in V_0, V(x(t)) > 0$.
- $\forall x \in V_0, \dot{V}(x(t)) = \frac{dV(x(t))}{dt} = \frac{\partial V(x(t))}{\partial x} \dot{x}(t) \leq 0$.

If $V(x(t)) > 0$ and $\dot{V}(x(t)) < 0$, the function $V(x(t))$ is considered a Lyapunov function in the strict sense and the origin is considered asymptotically stable.

Exponential stability The origin is an exponentially stable equilibrium point for the system (2.5) if there exists a continuous and differentiable function $V(x(t))$, constants $\alpha, \beta, \gamma > 0; p \geq 0$ and if there exists a vicinity V_0 such that

- $\forall x \in \alpha \|x\|^p \leq V(x(t)) < \beta \|x\|^p$.
- $\forall x \in V_0, \dot{V}(x(t)) < -\gamma V(x(t))$.

2.5.2 Types of Lyapunov functions

The difficulty of Lyapunov stability method lies in the determination of these functions. However, there are families of Lyapunov functions that are often used and whose adoption depends on the nature of the system to be studied (linear systems, piecewise continuous

systems, delay systems, uncertain linear systems, etc.). In this thesis, we are interested in the stability by quadratic Lyapunov functions.

2.5.2.1 Quadratic function

the most classic choice is to use a quadratic form:

$$V(x(t)) = x(t)^T P x(t) \quad P = P^T > 0 \quad (2.15)$$

This type of function, adopted to study the stability of linear systems, is also used in the case of multi-models [TW04]. Finding such a function amounts to finding a definite positive matrix. In the case of the multi-model approach, the convex formulation of the problem easily allows the extraction of such a function when it exists. The disadvantage of the method lies in obtaining very conservative stability conditions [Cha02].

2.5.2.2 Poly-quadratic function [Cha02]

This function has the following form:

$$V(x(t), \xi(t)) = x(t)^T \sum_{i=1}^r \mu_i(\xi(t)) P_i x(t) \quad (2.16)$$

with

$$\begin{aligned} P_i &> 0, \\ \mu_i(\xi(t)) &> 0, \\ \sum_{i=1}^r \mu_i(\xi(t)) &= 1. \end{aligned}$$

It allows, in the case of the multi-model approach, to relax the constraints imposed by the quadratic method. This type of function is also more general in the sense that it includes the quadratic case, because it suffices to choose $P_i = P, i \in I_n$ to reduce to the case of quadratic functions. It is also interesting to note that, as opposed to the quadratic method, this type of function takes into account the speed of variation of the decision variables of the continuous multi-model, which explains the reduction in the conservatism of the method [BPB01, CMR00, Cha02] [CMR00].

2.5.2.3 Parametric affine function

This type of function has the following form:

$$V(x(t)) = x(t)^T P(\theta)x(t) \quad (2.17)$$

with

$$P(\theta) = P_0 + \theta_1 P_1 + \dots + \theta_r P_r > 0$$

is often used to study time-varying linear systems with uncertain parameters of the type:

$$\dot{x}(t) = A(\theta)x(t) \quad (2.18)$$

with

$$A(\theta) = A_0 + \theta_1 A_1 + \dots + \theta_r A_r \quad (2.19)$$

Where the parameters and their variations are bounded. Expression (2.17) generalizes the quadratic Lyapunov functions which correspond to, $P_1 = \dots = P_k = 0$. They are less conservative than the quadratic functions because they take into account the variations of the parameters. The quality of the results obtained depends on the choice of the type of Lyapunov function relative to the nature of the system studied [Cha02].

2.5.2.4 Piecewise continuous functions

One can distinguish between piecewise continuous linear Lyapunov functions and piecewise continuous quadratic Lyapunov functions [DLPT20] [Poo19]. These non-quadratic functions have also been the subject of applications in the case of fuzzy systems [CGAL19]. One can also distinguish the piecewise quadratic functions of the form:

$$V(x(t)) = \max(V_1(x(t)), \dots, V_i(x(t)), \dots, V_n(x(t))) \quad (2.20)$$

With

$$V_i(x(t)) = x(t)^T P_i x(t), \quad P_i > 0, i \in I_i \quad (2.21)$$

This type of function has been studied in the case of linear time variant systems [BEGFB94] and has the advantage of being less conservative than quadratic functions [Cha02].

2.5.2.5 Line integral Lyapunov function

The line integral Lyapunov function is a useful tool for the analysis and design of fuzzy control systems as it allows for the development of stability conditions without considering the time derivatives of the membership functions. This makes it a simple and computationally efficient method for analysing the stability of fuzzy control systems, Rhee et al. [RW06] proposed the following line integral Lyapunov function:

$$V(x(t)) = 2 \int_{\Gamma(0,x)} g(\bar{\omega}) d\bar{\omega} \quad (2.22)$$

where $\bar{\omega} \in \mathfrak{R}^n$, and $d\bar{\omega}$ denote a dummy vector for the integral and an infinitesimal displacement vector.

$\Gamma(0, x)$ represent the path from $0 \rightarrow x$

Consider $g(x)$ to be a force vector at x , and then the proposed Lyapunov function $V(x(t))$ in (2.22) can be interpreted as the work that has been performed in $g(x)$ from zero to x . This function resembles an energy form that ensures the following conditions:

- $V(x(t))$ is a smooth function.
- positive definite.
- radially unbounded.

However, if this function is dependent on $\Gamma(0, x)$, then the two last conditions can not be satisfied. Therefore, it is essential to ensure that $V(x(t))$ must be path-independent. To do so, a necessary and sufficient condition is required.

$$\frac{\partial g_i(x)}{\partial x_j} = \frac{\partial g_j(x)}{\partial x_i} \quad \text{for } i, j = 1, \dots, n \quad (2.23)$$

According to 2.23, Meredef et al. [MHB⁺22] proposed the following equation:

$$g(x) = \left(\bar{P} + \sum_{i=1}^r \mu_i(x) E_i \right) x \quad (2.24)$$

$$\bar{P} = \bar{P}^T = \begin{bmatrix} 0 & P_{12} & P_{13} & \dots & P_{1n} \\ * & 0 & P_{23} & \dots & P_{2n} \\ \vdots & \vdots & \ddots & & \vdots \\ * & * & * & \dots & 0 \end{bmatrix}$$

$$E_i = \begin{bmatrix} E_{11} & E_{12} & \dots & E_{1n} \\ E_{21} & E_{22} & \ddots & E_{2n} \\ \vdots & \ddots & \ddots & \vdots \\ E_{n1} & E_{n2} & \dots & E_{nn} \end{bmatrix} \times I_{n \times n}$$

2.6 Stability of Takagi-Sugeno fuzzy systems

The stability of non-linear systems has been the subject of many studies. Lyapunov's theory is the fundamental tool. The main concept of this theory is based on the idea that; if there is a function having energy form is dissipated in time, then it tends towards an equilibrium point. In this context, the use of the Lyapunov function is a measure of the distance between the state variables and the equilibrium point.

The most classical choice consists in choosing a Lyapunov function in the quadratic form which is our choice in this work.

2.6.1 Quadratic Stability of Takagi-Sugeno fuzzy Models

Our objective is to ensure the stability of the fuzzy systems of Takagi-Sugeno, and we privilege the use of the quadratic stabilisation of the system by the second method of Lyapunov. This stability is guaranteed if the conditions in the form of a set of linear matrix inequalities (LMIs) of the following theorems are satisfied.

Theorem 2.6.1:

The TS fuzzy model described by (2.13), is asymptotically stable if there exists a positive definite P matrix such that the following *LMI* holds:

$$A_i^T P + P A_i < 0 \quad i = 1, \dots, r \quad (2.25)$$

Proof

$$V(x(t)) = x(t)^T P x(t) \quad P = P^T > 0 \quad (2.26)$$

The autonomous TS fuzzy model (2.13) ($u(t) = 0$) is stable if:

$$\dot{V}(x(t)) = \dot{x}^T(t) P x(t) + x^T P \dot{x}(t) < 0 \quad (2.27)$$

than

$$\dot{V}(x(t)) = x(t)^T \left(\sum_{i=1}^r h_i(\xi(t)) (A_i^T P + P A_i) \right) x(t) < 0 \quad (2.28)$$

We draw the reader's attention to the fact that many examples show that a fuzzy system of TS has unstable sub-models, but it may be stable, and vice versa.

The stability conditions of Theorem 2.6.1 are conservative since the premise variables are not taken into account. The problem of conservatism of the stability conditions is reduced at the cost of a large number of LMI's.

2.6.2 Alternative Approaches to Stability Analysis in Takagi-Sugeno fuzzy Models

In the literature, researchers have proposed methods to minimize the effect of the conservatism of the stability conditions [Cha02, Kru07, Mor01, Akh04]. They have explored alternative approaches to stability analysis, aiming to address the limitations of classical quadratic Lyapunov functions and provide more flexibility and less conservative results in the context of Takagi-Sugeno fuzzy systems.

These alternative approaches include polyquadratic and non-quadratic Lyapunov functions, which help relax stability constraints. However, the complexity of the stability conditions and the associated computational burden can increase depending on the chosen approach.

It is essential to note that the interpolation of stable sub-models is not necessarily stable. In some cases, it can be challenging to find a common P matrix satisfying the LMIs simultaneously. Researchers have studied several approaches, in particular, the use of polyquadratic Lyapunov functions and non-quadratic Lyapunov functions based on a piecewise continuous function. These types of functions have been used in the context of LPV systems and Takagi-Sugeno systems, providing less restrictive stability conditions

than quadratic stability conditions. However, they are expressed in terms of Bilateral Matrix Inequalities (BMI), which are more challenging to solve than LMIs.

In conclusion, alternative approaches to stability analysis have been explored to address the limitations of classical quadratic Lyapunov functions, providing more flexibility and less conservative results in the context of Takagi-Sugeno fuzzy systems.

2.7 Conclusion

The multi-model approach is a useful technique for modelling non-linear systems, as it allows for accurate representation of the system's behaviour in different operating zones. The different multi-model structures and methods for obtaining multi-models provide a range of options for modelling non-linear systems. The stability analysis of dynamic systems is an essential aspect of system modelling, and the techniques discussed in this chapter, including Lyapunov's stability analysis and the quadratic stability of Takagi-Sugeno fuzzy models, are important for ensuring the stability and reliability of the model. Overall, the multi-model approach is a powerful tool for modelling non-linear systems and can provide valuable insights into the behaviour of complex systems.

State Estimation of TS Multi-Model

3.1	Introduction	66
3.1.1	The different types of observers of non-linear systems	68
3.2	Takagi-Sugeno multi-model State Observer	69
3.2.1	Measurable premise variables (<i>MPV</i>)	70
3.2.2	Non-measurable premise variables (<i>NMPV</i>)	71
3.3	Structure of state multi gain observer based on the Lipschitz approach	72
3.4	State and unknown input observer	75
3.4.1	Structure of robust proportional integral (PI) observer	75
3.4.2	Structure of the proportional multi integral (PMI) observer	81
3.5	Conclusion	85

3.1 Introduction

State estimation in the context of nonlinear systems presents unique challenges, particularly when dealing with observability and the presence of disturbances, unknown inputs, and noise. This chapter focuses on addressing these challenges by exploring various observer techniques. The goal is to develop robust and accurate state estimation methods that can handle nonlinear dynamics effectively.

The chapter begins by providing an overview of the state-of-the-art approaches to observability in nonlinear systems. A comprehensive analysis of different observer types designed for nonlinear systems is presented. This includes high-gain observers, sliding mode observers, and extended Kalman filters, among others. The strengths and limi-

tations of each approach are discussed, providing valuable insights into their practical applicability.

One specific observer technique explored in this chapter is the Takagi-Sugeno multi-model state observer. This observer leverages measurable premise variables (MPV) to estimate system states accurately. It also incorporates non-measurable premise variables (NMPV) to capture the system's dynamics that cannot be directly measured. The structure and functioning of this observer are explained in detail.

Another approach discussed in the chapter is the state multi-gain observer based on the Lipschitz approach. This observer exploits the Lipschitz condition, a fundamental concept in nonlinear analysis, to design an observer that is robust and accurate. The chapter provides a comprehensive explanation of the observer's structure and its theoretical foundations.

To address the challenges posed by disturbances, unknown inputs, and noise, the chapter introduces the state and unknown input observer. This observer incorporates both proportional and integral actions to enhance estimation accuracy and robustness. The robust proportional integral (PI) observer and the proportional multi-integral (PMI) observer are presented, along with their respective structures.

The non-linear system considered is that of the form (1.2)

Definition 1 (*Indistinguishability*). *a pair of states (x_0, x'_0) is said to be indistinguishable if for any input $u(t)$ and for any $t \geq 0$*

$$y(x_0, u, t) = y(x'_0, u, t)$$

Definition 2 (*Observability and low local observability*). *The non-linear system (1.2) is observable if it does not admit an indistinguishable pair. On the other hand, a system is weakly observable at $x_0 \in V$, if there exists an open neighbourhood $V'(x_0) \subset V$ containing x_0 , such that for any neighbourhood $V'' \subset V'(x_0)$ of x_0 , for any point $x_1 \in V''(x_0)$, the pairs (x_0, x_1) are distinguishable.*

Definition 3 (*Observability space*). *The observation space for a non-linear system is defined as the smallest real vector space $(O(h))$ of class function \mathbb{C} which contains the components of $h(h_1, h_2, \dots, h_n)$ and which is closed by Lie derivation.*

Definition 4 (*Observer*). *We call an observer of the dynamical system (1.2) any auxiliary dynamical system in the following form:*

$$\dot{\hat{x}}(t) = \hat{f}(\hat{x}(t), u(t), y(t)) \quad (3.1)$$

We say that the observer (3.1) is a global observer if the estimation error $e(t)$ either satisfy the following condition:

$$\|e(t)\| = \|x(t) - \hat{x}(t)\| \longrightarrow 0 \text{ When } t \longrightarrow \infty \quad (3.2)$$

3.1.1 The different types of observers of non-linear systems

In the literature, Many works concerning the development of observers for all types of systems have been carried out since the founding works of Luenberger, The synthesis of state observers of non-linear systems is more difficult than those of linear systems. In general, there are three approaches to observer synthesis.

3.1.1.1 Extended Observers

The Extended Kalman Filter (*EKF*) and Luenberger's observer are two techniques based on the linearization of the system around an operating point.

- **The Extended Kalman Filter** The Kalman filter, designed initially for stochastic linear systems, the *EKF* extended filter consists of using the standard Kalman filter equations on the nonlinear model after linearization around an operating point [BA99]. Despite the proofs of stability and convergence established in the case of linear systems cannot be extended generally to the case of nonlinear systems, but this method remains the most popular and widely studied in the field of observation of non-linear systems [SG92].
- **Luenberger's observer extended** This type of observer intervenes, either at the level of the original system with a constant gain which must calculate by placing poles, or through a change of coordinates with a gain depending on the state to be estimated [Zer11]. This type of observer, can cause instabilities which appear while moving away from the point of operation, it is for that, it is seldom used in the practice.

3.1.1.2 Observers in canonical form

These techniques are based on the change of the coordinates in order to use the non-linear transformation by the Lie method, the new system is written in a quasi-linear canonical form [BEN]. The advantage of these approaches is that after the transformation, the synthesis of the observer is simple, but the problem lies in the characterization of the system having a observability canonical form requested [KI83], [LB01].

3.1.1.3 High-gain observers (*Lipschitz Observer*):

Are observers based on the Lyapunov stability conditions, The first works of this type of observers are carried out by [Tha73]. This type of observer is used in general for systems of Lipschitz form, its name (*High-gain*) is due to the fact that the gain of the observer is large enough to compensate for the non-linearity of the system, The major problem of this technique lies in the sensitivity to measurement noise when the gains obtained are high.

3.1.1.4 Generalized Luenberger observers

The generalized Luenberger observer was proposed by [AK01], the idea of this technique is to add a second gain inside the non-linear part of the system to the gain of the Luenberger observer. an extension of the technique (*GLO*) to the case of monotonic multi-variable systems has been proposed by [FA03]. The disadvantage of *GLO* is that it is applicable to systems where the Jacobian of each component of the non-linear function is a square matrix.

3.1.1.5 Observers based on contraction theory

This observation technique was introduced in [LS98] it is based on contraction theory as a tool for analysing the convergence between the observer and the model [Zem07]

3.2 Takagi-Sugeno multi-model State Observer

Let's consider the following Takagi-Sugeno (T-S) fuzzy model, where the output is a linear function of the state:

$$\begin{cases} \dot{x}(t) = \sum_{i=1}^r h_i(\xi(t))(A_i x(t) + B_i u(t)) \\ y(t) = Cx(t) \end{cases} \quad (3.3)$$

Most observers designed for the T-S fuzzy model extend the Luenberger observer proposed for linear systems [Dav71]. This extension is described by the following equations:

$$\begin{cases} \dot{\hat{x}}(t) = \sum_{i=1}^r h_i(\hat{\xi}(t))(A_i \hat{x}(t) + B_i u(t) + L_i(y(t) - \hat{y}(t))) \\ \hat{y}(t) = C\hat{x}(t) \end{cases} \quad (3.4)$$

Here, $\hat{x}(t)$ and $\hat{\xi}$ are the estimated state and the estimated decision variables $\xi(t)$, respectively. The observer synthesis problem (3.4) involves finding the constant gains L_i that ensure asymptotic convergence of the estimation error to zero. This task involves examining the stability of the system that generates the state estimation error, defined as:

$$e(t) = x(t) - \hat{x}(t) \quad (3.5)$$

The estimation error (3.5), is a system of equations dependent on the premise variables $\xi(t)$. These variables may be measurable or non-measurable.

3.2.1 Measurable premise variables (MPV)

Most work on state observer synthesis for systems described by the T-S representation assumes that premise variables are measurable, i.e., $\hat{\xi}(t) = \xi(t)$. This implies that the observer shares the same premise variables as the system model, allowing for factorization by activation functions when evaluating the error dynamics estimate (3.5), which can be written as [Akh04, Nag10]:

$$\dot{e}(t) = \sum_{i=1}^r h_i(\xi(t))(A_i - L_i C)e(t) \quad (3.6)$$

Determining the L_i gains of the observer requires a system stability analysis (3.6), through which we obtain the LMI's conditions by introducing a quadratic function of the form $V(x(t)) = x^T(t)Px(t)$.

Theorem 3.2.1:

The state estimation error asymptotically converges to zero if there exists a matrix $P = P^T > 0 \in \mathbb{R}^{n \times n}$ and matrices $K_i \in \mathbb{R}^{n \times m}$, such that the following conditions hold [PCLT98]:

$$PA_i + A_i^T P - K_i C - C^T K_i^T < 0 \quad i = 1, \dots, r \quad (3.7)$$

The observer gains can be obtained from the equation:

$$L_i = P^{-1} K_i \quad (3.8)$$

Several studies have focused on improving observer performance, using non-quadratic Lyapunov functions to study system stability [Kru07, THW03], and designing an observer with unknown inputs [ACR⁺06, IMRM09, ACMR04, ALA20].

3.2.2 Non-measurable premise variables (NMPV)

Most real-world processes are inherently non-linear and involve non-measurable premise variables. There are works in the literature that address these situations, such as [IMRM10], [BPD01], and [NKMM⁺10].

Actual processes are generally non-linear in nature with non-measurable premise variables. In the literature, there may be works that discuss this type of situation, we cite here: [IMRM10],[BPD01] and [NKMM⁺10]. In [BP00] the Thau-Luenberger approach is proposed taking into account state estimation convergence conditions towards zero. The estimation error dynamic (3.6) is then written in the form [Ich09, Akh04, Nag10]:

$$\dot{e}(t) = \sum_{i=1}^r h_i(\xi(t))(A_i x(t) + B_i u(t)) - \sum_{i=1}^r h_i(\hat{\xi}(t))(A_i \hat{x}(t) + B_i u(t) + L_i C e(t)) \quad (3.9)$$

Theorem 3.2.2:

The state estimation error between the TS model and the observer converges asymptotically to zero, if there are symmetric and positive definite matrices $P, Q \in \mathbb{R}^{n \times n}$ and matrices $K_i \in \mathbb{R}^{n \times m}$ as well as a positive scalar γ such that:

$$PA_i + A_i^T P - K_i C - C^T K_i^T < Q \quad i = 1, \dots, r \quad (3.10)$$

$$\begin{bmatrix} -Q + \gamma^2 I & P \\ P & -I \end{bmatrix} < 0 \quad (3.11)$$

The proof of this result can be found in Bergsten et al. [BPD01].

3.3 Structure of state multi gain observer based on the Lipschitz approach

The main interest of this type of observers is its robustness with respect to modeling uncertainties. the multi-observer expression is presented in following equation [IMRM07]:

$$\begin{cases} \dot{\hat{x}}(t) = \sum_{i=1}^r h_i(\hat{\xi}(t))(A_i \hat{x}(t) + B_i u(t) + L_i(y(t) - \hat{y}(t))) \\ \hat{y}(t) = C \hat{x}(t) \end{cases} \quad (3.12)$$

Stability conditions

The state estimation error is written as follows:

$$e = x(t) - \hat{x}(t) \quad (3.13)$$

The dynamics of this error is obtained using the equations (2.18), (2.19) et (3.13) :

$$\dot{e}(t) = \sum_{i=1}^r (A_i(h_i(x(t))x(t) - h_i(\hat{x}(t))\hat{x}(t)) + B_i(h_i(x(t)) - h_i(\hat{x}(t)))u - h_i(\hat{x}(t))L_i C(x(t) - \hat{x}(t))) \quad (3.14)$$

If we add and subtract from the right-hand side of equation (3.14) the term $A_i h_i(\hat{x}(t))e(t)$, we obtain:

$$\dot{e}(t) = \sum_{i=1}^r (A_i \delta_i + B_i \Delta_i + h_i(\hat{x}(t))\bar{A}_i e(t)) \quad (3.15)$$

where:

$$\begin{cases} \delta_i = (h_i(x(t)) - h_i(\hat{x}(t)))x(t) \\ \Delta_i = (h_i(x(t)) - h_i(\hat{x}(t)))u(t) \\ \bar{A}_i = A_i - L_i C \end{cases} \quad (3.16)$$

We take into consideration the following Lyapunov function to show the asymptotic convergence of the state estimation error:

$$V(e(t)) = e(t)^T P e(t) \quad (3.17)$$

Where the derivative of the Lyapunov function is given by:

$$\dot{V}(e(t)) = \dot{e}^T(t)Pe(t) + e(t)^T P\dot{e}(t) \quad (3.18)$$

by the substituting equation (3.15) into equation (3.18), we find:

$$\begin{aligned} \dot{V}(e(t)) = & \sum_{i=1}^r (\delta_i^T A_i^T Pe(t) + e^T(t)PA_i\delta_i + \Delta_i^T B_i^T Pe(t) + e^T(t)PB_i\Delta_i \\ & + h_i(\hat{x}(t))(e^T(t)\bar{A}_i^T Pe(t) + e^T(t)P\bar{A}_i e(t)) \end{aligned} \quad (3.19)$$

Assumptions

In this work, we consider that:

1. The activation functions are Lipschitzian, so:

$$|h_i(x(t)) - h_i(\hat{x}(t))| \leq M_i|x(t) - \hat{x}(t)| \quad (3.20)$$

where M_i is a positive scalar representing the Lipschitz constant.

2. The system's input signal $u(t)$ and state $x(t)$ are both bounded.

$$\begin{cases} \|x(t)\| \leq B_1 \\ \|u(t)\| \leq B_2 \end{cases} \quad (3.21)$$

with B_1 and B_2 positive scalars.

Given the definition (3.16) and assumptions 3.2 and 3.3, we then have:

$$\begin{cases} |\delta_i| \leq M_i\beta_1|e(t)| \\ |\Delta_i| \leq M_i\beta_2|e(t)| \end{cases} \quad (3.22)$$

Then:

$$\begin{aligned} \delta_i^T A_i^T Pe(t) + e^T(t)PA_i\delta_i & \leq \delta_i^T \delta_i + e^T(t)PA_iA_i^T Pe(t) \\ & \leq M_i^2\beta_1^2 e^T(t)e(t) + e^T(t)PA_iA_i^T Pe(t) \end{aligned} \quad (3.23)$$

$$\begin{aligned} \Delta_i^T B_i^T Pe(t) + e^T(t)PB_i\Delta_i & \leq \Delta_i^T \Delta_i + e^T(t)PB_iB_i^T Pe(t) \\ & \leq M_i^2\beta_2^2 e^T(t)e(t) + e^T(t)PB_iB_i^T Pe(t) \end{aligned} \quad (3.24)$$

Using these upper bounds, the derivative of the function of Lyapunov (3.25) obeys the inequality:

$$\dot{V}(e(t)) \leq \sum_{i=1}^r e^T(t)(h_i(\hat{x}(t))(\bar{A}_i^T P + p\bar{A}_i) + M_i^2(\beta_1^2 + \beta_2^2)I$$

$$+ PA_i A_i^T P + PB_i B_i^T P)e(t) \quad (3.25)$$

The negativity of the derivative of the Lyapunov function is therefore ensured if [IMRM07]:

$$h_i(\hat{x})(\bar{A}_i^T P + P\bar{A}_i) + M_i^T(\beta_1^2 + \beta_2^2)I - PA_i A_i^T P + PB_i B_i^T P < 0 \quad (3.26)$$

We can consider that the terms $A_i\delta_i + B_i\Delta_i$ of the equation (3.15) constitute a disturbance. The study of the convergence of the state estimation error is therefore reduced to the study of the stability of a disturbed system.

Suppose that for a symmetric matrix Q , there exists a symmetric positive definite matrix P such that:

$$h_i(\hat{x})(\bar{A}_i^T P + P\bar{A}_i) < Q \quad (3.27)$$

This inequality leads to:

$$(A_i - L_i C)^T P + P(A_i - L_i C) < Q \quad (3.28)$$

By transferring the inequality (3.28) into (3.26) we obtain:

$$Q + M_i^2(\beta_1^2 + \beta_2^2)I + PA_i A_i^T P + PB_i B_i^T P < 0 \quad (3.29)$$

Note that the matrix inequalities (3.28) and (3.29) are nonlinear with respect to P and L_i . However, if we pose the change of variable:

$$K_i = PL_i \quad (3.30)$$

and if we use Schur's complement, we get:

$$A_i^T P - PA_i - C^T K_i^T - K_i C < -Q \quad (3.31)$$

$$\begin{bmatrix} -Q + \theta_i I & PA_i & B_i \\ A_i^T P & -I & 0 \\ B_i^T P & 0 & -I \end{bmatrix} < O \quad (3.32)$$

$$\theta_i = M_i^2(\beta_1^2 + \beta_2^2)$$

Thus (3.31) and (3.32) are LMIs with respect to P and L_i .

Calculation of the Lipschitz constant

The Lipschitz constant involved in equation (3.20) is calculated using expansions of $\mu_i(x(t))$ in the Taylor series with residue integral to order 0 in the vicinity of $\hat{x}(t)$:

$$\begin{aligned}
 \mu_i(x) &= \mu_i(\hat{x}) + \int_{\hat{x}}^x \dot{\mu}_i(t) dt \\
 \mu_i(x) - \mu_i(\hat{x}) &= \int_{\hat{x}}^x \dot{\mu}_i(t) dt \\
 |\mu_i(x) - \mu_i(\hat{x})| &\leq \left| \int_{\hat{x}}^x \dot{\mu}_i(t) dt \right| \\
 &\leq \int_{\hat{x}}^x |\dot{\mu}_i(t)| dt \\
 &\leq M_i |x - \hat{x}|
 \end{aligned} \tag{3.33}$$

Since we are going to choose Lipschitz activation functions (continuous and differentiable), it suffices to study the extrema of the function $\dot{\mu}_i(x(t))$ to find the value of M_i .

3.4 State and unknown input observer

State estimation in the presence of disturbances, unknown inputs, and noise is a challenging task in control systems. Convergence of the state estimation error to zero cannot be guaranteed under these conditions. To address these challenges, a robust state and unknown inputs observer can be employed. This observer incorporates both proportional and integral actions, providing an additional degree of freedom in the synthesis process. By using the \mathcal{L}_2 norm, the observer can quantify and minimize the impact of disturbances and noise on the estimation process. This enhances the accuracy and robustness of state estimation, making it a promising solution for practical control and diagnosis system applications.

3.4.1 Structure of robust proportional integral (PI) observer

Consider the following T-S fuzzy system with weighting functions μ_i depending on the state of the system:

$$\begin{cases} \dot{x}(t) = \sum_{i=1}^r h_i(x(t))(A_i x(t) + B_i u(t) + E_i \delta(t) + W_i \omega(t)) \\ y(t) = Cx(t) + G\delta(t) + W\omega(t) \end{cases} \tag{3.34}$$

Where $A_i \in \mathfrak{R}^{n \times n_x}$, $B_i \in \mathfrak{R}^{n \times n_u}$, $E_i \in \mathfrak{R}^{n \times n_\delta}$, are the state, input, and the influence matrices respectively, $W_i \in \mathfrak{R}^{n \times n_\omega}$ is the influence matrices of the noises $\omega(t)$ affecting the states and measurement, $C \in \mathfrak{R}^{n_y \times n}$ is the output matrix. The proposed observer can estimate the states and unknown inputs simultaneously of the global T-S fuzzy system (3.34)[IMRM09].

The \mathcal{L}_2 norm approach

State estimation in control systems typically relies on a mathematical model of the system dynamics and measurements collected from the system. However, it is common for the system model to be imperfect, and disturbances may not be accurately accounted for in the model. As a result, the convergence of the state estimation error to zero cannot be guaranteed.

To address this challenge, the \mathcal{L}_2 norm, which is a direct extension of the H_∞ norm [Wei12, VDS92], has been employed to evaluate the performance of state estimation algorithms. The \mathcal{L}_2 norm provides a measure of the energy or power of a signal. In the context of state estimation, it quantifies the energy of the estimation error, which represents the discrepancy between the true state and the estimated state. One advantage of using the \mathcal{L}_2 norm is its ability to handle systems with time-varying parameters. In such cases, where the system parameters change over time, the \mathcal{L}_2 norm allows for the evaluation of the estimation error and the determination of an upper bound on the gain between the energy of the input and the energy of the output. This upper bound holds true for all admissible parametric trajectories of the system [Bar01, Nag10].

The \mathcal{L}_2 norm approach provides a rigorous framework for quantifying the performance of state estimation algorithms, even in the presence of modeling uncertainties, perturbation, and unmodeled disturbances.

Definition 5 (*The \mathcal{L}_2 norm of signal*). The \mathcal{L}_2 norm of a square integrable signal $s(t)$ is denoted and defined by:

$$\|s(t)\|_2 = \left(\int_0^{+\infty} s(t)^T s(t) dt \right)^{1/2} \quad (3.35)$$

Definition 6 (*the induced \mathcal{L}_2 norm of a system*). The induced \mathcal{L}_2 norm of a system is defined by:

$$\sup_{\|w(t)\|_2^2 \neq 0} \frac{\|y(t)\|_2^2}{\|u(t)\|_2^2}, \quad (3.36)$$

where $u(t)$ and $y(t)$ are respectively the input and output signals with bounded energy, within the meaning of the $\|\cdot\|_2$ norm of the considered system. This norm is a measure of the greater rate of energy amplification of $u(t)$ over $y(t)$.

Assumptions

In this work, we consider that:

- The non linear system is stable, and the pair (A_i, C) , (\bar{A}_i, \bar{C}) are observable.
- The signals $u(t)$, $\delta(t)$, and $\omega(t)$ are bounded.
- The unknown inputs $\delta(t)$ are assumed to be constant.

The considered observer is given by [IMRM09]:

$$\begin{cases} \dot{\hat{x}}(t) = \sum_{i=1}^r h_i(\hat{x}(t))(A_i\hat{x}(t) + B_iu(t) + E_i\hat{\delta}(t) + L_{Pi}(y(t) - \hat{y}(t))) \\ \hat{y}(t) = C\hat{x}(t) + G\hat{\delta}(t) \\ \dot{\hat{\delta}}(t) = \sum_{i=1}^r h_i(\hat{x}(t))L_{Ii}(y(t) - \hat{y}(t)) \end{cases} \quad (3.37)$$

Where $L_{Pi} \in \mathfrak{R}^{n_x \times n_y}$, and $L_{Ii} \in \mathfrak{R}^{n_\delta \times n_y}$ are the proportional and integral gains respectively. $\hat{x}(t)$, and $\hat{\delta}(t)$ represent the states and the unknown inputs estimation.

The TS multi-model (3.34) can be rewritten as a perturbed system in the following form [IMRM09]:

$$\dot{x}(t) = \sum_{i=1}^r h_i(\hat{x}(t))(A_i x(t) + B_i u(t) + E_i \delta(t) + W_i \omega(t) + v(t)) \quad (3.38)$$

where:

$$v(t) = \sum_{i=1}^r (h_i(x(t)) - h_i(\hat{x}(t)))(A_i x(t) + B_i u(t) + E_i \delta(t) + W_i \omega(t)) \quad (3.39)$$

Based on the convex sum property and the above assumptions, the term $v(t)$ is bounded and

$$\mathbf{IF} \hat{x}(t) \rightarrow x(t), \quad \mathbf{THEN} v(t) \rightarrow 0.$$

The TS multi-model (3.38) and the proposed PIO (3.37) can be written under the following augmented forms [IMRM09]:

$$\begin{cases} \dot{x}_a(t) = \sum_{i=1}^r h_i(\hat{x}(t))(\bar{A}_i x_a(t) + \bar{B}_i u(t) + \bar{\Gamma}_i \bar{\omega}(t)) \\ y(t) = \bar{C} x_a(t) + \bar{D} \bar{\omega}(t) \end{cases} \quad (3.40)$$

and

$$\begin{cases} \dot{\hat{x}}_a(t) = \sum_{i=1}^r h_i(\hat{x}(t))(\bar{A}_i \hat{x}_a(t) + \bar{B}_i u(t) + \bar{L}_i(y(t) - \hat{y}(t))) \\ \hat{y}(t) = \bar{C} \hat{x}_a(t) \end{cases} \quad (3.41)$$

where:

$$x_a(t) = \begin{bmatrix} x(t) \\ \delta(t) \end{bmatrix}, \quad \bar{\omega}(t) = \begin{bmatrix} v(t) \\ \omega(t) \end{bmatrix}.$$

with

$$\bar{A}_i = \begin{bmatrix} A_i & E_i \\ 0 & 0 \end{bmatrix}, \quad \bar{B}_i = \begin{bmatrix} B_i \\ 0 \end{bmatrix}, \quad \bar{C} = [C \ G], \quad \bar{D} = [0 \ W], \quad \bar{\Gamma}_i = \begin{bmatrix} I & W_i \\ 0 & 0 \end{bmatrix}.$$

and

$$\bar{L}_i = \begin{bmatrix} L_{Pi} \\ L_{Ii} \end{bmatrix}.$$

Let us consider the state estimation error of the augmented system:

$$e_a(t) = x_a(t) - \hat{x}_a(t) \quad (3.42)$$

The dynamics of error $e_a(t)$ is represented by:

$$\dot{e}_a(t) = \sum_{i=1}^r h_i(\hat{x}(t))((\bar{A}_i - \bar{L}_i \bar{C})e_a(t) + (\bar{\Gamma}_i - \bar{L}_i \bar{D})\bar{\omega}(t)) \quad (3.43)$$

Based on the above assumptions, the gain matrices \bar{L}_i of the proposed observer are determined in order to guarantee the stability of the augmented system even if $\bar{\omega}(t)$ different from zero.

Lemma 1:[IMRM09] Consider the TS multi-model defined by:

$$\begin{cases} \dot{x}(t) = \sum_{i=1}^r h_i(\xi(x(t)))(A_i x(t) + B_i u(t)) \\ y(t) = Cx(t) \end{cases} \quad (3.44)$$

The fuzzy system described by (3.44) is stable and guarantee the \mathcal{L}_2 -gain condition $\frac{\|y(t)\|_2}{\|u(t)\|_2} < \gamma$, if there exists a common positive definite matrix P such that

$$\begin{bmatrix} A_i^T P + P A_i + C^T C & P B_i \\ B_i^T P & -\gamma^2 I \end{bmatrix} < 0 \quad (3.45)$$

Theorem 3.4.1:

The PIO (3.41), estimating the unknown inputs and state of the fuzzy system (3.40) with minimizing the \mathcal{L}_2 -gain $\bar{\gamma}$ of the unknown inputs on the augmented state estimation error e_a , is obtained by finding a common positive definite matrix P , matrices M_i and a positive scalars $\bar{\gamma}$ such that for $i = 1, \dots, r$:

$$\begin{bmatrix} \bar{A}_i^T P + P \bar{A}_i - M_i \bar{C} - \bar{C}^T M_i^T + I & P \bar{\Gamma}_i - M_i \bar{D} \\ \bar{\Gamma}_i^T P - \bar{D}^T M_i^T & -\bar{\gamma} I \end{bmatrix} < 0 \quad (3.46)$$

where $\gamma = \sqrt{\bar{\gamma}}$.

The observer gains (3.41) are given by:

$$\bar{L}_i = P^{-1} M_i \quad (3.47)$$

Proof:

The PIO estimates the states and unknown input if:

$$\lim_{t \rightarrow \infty} e(t) = 0 \quad (3.48)$$

where: $e(t) = x_a(t) - \hat{x}_a(t)$

To study the convergence of the state estimation error, we consider the following quadratic Lyapunov function:

$$V(t) = e^T(t) P e(t); \quad (3.49)$$

where P is symmetric positive definite matrix ($P = P^T > 0$).

The augmented state estimation error converges asymptotically towards zero if:

$$V(t) > 0 \quad \text{and} \quad \dot{V}(t) < 0$$

The derivative of the Lyapunov function along the trajectory of (17) is given by:

$$\dot{V}(t) = \dot{e}^T(t) P e(t) + e^T(t) P \dot{e}(t) \quad (3.50)$$

by the substituting equation (3.43) into equation (3.50), we find:

$$\dot{V}(t) = e^T(t) (\bar{A}_i^T - \bar{C}^T \bar{L}_i^T) P e(t) + \bar{w}^T(t) (\bar{\Gamma}_i^T - \bar{D}^T \bar{L}_i^T) P e(t)$$

$$+ e^T(t)P((\bar{A}_i^T - \bar{L}_i\bar{C})e(t)) + e^T(t)P((\bar{\Gamma}_i^T - \bar{L}_i\bar{D})\bar{w}(t)) \quad (3.51)$$

$$\begin{aligned} \dot{V}(t) = & e^T(t)((\bar{A}_i^T - \bar{C}^T\bar{L}_i^T)P + P(\bar{A}_i^T - \bar{L}_i\bar{C}_i))e(t) + \bar{w}^T(t)(\bar{\Gamma}_i^T - \bar{D}^T\bar{L}_i^T)Pe(t) \\ & + e^T(t)P((\bar{\Gamma}_i^T - \bar{L}_i\bar{D})\bar{w}(t)) \end{aligned} \quad (3.52)$$

According to the above assumptions $\bar{w}(t)$ is bounded, and based on lemma1:

$$\| e_a(t) \|_2 < \gamma \| \bar{w}(t) \|_2$$

$$\begin{aligned} \dot{V}(t) - \gamma^2\bar{w}^T\bar{w} = & e^T(t)((\bar{A}_i^T - \bar{C}^T\bar{L}_i^T)P + P(\bar{A}_i^T - \bar{L}_i\bar{C}_i))e(t) \\ & + \bar{w}^T(t)(\bar{\Gamma}_i^T - \bar{D}^T\bar{L}_i^T)Pe(t) + e^T(t)P((\bar{\Gamma}_i^T - \bar{L}_i\bar{D})\bar{w}(t)) - \gamma^2\bar{w}^T\bar{w} \end{aligned} \quad (3.53)$$

$$\dot{V}(t) - \gamma^2\bar{w}^T\bar{w} = \begin{bmatrix} e \\ \bar{w} \end{bmatrix}^T \begin{bmatrix} \bar{A}_i^T P + P\bar{A}_i - P\bar{L}_i\bar{C} - \bar{C}^T\bar{L}_i^T P + I & P\bar{\Gamma}_i - P\bar{L}_i\bar{D} \\ \bar{\Gamma}_i^T P - \bar{D}^T\bar{L}_i^T P & -\gamma^2 I \end{bmatrix} \begin{bmatrix} e \\ \bar{w} \end{bmatrix} \quad (3.54)$$

Then, we obtain:

$$\begin{bmatrix} \bar{A}_i^T P + P\bar{A}_i - P\bar{L}_i\bar{C} - \bar{C}^T\bar{L}_i^T P + I & P\bar{\Gamma}_i - P\bar{L}_i\bar{D} \\ \bar{\Gamma}_i^T P - \bar{D}^T\bar{L}_i^T P & -\gamma^2 I \end{bmatrix} < 0 \quad (3.55)$$

Using the following changes:

$$\bar{\gamma} = \gamma^2, M_i = P\bar{L}_i.$$

The linear matrix inequalities formulation in theorem 1 are obtained.

Remark: The minimization of \mathcal{L}_2 -gain affect the dynamics of unknown inputs and state estimation error. we can solve this problem with the pole assignment approach.

$$\{z \mid Re(z) < -\lambda\}, \quad \lambda > 0 \quad (3.56)$$

In order to impose $Re(\lambda_i) < -\lambda$ where λ_i are the eigenvalues of \bar{A}_i and $\lambda > 0$, the following constraint is added to the LMI in theorem 1.

$$P(\bar{A}_i + \lambda I) + (\bar{A}_i + \lambda I)^T P - M_i\bar{C} - \bar{C}^T M_i^T < 0 \quad (3.57)$$

This approach remains effective in practical cases where assumption 1 is not satisfied. However, it is important to note that the effectiveness of this method relies on the assumption that the unknown inputs vary slowly. If the unknown inputs change rapidly, the state and unknown inputs estimation using this method may be inaccurate.

In the next section, an alternative method for state and unknown inputs estimation is introduced. This method utilizes the proportional multiple integral observer. One of the key advantages of this observer is that it does not rely on assumption 3 in its theoretical proof. As a result, it becomes possible to estimate a larger class of unknown inputs. This makes the proportional multiple integral observer an interesting and valuable approach for state and unknown inputs estimation in a variety of scenarios.

3.4.2 Structure of the proportional multi integral (PMI) observer

In this section, we relax the working assumption 3, which assumes that the unknown inputs $d(t)$ are constant. Instead, we consider a more general class of signals that includes unknown inputs in polynomial form. It is important to note that the estimation quality of the state and unknown inputs using a proportional integral (PI) observer, as discussed in the previous section, may degrade when the unknown inputs undergo rapid variations.

The main objective of this section is to present a method that enables the simultaneous estimation of the system's state and the unknown inputs, even when assumption 3 is not satisfied. By considering a broader range of unknown input variations, we aim to address the limitations of the PI observer and enhance the accuracy of the estimation process.

Let us consider the multiple model with unmeasurable premise variables described in (3.34). The unknown input is assumed to be a bounded time varying signal with null q^{th} derivative:

Assumptions

In this work, we consider that:

- The non linear system is stable, and the pair (A_i, C) , (\tilde{A}_i, \tilde{C}) are observable.
- The signals $u(t)$, $\delta(t)$, and $\omega(t)$ are bounded.

- The unknown inputs $\delta(t)$ are assumed to be a bounded time varying signal with null q^{th} derivative $d^{(q)}(t) = 0$.

Generally, the application of a proportional integral (PI) observer assumes that the unknown input is constant (i.e., $\dot{d} = 0$). As a result, the estimation of unknown inputs that satisfy condition $d^{(q)}(t) = 0$ cannot be achieved with high precision using a PI observer. In such cases, the proportional multiple integral (PMI) observer is more suitable as it allows for the estimation of the $(q - 1)^{th}$ derivatives of the unknown input, resulting in improved precision of the estimated unknown inputs.

In a diagnostic framework, condition $d^{(q)}(t) = 0$ therefore makes it possible to take into consideration a large class of faults affecting the system: step, ramp, etc. In general, $d^{(1)}(t), d^{(2)}(t), \dots, d^{(q-1)}(t)$ represent the successive derivatives of $d(t)$ which we will define in the form of following state:

$$\begin{bmatrix} \dot{d}(t) \\ \dot{d}_1(t) \\ \vdots \\ \dot{d}_{q-1}(t) \end{bmatrix} = \begin{bmatrix} d_1(t) \\ d_2(t) \\ \vdots \\ d_q(t) \end{bmatrix} \quad (3.58)$$

In this section, we consider the generalization of the PMI observer to Takagi-Sugeno (T-S) systems. The PMI observer for linear descriptor systems, proposed in [IMRM09], serves as the basis for extending its application to T-S systems. By incorporating the PMI observer into the T-S framework, we aim to enhance the estimation accuracy of unknown inputs that do not satisfy condition $d^{(q)}(t) = 0$.

The considered general observer is given by [IMRM09]:

$$\left\{ \begin{array}{l} \dot{\hat{x}}(t) = \sum_{i=1}^r h_i(\hat{x}(t))(A_i \hat{x}(t) + B_i u(t) + E_i \hat{\delta}_0(t) + L_{P_i}(y(t) - \hat{y}(t))) \\ \hat{y}(t) = C \hat{x}(t) + G \hat{\delta}(t) \\ \dot{\hat{\delta}}_0(t) = \sum_{i=1}^r h_i(\hat{x}(t)) L_{I_i}^0 (y(t) - \hat{y}(t)) + \hat{\delta}_1(t) \\ \dot{\hat{\delta}}_1(t) = \sum_{i=1}^r h_i(\hat{x}(t)) L_{I_i}^1 (y(t) - \hat{y}(t)) + \hat{\delta}_2(t) \\ \vdots \\ \dot{\hat{\delta}}_{q-2}(t) = \sum_{i=1}^r h_i(\hat{x}(t)) L_{I_i}^{q-2} (y(t) - \hat{y}(t)) + \hat{\delta}_{q-1}(t) \\ \dot{\hat{\delta}}_{q-1}(t) = \sum_{i=1}^r h_i(\hat{x}(t)) L_{I_i}^{q-1} (y(t) - \hat{y}(t)) \end{array} \right. \quad (3.59)$$

where $\hat{\delta}_i, i = 1, 2, \dots, (q-1)$ are the estimation of the $(q-1)$ first derivatives of the unknown input $d(t)$.

The TS fuzzy model (3.38) and the proposed PMI (3.59) can be written under the following augmented forms [IMRM09]:

$$\left\{ \begin{array}{l} \dot{x}_a(t) = \sum_{i=1}^r h_i(\hat{x}(t)) (\tilde{A}_i x_a(t) + \tilde{B}_i u(t) + \tilde{\Gamma}_i \tilde{\omega}(t)) \\ y(t) = \tilde{C} x_a(t) + \tilde{D} \tilde{\omega}(t) \end{array} \right. \quad (3.60)$$

and

$$\left\{ \begin{array}{l} \dot{\hat{x}}_a(t) = \sum_{i=1}^r h_i(\hat{x}(t)) (\tilde{A}_i \hat{x}_a(t) + \tilde{B}_i u(t) + \tilde{L}_i (y(t) - \hat{y}(t))) \\ \hat{y}(t) = \tilde{C} \hat{x}_a(t) \end{array} \right. \quad (3.61)$$

where:

$$x_a(t) = \begin{bmatrix} x(t) \\ \delta(t) \\ \delta_1(t) \\ \vdots \\ \delta_q(t) \end{bmatrix}, \quad \tilde{\omega}(t) = \begin{bmatrix} v(t)^T \\ \omega(t)^T \\ \delta^q(t)^T \end{bmatrix}.$$

with

$$\tilde{A}_i = \begin{bmatrix} A_i & E_i & 0 & \dots & 0 & 0 \\ 0 & 0 & I_s & \dots & 0 & 0 \\ 0 & 0 & 0 & \ddots & 0 & 0 \\ \vdots & \vdots & \vdots & \vdots & \vdots & \vdots \\ 0 & 0 & 0 & \dots & 0 & I_s \\ 0 & 0 & 0 & \dots & 0 & 0 \end{bmatrix}, \quad \tilde{B}_i = \begin{bmatrix} B_i \\ 0 \\ \vdots \\ 0 \end{bmatrix}, \quad \tilde{\Gamma}_i = \begin{bmatrix} \Gamma_i^T \\ 0 \\ \vdots \\ 0 \end{bmatrix}, \quad \tilde{C} = [C \ G \ 0 \ \dots \ 0 \ 0].$$

where 0 represents null matrix with appropriate dimensions.

and \tilde{L}_i is:

$$\tilde{L}_i = \begin{bmatrix} L_{P_i} \\ L_{I_i}^0 \\ L_{I_i}^1 \\ \vdots \\ L_{I_i}^{q-2} \\ L_{I_i}^{q-1} \end{bmatrix}.$$

The state estimation error of the augmented system presented as follow:

$$e(t) = x(t) - \hat{x}(t), e_0(t) = \delta(t) - \hat{\delta}_0(t), \dots, e_{q-1}(t) = \dot{\delta}_{q-1}(t) - \hat{\delta}_{q-1}(t) \quad (3.62)$$

The dynamics of error $e_a(t)$ is represented by:

$$\left\{ \begin{array}{l} \dot{e}(t) = \sum_{i=1}^r h_i(\hat{x}(t))((A_i - L_{P_i}C)e(t) + (\Gamma_i - L_{P_i}\bar{W})\tilde{\omega}(t) + (E_i - L_{P_i}G)e_0(t)) \\ \dot{e}_0(t) = \sum_{i=1}^r h_i(\hat{x}(t))(-L_{I_i}^0Ce(t) + e_1(t) - L_{I_i}^0\bar{W}\tilde{\omega}(t) - L_{I_i}^0Ge_0(t)) \\ \dot{e}_1(t) = \sum_{i=1}^r h_i(\hat{x}(t))(-L_{I_i}^1Ce(t) + e_2(t) - L_{I_i}^1\bar{W}\tilde{\omega}(t) - L_{I_i}^1Ge_0(t)) \\ \vdots \\ \dot{e}_{q-2}(t) = \sum_{i=1}^r h_i(\hat{x}(t))(-L_{I_i}^{q-2}Ce(t) + e_{q-1}(t) - L_{I_i}^{q-2}\bar{W}\tilde{\omega}(t) - L_{I_i}^{q-2}Ge_0(t)) \\ \dot{e}_{q-1}(t) = \sum_{i=1}^r h_i(\hat{x}(t))(-L_{I_i}^{q-1}Ce(t) - L_{I_i}^0\bar{W}\tilde{\omega}(t) - L_{I_i}^{q-1}Ge_0(t)) \end{array} \right. \quad (3.63)$$

where:

$$\Gamma_i = \begin{bmatrix} I_n & W_i \end{bmatrix}, \quad \bar{W} = \begin{bmatrix} 0 & W \end{bmatrix},$$

The dynamics of error $e_a(t)$ is of the equation 3.63 can be represented as follow:

$$\dot{\tilde{e}}_a(t) = \sum_{i=1}^r h_i(\hat{x}(t))((\tilde{A}_i - \tilde{L}_i\tilde{C})e_a(t) + (\tilde{\Gamma}_i - \tilde{L}_i\bar{W})\tilde{\omega}(t)) \quad (3.64)$$

where:

$$\tilde{e}_a = \begin{bmatrix} e \\ e_0 \\ e_1 \\ \vdots \\ e_{q-2} \\ e_{q-1} \end{bmatrix}$$

Theorem 3.4.2:

The Proportional Multi Integral (PMI) Observer (3.61), designed to estimate the state and unknown inputs Simultaneously of the fuzzy system (3.60) while minimizing the \mathcal{L}_2 -gain $\bar{\gamma}$ of the unknown inputs on the augmented state estimation error e_a , can be obtained by determining a positive definite matrix P , matrices M_i , and positive scalar $\bar{\gamma}$ that satisfy the following conditions for $i = 1, \dots, r$:

$$\begin{bmatrix} \tilde{A}_i^T P + P \tilde{A}_i - M_i \tilde{C} - \tilde{C}^T M_i^T + \tilde{C}^T \tilde{C} & P \tilde{\Gamma}_i - M_i \tilde{W} \\ \tilde{\Gamma}_i^T P - \tilde{W}^T M_i^T & -\bar{\gamma} I \end{bmatrix} < 0 \quad (3.65)$$

The gains of the observer are derived from:

$$M_i = P \tilde{L}_i$$

and the attenuation level is calculated by:

$$\gamma = \sqrt{\bar{\gamma}}$$

Theorem 3.4.2 presents the conditions for designing the Proportional Multi Integral (PMI) Observer, which aims to estimate the unknown inputs and state of the fuzzy system while minimizing the \mathcal{L}_2 -gain $\bar{\gamma}$ of the unknown inputs on the augmented state estimation error \tilde{e}_a . By finding appropriate values for the positive definite matrix P , matrices M_i , and positive scalar $\bar{\gamma}$, the PMI Observer can be effectively designed to achieve accurate estimation results.

The inequality (3.65) represents the key stability and performance conditions for the PMI Observer. It ensures that the augmented state estimation error remains bounded, while minimizing the \mathcal{L}_2 -gain of the unknown inputs. By satisfying these conditions, the PMI Observer demonstrates its capability to provide robust and accurate estimation of the unknown inputs and state of the fuzzy system.

3.5 Conclusion

In conclusion, this chapter explores various observer techniques for state estimation in nonlinear systems. It highlights the state-of-the-art approaches to observability and discusses specific observer methods, such as the Takagi-Sugeno multi-model observer and

the state multi-gain observer based on the Lipschitz approach. Additionally, the chapter introduces the state and unknown input observer, which offers improved estimation accuracy and robustness. By incorporating proportional and integral actions, these observers provide valuable tools for state estimation in challenging nonlinear systems.

State and Unknown Estimation of the Synchronous Reluctance Machine (SynRM)

4.1 Introduction	87
4.2 Application to synchronous reluctance motor	88
4.2.1 TS model design of SynRM	89
4.2.2 Syntax code in MATLAB	90
4.3 Simulation results and comparative analysis	92
4.4 Hardware-in-the-loop validation	97
4.5 Conclusions	108

4.1 Introduction

This chapter focuses on the practical application of the observer techniques discussed in Chapter 3 to a synchronous reluctance motor (SynRM). The chapter explores the design and implementation of a Takagi-Sugeno (TS) model-based observer for the SynRM system. The goal is to demonstrate the effectiveness and performance of the observer in estimating the states of the SynRM under various operating conditions.

The chapter begins by presenting the application of the observer to the SynRM system. The TS model design for the SynRM is discussed in detail, highlighting the modeling

considerations and the construction of the TS model. The TS model serves as the basis for developing the observer for state estimation.

To facilitate the implementation of the observer, the chapter provides syntax code in MATLAB. This code offers a practical guide for readers to understand and implement the observer algorithm in a real-world scenario. The MATLAB code includes the necessary functions and calculations required for the observer design and estimation process.

The chapter presents the simulation results obtained from applying the observer to the SynRM system. The performance of the observer in estimating the states of the motor under various operating conditions is evaluated and analyzed. A comparative analysis is conducted to assess the effectiveness of the observer in comparison to other existing methods. The results provide insights into the accuracy, robustness, and overall performance of the observer in practical applications.

To further validate the observer's effectiveness and practical applicability, the chapter includes a hardware-in-the-loop validation. This validation involves implementing the observer on real hardware and testing its performance in a real-time setup. The experimental results and observations obtained from the hardware-in-the-loop validation provide valuable insights into the practical feasibility and performance of the observer in a real-world SynRM system.

4.2 Application to synchronous reluctance motor

Several studies are devoted to the state estimation problem for synchronous reluctance motor. Unfortunately, the majority of those works cannot be determined the unknown inputs. Mynar et al [MVB20], proposed an adaptive observer using extended Kalman filter to estimate the speed rotor and inductance parameters in which the observer gains are obtained with online technique. In order to achieve the fault detection problem, a Luenberger observer has been proposed in Mahmoudi et al. [MJC⁺21], to estimate only the stator current. For this reason, a PIO algorithm is proposed in this paper to solve this problem.

In this section the proposed observer is applied to a synchronous reluctance motor in order to reconstruct the unknown inputs and state variables . First the synchronous reluctance motor fuzzy model is presented.

4.2.1 TS model design of SynRM

The TS fuzzy model is built to design the proposed observers allowing the unknown inputs and state estimation. The most method to obtain a TS model is the non linear sector transformation, this approach allows exactly transform the non linear system into a fuzzy model with four linear sub-system.

Terms (i_q, Ω) are mainly contribute on the non-linearity of system, so it is natural to define these terms as a premise variables.

$$\begin{cases} \xi_1(t) = i_q \\ \xi_2(t) = \Omega \end{cases}$$

The non linear terms $\xi(t)$ can be writing under the following shape:

$$\xi_j(t) = F_{1j}(t) \cdot \bar{\xi}_j + F_{2j}(t) \cdot \underline{\xi}_j \quad j = \{1, 2\} \quad (4.1)$$

where:

$$\begin{cases} F_{1j} = \frac{\xi_j(t) - \underline{\xi}_j}{\bar{\xi}_j - \underline{\xi}_j} \\ F_{2j} = \frac{\bar{\xi}_j - \xi_j(t)}{\bar{\xi}_j - \underline{\xi}_j} \end{cases} \quad (4.2)$$

Thus, the LPV system (1.28) is equivalently written under the TS fuzzy model form:

$$\begin{cases} \dot{x}(t) = \sum_{i=1}^4 h_i(\xi(t))(A_i x(t) + B_i u(t) + E_i \delta(t)) \\ y(t) = Cx(t) \end{cases} \quad (4.3)$$

$$h_1(\xi(t)) = M_1(\xi_1(t)) \times N_1(\xi_2(t)); \quad h_2(\xi(t)) = M_1(\xi_1(t)) \times N_2(\xi_2(t))$$

$$h_3(\xi(t)) = M_2(\xi_1(t)) \times N_1(\xi_2(t)); \quad h_4(\xi(t)) = M_2(\xi_1(t)) \times N_2(\xi_2(t))$$

The machine studies is a (2.2 kW) SynRM whose parameters are presented in Table 1. The constant matrices in (4.3) defining the four linear sub-systems, are determined by using the pair $(\bar{\xi}_j, \underline{\xi}_j)$ and non linear matrices in (1.28).

$$\begin{aligned}
 A_1 &= \begin{bmatrix} 9 & 0 & 4.73 \\ -4644.4 & -38 & 0 \\ 317.5 & 0 & -0.02 \end{bmatrix}, A_2 = \begin{bmatrix} -9 & 0 & 4.73 \\ -84.4 & -38 & 0 \\ 317.5 & 0 & -0.02 \end{bmatrix}, \\
 A_3 &= \begin{bmatrix} -9 & 0 & 0 \\ -4644.4 & -38 & 0 \\ 0 & 0 & -0.02 \end{bmatrix}, A_4 = \begin{bmatrix} -9 & 0 & 0 \\ -84.4 & -38 & 0 \\ 0 & 0 & -0.02 \end{bmatrix}, \\
 B_i &= \begin{bmatrix} 5.26 & 0 \\ 0 & 22.22 \\ 0 & 0 \end{bmatrix}, E_i = \begin{bmatrix} 0 \\ 0 \\ -73 \end{bmatrix}.
 \end{aligned}$$

Table 4.1: SynRM parameters[YMEC14]

Rated power	P_N	2.2KW
Rated voltage	V_N	220/380V
Rated speed	Ω	1500rpm
stator resistance	R_s	1.71 Ω
direct axe Inductance d	L_d	0.15 H
quadrature axe Inductance q	L_q	0.04 H
Number of pole pairs	n_p	2
Moment of inertia	J	0.0137Kg.m ²
friction coefficient	f	0.00036Nm/rad/s

4.2.2 Syntax code in MATLAB

In order to design the MGO, PIO observer we establish the LMI (constraints) algorithm to search the observer gains (3.47)

Step 1:

After calculating the matrices coefficients A_i of the TS fuzzy model.

Then, initialize the system parameters in MATLAB.

Step 2:

Define the LMI constraints of MGO to guarantee the feasibility of (3.31)

```

» P = sdpvar (3,3,'symmetric');
» M1 = sdpvar(3,3); M2 = sdpvar(3,3);
» M3 = sdpvar(3,3); M4 = sdpvar(3,3);
» F = set(P>zeros(3,3));
» LMI (3.31) and (3.32)

```

Define the LMI constraints of PIO to guarantee the feasibility of (3.46)

```

» P = sdpvar (4,4,'symmetric');
» M1 = sdpvar(4,3); M2 = sdpvar(4,3);
» M3 = sdpvar(4,3); M4 = sdpvar(4,3);
» F = set(P>zeros(4,4));
» LMI (3.46) and (3.57)

```

Step 3:

Solved, the convex optimization problem by using an semidefinite solver "SeDuMi".

The gains matrices of the fuzzy multi-gain observer (MGO) and proportional integral observer (PIO) are given, respectively, as follows:

$$L_{MGO1} = \begin{bmatrix} 584 & -89 & 9 \\ -93 & 3863 & 917 \\ 52 & -974 & 22720 \end{bmatrix}, L_{MGO2} = \begin{bmatrix} 584 & -89 & 9 \\ -93 & 3863 & -917 \\ 52 & -974 & 22720 \end{bmatrix}, \\
 L_{MGO3} = \begin{bmatrix} 584 & -89 & 8 \\ -92 & 3841 & -898 \\ 23 & -854 & 22741 \end{bmatrix}, L_{MGO4} = \begin{bmatrix} 584 & -89 & 8 \\ -92 & 3841 & -898 \\ 23 & -854 & 22741 \end{bmatrix}.$$

$$\bar{L}_{PI1} = \begin{bmatrix} 43.8 & -5396.4 & 5353.4 \\ -2145.8 & -3636.2 & 5782.8 \\ -649.8 & -8063.2 & 8713.7 \\ 1123.9 & 795.4 & -1919.2 \end{bmatrix}, \bar{L}_{PI2} = \begin{bmatrix} -287.1 & -379.34 & 667.45 \\ -652.79 & -144.28 & 798.04 \\ -868.68 & -616.39 & 1486 \\ 1054.9 & 88.665 & -1143.4 \end{bmatrix},$$

$$\bar{L}_{PI3} = \begin{bmatrix} 446.53 & -5250.4 & 4804.8 \\ -1731.7 & -3533.3 & 5266 \\ -57.2 & -7827.9 & 7886.1 \\ 831.98 & 878.9 & -1710.9 \end{bmatrix}, \bar{L}_{PI4} = \begin{bmatrix} 114.1 & -245.8 & 132.8 \\ -253.5 & -66.7 & 321.3 \\ -278.0 & -425.9 & 704.9 \\ 756.8 & 210.5 & -967.3 \end{bmatrix}.$$

The gain of Luenberger observer is given as follows:

$$L_{Luen} = \begin{bmatrix} 94 & 100 & 2500 \end{bmatrix}^T.$$

4.3 Simulation results and comparative analysis

To show the effectiveness of the proposed PIO observer, a Luenberger observer (LO) [MJC⁺21] and a fuzzy multi-gain observer (MGO) [IMR16] are adopted for comparison purposes, under both different speed and load disturbance conditions. The performance of the different techniques were tested through MATLAB/Simulink environment. To study the observers reliability versus the external perturbations, a random noise signal of 0.5 amplitude is added to the observer inputs. These simulations were carried out with a 200kHz sampling frequency.

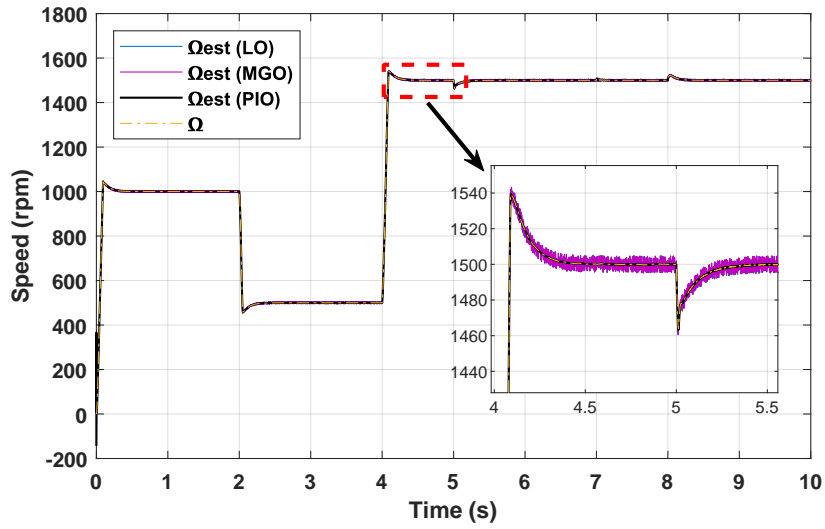


Fig 4.1: Rotor speed and its estimation via (LO - MGO - PIO).

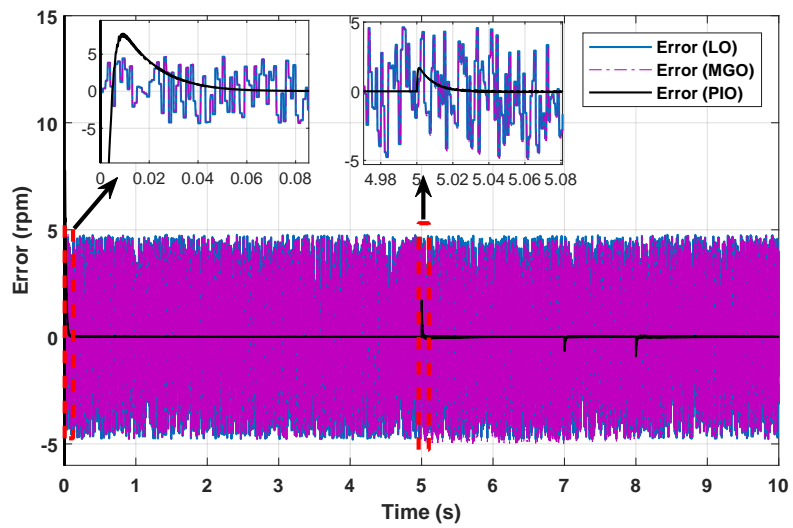


Fig 4.2: Error of the rotor speed.

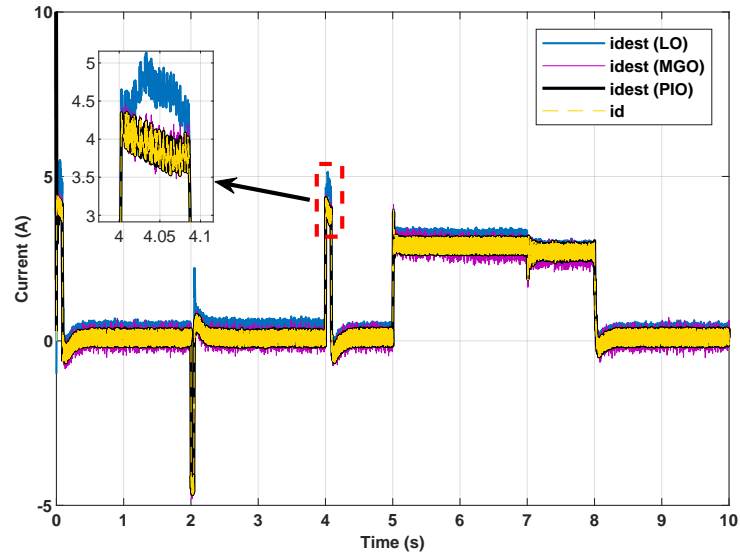


Fig 4.3: The d-axis stator current and its estimation via (LO - MGO - PIO).

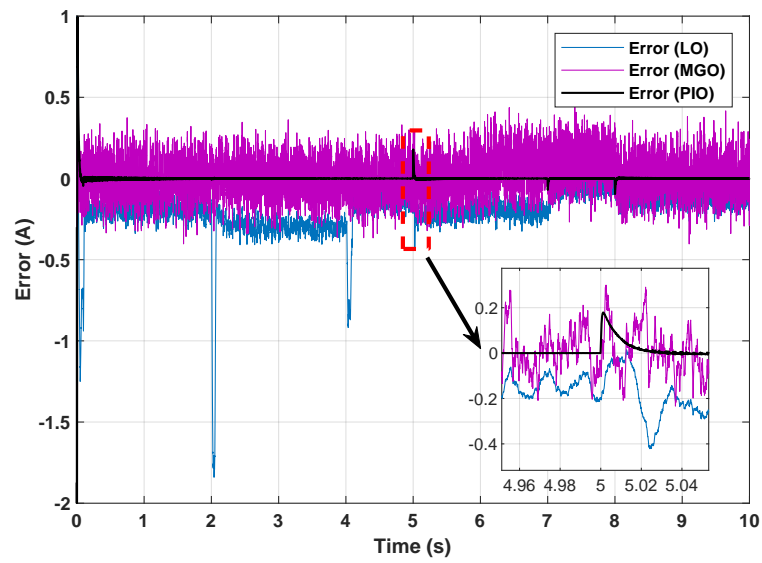


Fig 4.4: Error of the d-axis stator current.

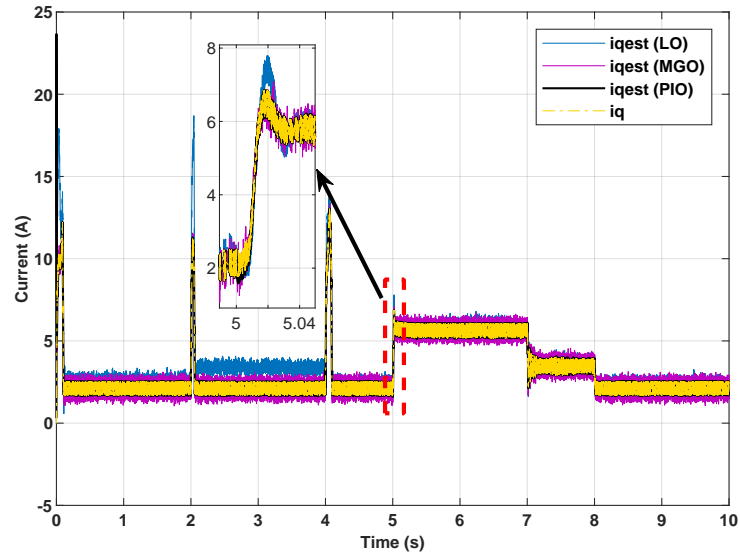


Fig 4.5: The q-axis stator current and its estimation via (LO - MGO - PIO).

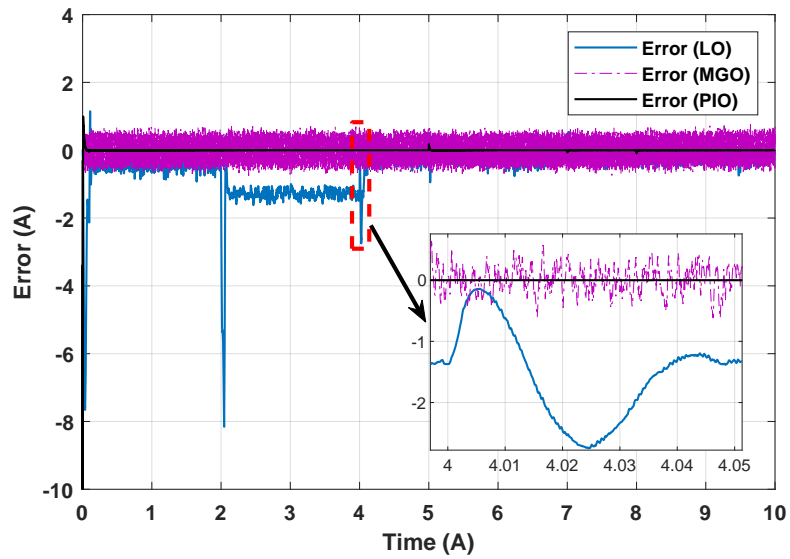


Fig 4.6: Error of the q-axis stator current.

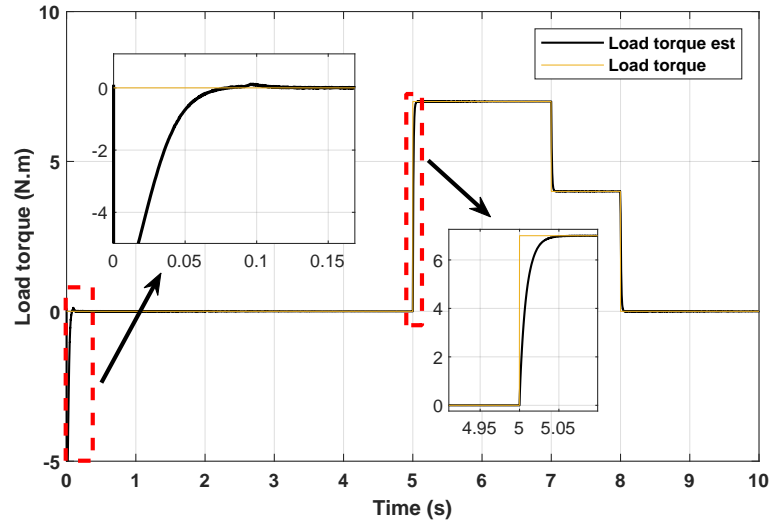


Fig 4.7: The Unknown load torque and its estimation via PIO.

Figures 4.1 to 4.7 show the rotor speed response, (d-axis, q-axis) stator currents, unknown load torque, and its estimation of the synchronous reluctance motor via proportional integral observer, Luenberger observer, and the fuzzy multi-gain observer under field-oriented control. Firstly, to test the systems tracking performance, the speed reference was increased from 0 to 1000rpm at $t = 0$ sec then a step-down from 1000 to 500rpm at $t = 2$ sec, and finally a step-up from 500 to 1500rpm at $t = 4$ sec. Secondly, a constant load torque of 7 Nm was applied at $t = 5$ sec, then it is stepped down to 4 Nm and 0 Nm at $t = 7$ sec and $t = 8$ sec, respectively.

Figure 4.1 indicates that the PIO tracks very well the real velocity for all the speed range. On the other hand, we find that the two proposed techniques [MJC⁺21] and [IMR16] give a degraded quality of observation and are noise-sensitive. Figure 4.2 illustrates the rotor speed error, which was between -5 and 5 rpm for the MGO and LO observers, and a negligible value for the proposed observer.

Figures 4.3 and 4.5 show the direct and quadrature axis stator current of the synchronous reluctance motor and their estimations via three approaches, under the proposed speed profile; Figures 4.4 and 4.6 show the estimation error of the stator currents. It is very clear that the proposed observer is insensitive to the noise and estimates the real values with high performance even at a low speed. On the other hand, we find that the other approaches give a degraded quality of estimation. Indeed, the Luenberger observer

presents a static error in the low speed ($t = 0\text{sec}$ to $t = 4\text{sec}$) and in the presence of the load torque ($t = 5\text{sec}$ to $t = 7\text{sec}$). As it is observed, the auxiliary system (PIO) is insensitive to the noise. It is clear from the obtained results that the errors between the real states and their estimations are negligible in different speed range and the observer shows its high performance even at the low speed, in addition to its insensitivity to the noise. From figure 4.7, it is clear that the PIO show a good agreement between the estimated and the real unknown input, on the other hand, both Luenberger and multi-gain observers are not able to estimate the unknown inputs. This is considered as one of the main strengths of the PIO.

Table 4 shows the comparison of the unknown input and state estimation errors between the PI, fuzzy multi-gain, and the Luenberger observers. As is seen in Table 4, the proposed technique provides the lowest currents and rotor speed error at all speed range and unknown inputs change conditions which confirms the high performance of the PIO even in extreme conditions (low speed, high load torque, and random noise). This makes the PIO more advantageous for industrial applications.

Table 4.2

Observer performance		LO	MGO	PIO
Mean square error	i_d (A)	0.2067	0.1352	0.00516
	i_q (A)	0.419	0.2219	0.00514
	Ω (rpm)	2.78	2.688	0.048
	Load torque (N.m)	/	/	0.004
Maximum error	i_d (A)	-1.9	0.54	0.18
	i_q (A)	-8.2	0.52	0.19
	Ω (rpm)	4.77	4.76	1.69
	Load torque (N.m)	/	/	7

4.4 Hardware-in-the-loop validation

Real-time HIL test bench is a way to bridge the gap between software-based simulation and real operational conditions [AADM19]. It has been proved as an effective approach to testing control and diagnosis algorithms in several fields, such as electric vehicle drive-

train, power electronics, and power systems [ZZOL19].

In order to validate the performance of the proposed PIO based on TS fuzzy model. A test bench is build in the MSE laboratory as shown in figure 4.8. A hardware in the loop platform is used to emulate the real behavior of synchronous reluctance motor. As presented in figure 4.9 the overall architecture of the hardware-in-the-loop is consist of two dSPACE1104 board cards, the first one is used to emulate both synchronous reluctance motor and voltage source inverter controlled by field-oriented control through MATLAB/Simulink. The second dSPACE is used for the observer application, where the sampling frequency is $10KHz$. We emphasize that the connection between the two board was done grace a digital analog and analog digital conversion blocks (DAC and ADC). The motor parameters are listed in Table 1.

Figures 4.10 to 4.23 show the PIO performance for synchronous reluctance motor under field-oriented control using the hardware experiment. For this reason, three different scenarios are tested as shown in Table 2.

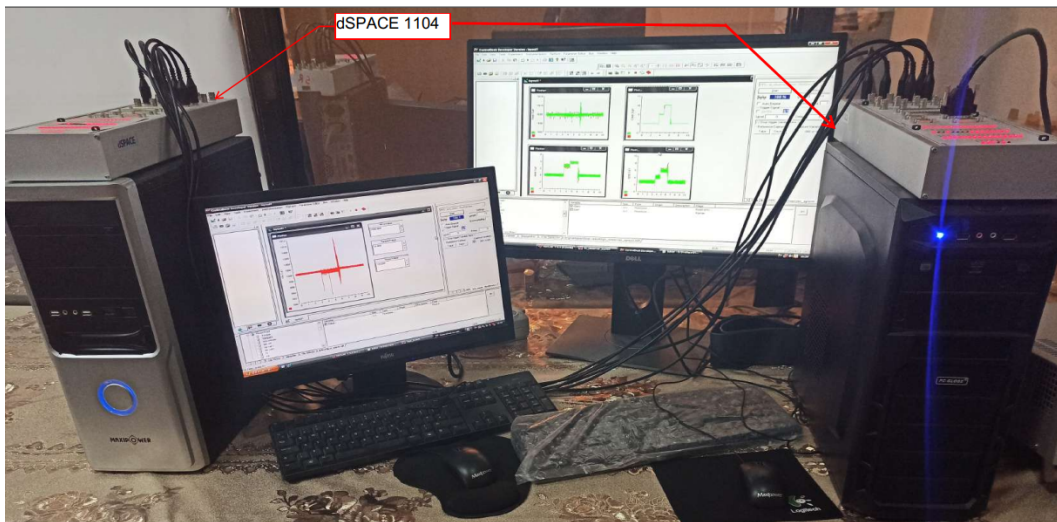


Fig 4.8: Test bench.

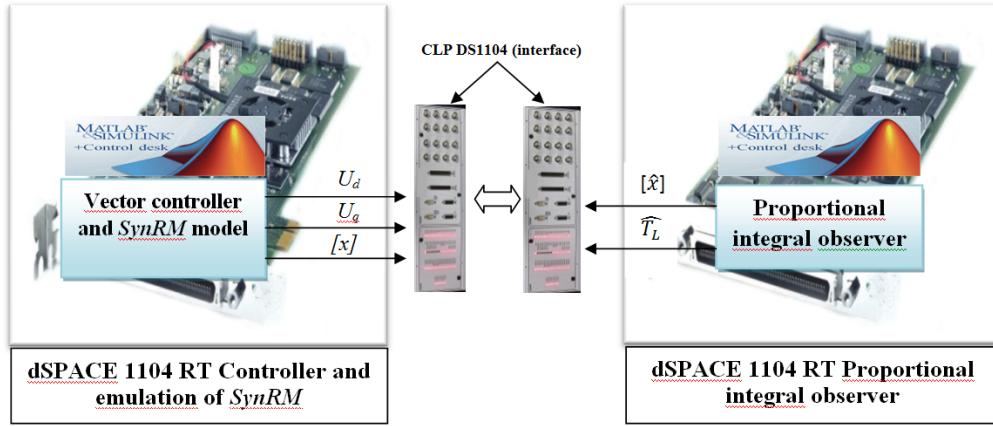


Fig 4.9: Overall architecture of the HIL test system.

Table 4.3

Cases	Speed profile	Load torque profile	Descriptions
1	Speed change step	No load torque	$\Omega : 0 \rightarrow 1500 \rightarrow 300 \rightarrow 1000(rpm/min)$ and $T_L = 0(N/m)$
2	Speed change step	Load torque step change	$\Omega : 0 \rightarrow 1000(rpm/min)$ and $T_L : 0 \rightarrow 5 \rightarrow 10 \rightarrow 0(N/m)$
3	Constant speed value	Load torque trapezoidal form	$\Omega = 1000(rpm/min)$ and $T_L : 0 \rightarrow 10 \rightarrow 0(N/m)$

Case 1 Observer performance under different speed references with no load torque

Firstly, in order to test the effectiveness of the proposed observer in speed tracking problem, a rapid variation in rotor speed reference is performed without load torque. The motor speed initially increases from 0 rpm to 1500 rpm at $t = 1.12$ sec, then, it decelerated to 300 rpm at $t = 3.91$ sec, and finally stepped up from 300 rpm to 1000 rpm at $t = 7.08$ sec.

Figures 4.10 to 4.13 shows the experimental results of rotor speed response, (d-axis, q-axis) stator currents, and its estimation under field oriented control. As it can be seen in figure 4.10, the estimate rotor speed follows perfectly the real out put with a fast settling

time (i.e., 28 ms) and without any noticeable ringing or overshoot (0.11 %), during all increase or decrease stage. In the zoom of figure 4.10 the magenta line represents the state estimated and the real values is represented by the black line.

Figures 4.12 and 4.13 present the d-q axis stator currents of the synchronous reluctance motor and their estimated, respectively, under the proposed speed profile. We can see in both figures, that the estimate states allow their real values with satisfactory performances. However, figure 4.11 illustrate the evolution of rotor speed error, which close to zero in a steady state (mean square error with 0.48%).

As it can be observed, the auxiliary system (PIO) is insensitive to the noise. It is clear from the obtained results that the errors between the real states and their estimated are negligible in different speed rang and the observer show its high performance even in the low speed and insensitivity to the noise.

Case 2 Observer performance under constant load torque

Secondly, in order to test the robustness of the proposed observer against the presence of unknown inputs, a constant load torque of 5 N.m was imposed at $t = 4,92$ sec, then it stepped up to 10 N.m at $t = 6,84$ sec. Figures 4.14 to 4.18 shows the performance of the PIO when the motor keeps running at speed of 1000 rpm and changes from no-load to load mode. It is clear from figure 4.14, that the estimated rotor speed tracks well the measured value without any noticeable ringing or overshoot, and the estimation errors remains very small (mean square error with 0.84%), where the zoomed graphs given the details of the few ripples. Figures 4.16 and 4.17, present the direct and quadrature components of the stator current and their estimated, respectively. As it can be observed, the stator currents estimation errors for both components (d and q) are near to zero for transient and steady states. Figure 4.18 depicts the load torque waveform. As can be seen, the load torque estimation converge to its real value with a fast settling time. A negligible overshoot appeared especially in transient state.

Case 3 Observer performance under variable load torque

Finally, a variable load torque was imposed for the motor when the rotor speed is equal 1000 rpm. As it can be observed from figure 4.19 the estimated speed tracks well the real value without any unacceptable peak or overshoot. Figure 4.20, present the speed

error, which is always negligible and there is no influence of load torque on the observation performance (mean square error with 0.96%). Figures 4.21 and 4.22 shows the d-q axis currents and their estimated, respectively, it is clear that the estimated currents follows perfectly its real values with a fast setting time and without any unacceptable peak or overshoot even in the presence of load torque. The quadrature component of the stator current value follows in a proportional manner the evolution of the load torque, as it illustrated in figure 4.20.

Figure 4.23 present the evolution of the load torque and thier estimated, as it can be seen in the zoom, the proposed observer has strong robustness to the unknown inputs in different values or variables profile. This make the PI-observer robust on variable load torque, speed and less sensitive to the noise.

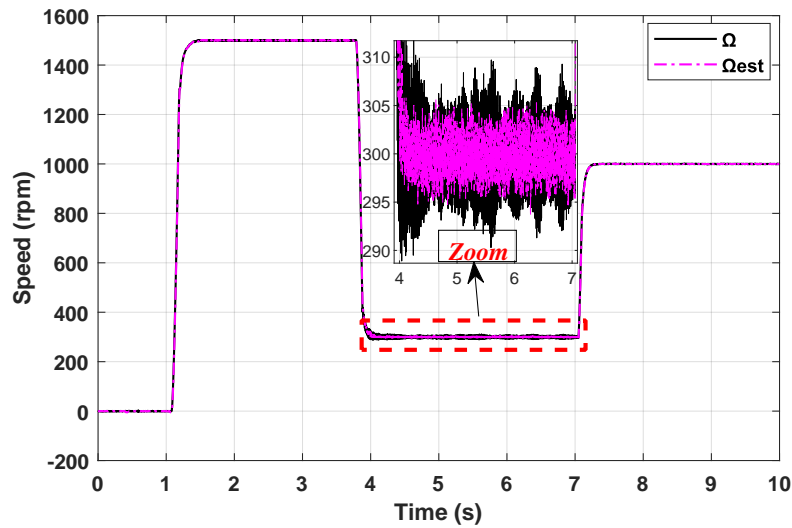


Fig 4.10: Rotor speed and its estimation case 1.

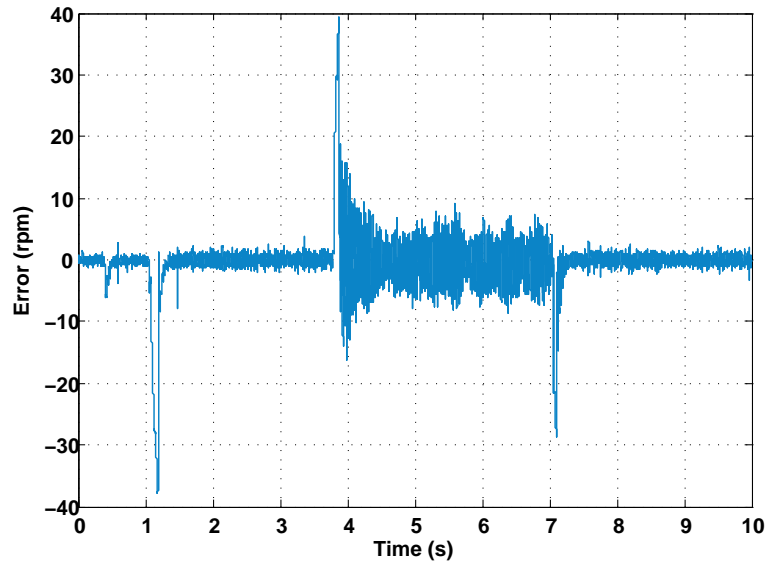


Fig 4.11: Error speed case 1.

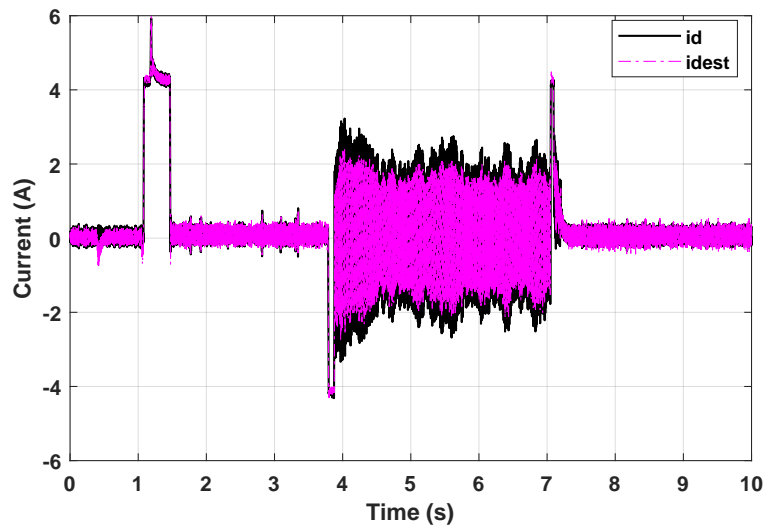


Fig 4.12: d-axis stator current and its estimation case 1.

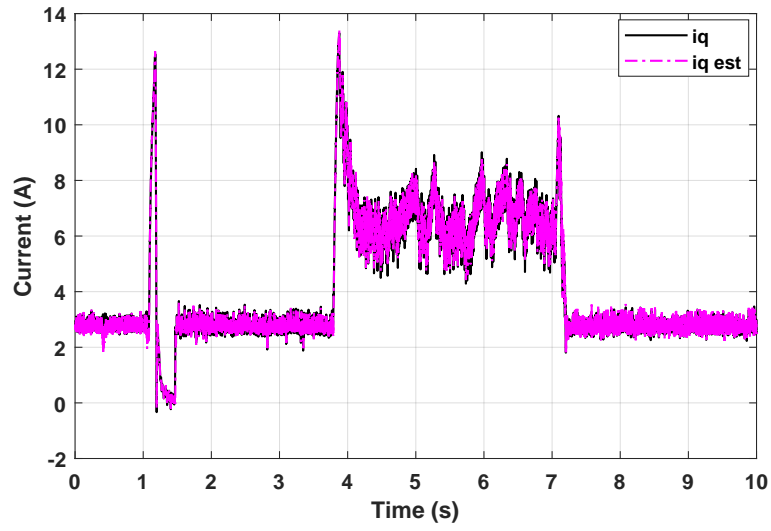


Fig 4.13: q-axis stator current and its estimation case 1.

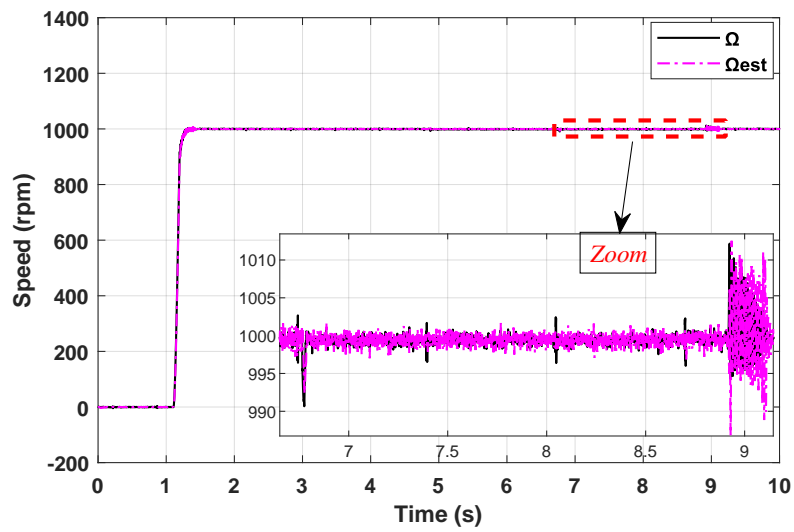


Fig 4.14: Rotor speed and its estimation case 2.

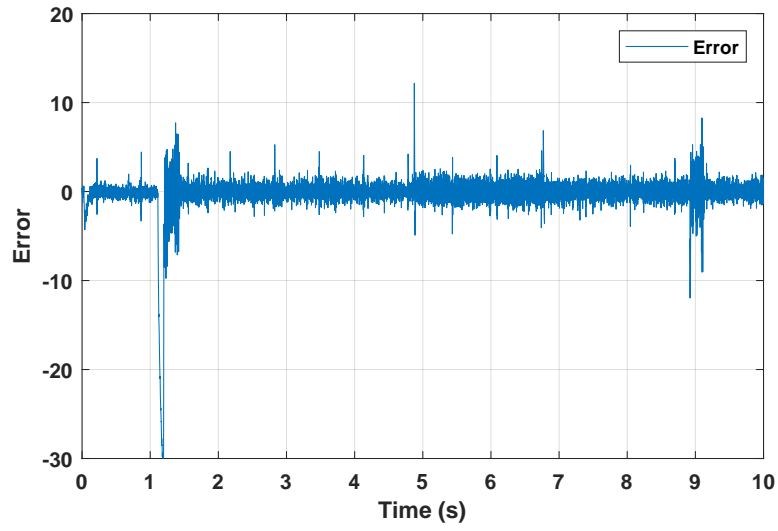


Fig 4.15: Error speed case 2.

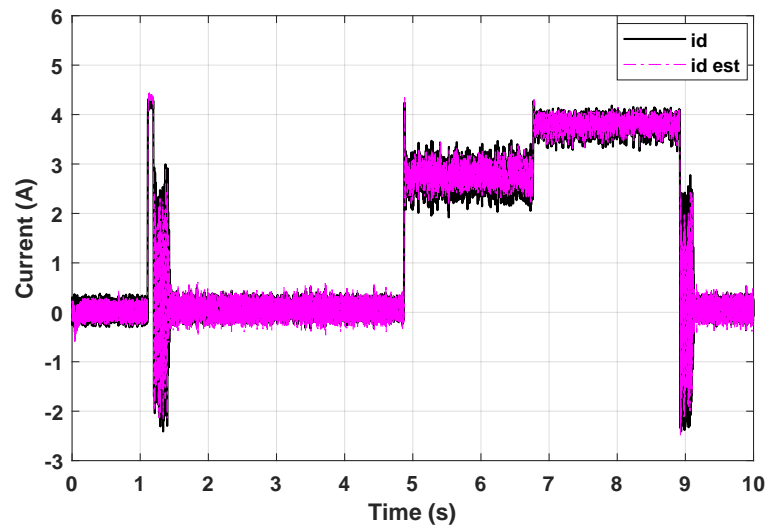


Fig 4.16: d-axis stator current and its estimation case 2.

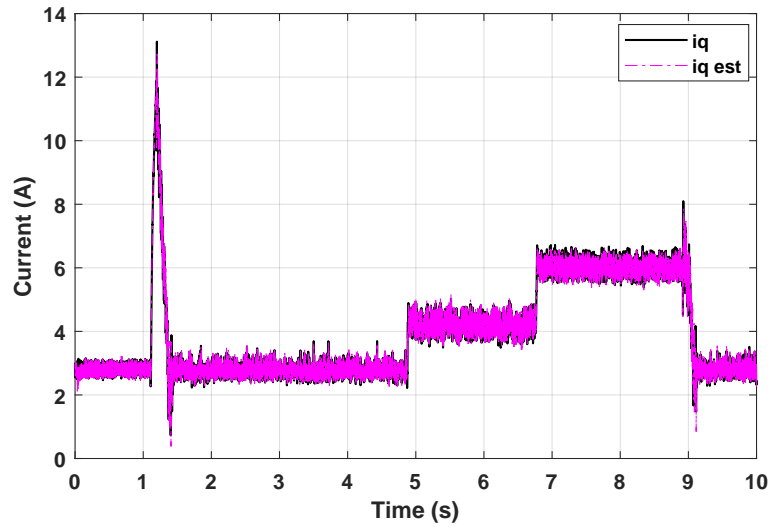


Fig 4.17: q-axis stator current and its estimation case 2.

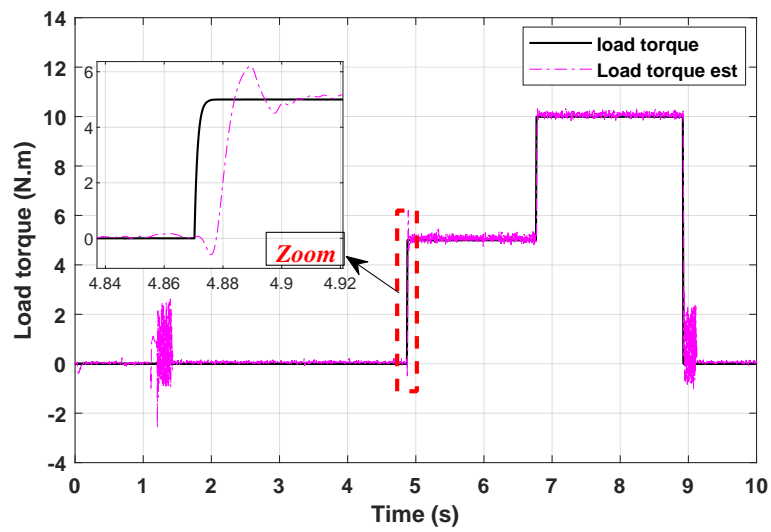


Fig 4.18: Unknown load torque and its estimation case 2.

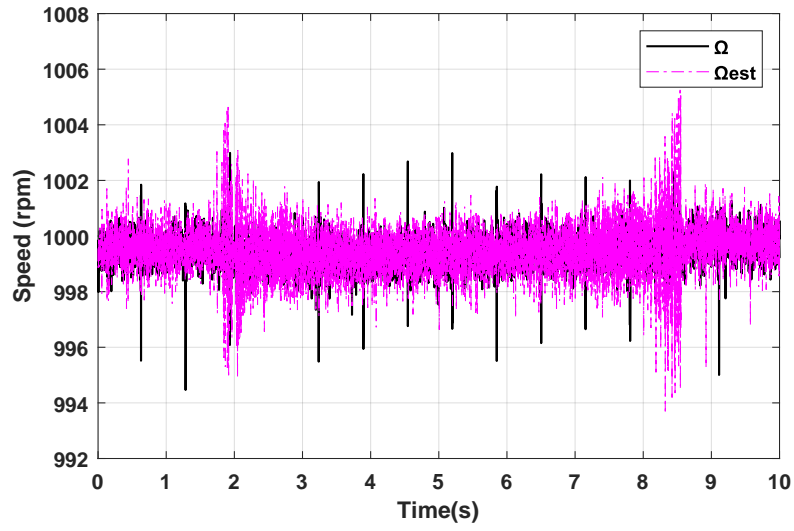


Fig 4.19: Rotor speed and its estimation case 3.

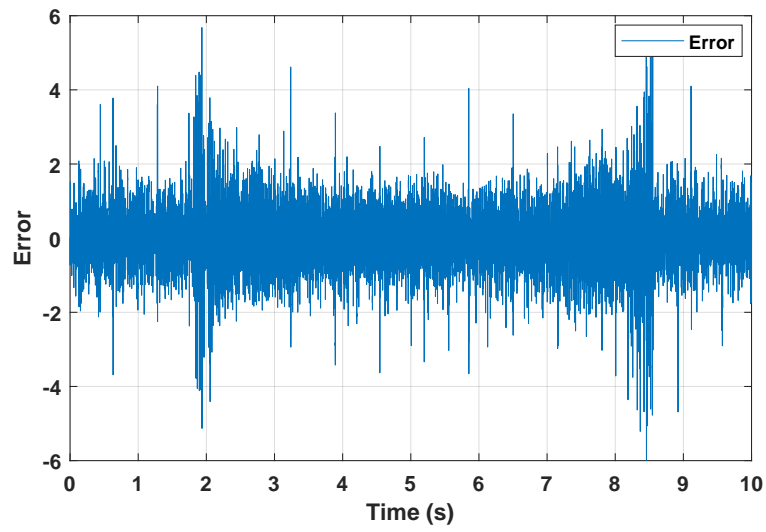


Fig 4.20: Error speed case 3.

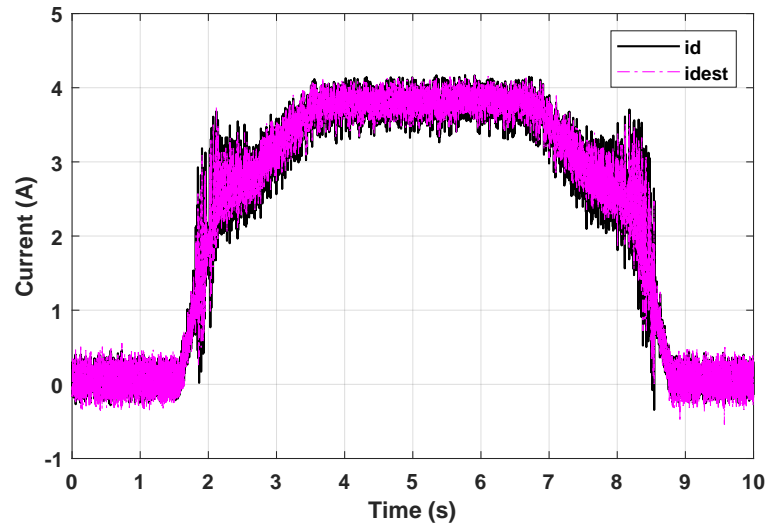


Fig 4.21: d-axis stator current and its estimation case 3.

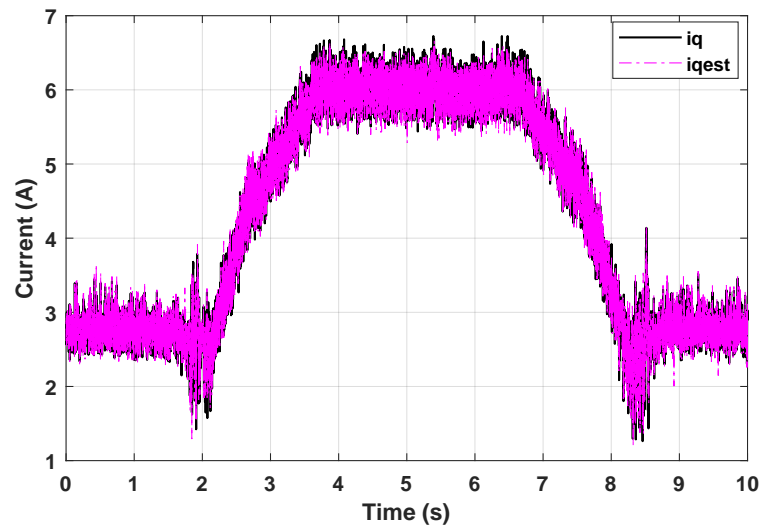


Fig 4.22: q-axis stator current and its estimation case 3.

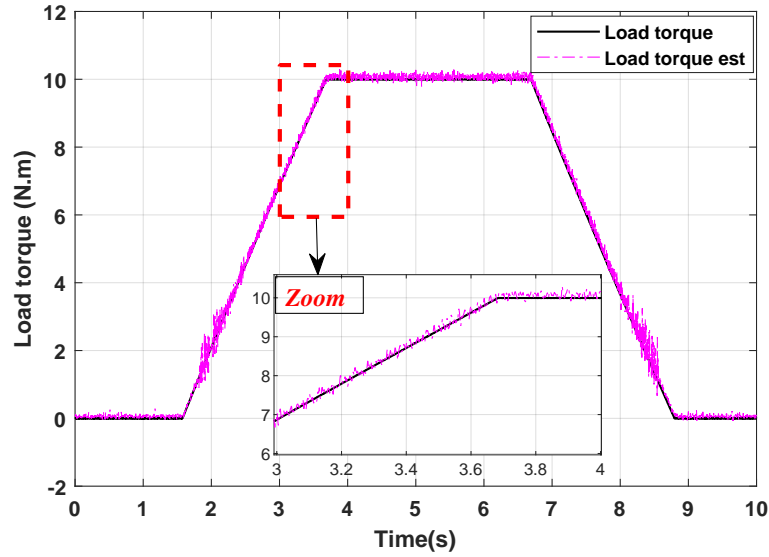


Fig 4.23: Unknown load torque and its estimation case 3.

Table 4.4

SynRM speed	Case 1	Case 2	Case 3
Maximum error (%)	2.6%	3.2%	0.56%
Mean square error (%)	0.48%	0.84%	0.96%
Overshoot (%)	0.11%	0.14%	—
Settling time (ms)	28ms	28ms	—

4.5 Conclusions

This chapter demonstrates the application of the observer techniques discussed in chapter 3 to a synchronous reluctance motor (SynRM). The TS model-based observer is designed and implemented for state estimation in the SynRM system. Through simulation results, comparative analysis, and hardware-in-the-loop validation, the chapter showcases the effectiveness, accuracy, and robustness of the observer in estimating the states of the SynRM under various operating conditions. The practical implementation and validation provide valuable insights into the practical applicability and performance of the observer in real-world scenarios, further emphasizing its potential for state estimation in SynRM systems.

General Conclusion

This thesis deals with the problem of modeling and state estimation of nonlinear systems represented in the form of fuzzy multi-models.

In the context of modeling, we favored the Takagi-Sugeno (T-S) approach because of its ease of use, particularly for studying stability and synthesizing observers and controllers. Two main structures of multi-models can be identified depending on whether the sub-models share the same state vector. The first structure is the decoupled multi-model, while the second is the fuzzy multi-model of Takagi-Sugeno, which has been at the origin of numerous developments in various fields of automation such as identification, state estimation, or control. Consequently, we represented the nonlinear model of the synchronous reluctance machine in the form of a fuzzy Takagi-Sugeno model, this representation is based on decomposition into a nonlinear sector.

In the context of state estimation, we synthesized three state observer structures for systems represented by a multi-model. The first observer (Lipschitzian observer) aims to estimate the states of the system while minimizing modeling uncertainties. The other two observers, with unknown inputs (proportional-integral gain and multi-integral), are intended for nonlinear systems affected by unknown inputs (disturbances). They allow for a simultaneous estimation of the state and unknown inputs of the system through an integral action improving state estimation. We applied these methods to a real process model, particularly that of synchronous reluctance machine.

To position our contribution in relation to existing work, we presented a state of the art on variable reluctance synchronous machines and fuzzy multi-models in the first two chapters. Our contributions were formulated in the third chapter of this dissertation, focused on the synthesis of robust observers in the face of modeling uncertainties and external disturbances (unknown inputs). In the last chapter, the example of a variable reluctance synchronous machine allowed us to illustrate the implementation of the results obtained, from the modeling phase to the observer synthesis phase.

The results demonstrate the interest in using advanced automation techniques in the

field of control and diagnosis of electric machines.

The problems discussed in this dissertation open up many perspectives for future work:

- fault detection and diagnosis methods based on a proportional-integral (PI) observer and multi-integral (PMI).
- Design of an observer-based controller whose stability is dealt with by means of linear and nonlinear Lyapunov functions.
- Design of a fault-tolerant control for nonlinear systems described by TS multi-models, and particularly for electric machines.

Annex

LMI Tools

LMI methods are based on formulating a given problem as an optimization problem with a linear objective and constraints in the form of Matrix Linear Inequalities (LMI). An LMI constraint in a vector $x \in \mathbb{R}^m$ is of the form

$$F(x) = F_0 + \sum_{i=1}^m x_i F_i \geq 0 \quad (4.4)$$

where the symmetric matrices $F_i = F_i^T \in \mathbb{R}^{N \times N}$, $i = 1, \dots, m$, are given.

Schur's complement

Consider three matrices $R(x) = R^T(x)$, $Q(x) = Q^T(x)$ and $S(x)$ affine with respect to the variable x . The following LMIs are equivalent:

$$\begin{bmatrix} Q(x) & S(x) \\ S^T(x) & R(x) \end{bmatrix} > 0,$$

$$R(x) > 0, Q(x) - S(x)R^{-1}(x)S^T(x) > 0,$$

$$Q(x) > 0, R(x) - S^T(x)Q^{-1}(x)S(x) > 0.$$

Bibliography

- [AADM19] Mahmoud Amin, Ghada A Abdel Aziz, James Durkin, and Osama A Mohammed. A hardware-in-the-loop realization of speed sensorless control of pma-synrm with steady-state and transient performances enhancement. *IEEE Transactions on Industry Applications*, 55(5):5331–5342, 2019. (page 97).
- [ACMR04] Abdelkader Akhenak, Mohammed Chadli, Didier Maquin, and José Ragot. State estimation of uncertain multiple model with unknown inputs. In *43rd IEEE Conference on Decision and Control, CDC'04*, page CDROM. IEEE, 2004. (pages 45, 71).
- [ACR⁺06] Abdelkader Akhenak, Mohammed Chadli, José Ragot, Didier Maquin, et al. Unknown input multiple observer based approach. application to secure communications. In *1st IFAC Conference on Analysis and Control of Chaotic Systems, CHAOS06, Reims, France*, 2006. (page 71).
- [AK01] Murat Arcaç and Petar Kokotović. Nonlinear observers: a circle criterion design and robustness analysis. *Automatica*, 37(12):1923–1930, 2001. (page 69).
- [Akh04] Abdelkader Akhenak. *Conception d'observateurs non linéaires par approche multimodèle: application au diagnostic*. PhD thesis, éditeur inconnu, 2004. (pages 50, 64, 70, 71).
- [AKK⁺15] Lassi Aarniovuori, Jere Kolehmainen, Antti Kosonen, Markku Niemelä, Huifeng Chen, Wenping Cao, and Juha Pyrhönen. Application of calorimetric method for loss measurement of a synrm drive system. *IEEE Transactions on Industrial Electronics*, 63(4):2005–2015, 2015. (page 5).
- [AKNM17] JAMAL DEHGHANI ASHKEZARI, Hassan Khajeroshane, Mohsen Niasati, and MOHAMMAD JAFAR MOJIBIAN. Optimum design and oper-

- ation analysis of permanent magnet-assisted synchronous reluctance motor. *Turkish Journal of Electrical Engineering & Computer Sciences*, 25(3):1894–1907, 2017. (page 5).
- [ALA20] Ahmed Amrane, Abdelkader Larabi, and Abdel Aitouche. Unknown input observer design for fault sensor estimation applied to induction machine. *Mathematics and Computers in Simulation*, 167:415–428, 2020. (pages 5, 71).
- [Ang01] Georgo Z Angelis. System analysis, modelling and control with polytopic linear models. 2001. (page 42).
- [BA99] M Boutayeb and D Aubry. A strong tracking extended kalman observer for nonlinear discrete-time systems. *Automatic Control, IEEE Transactions on*, 44(8):1550–1556, 1999. (page 68).
- [Bar01] Gabriela Iuliana Bara. *Estimation d'état des systèmes linéaires à paramètres variants*. PhD thesis, INPL-Institut National Polytechnique de Lorraine, 2001. (page 76).
- [BEGFB94] Stephen P Boyd, Laurent El Ghaoui, Eric Feron, and Venkataramanan Balakrishnan. *Linear matrix inequalities in system and control theory*, volume 15. SIAM, 1994. (page 61).
- [Bel08] Christian Belalahy. *Dimensionnement d'une machine synchro-réductante à excitation homopolaire par réseaux de perméances*. PhD thesis, Institut National Polytechnique de Lorraine, 2008. (pages 12, 13).
- [BEN] Mohamed BENALLOUCH. Observation des systemes non-linéaires a entrées inconnues-applicationa la pilea combustible de type pem these. (page 69).
- [Bez13] Souad Bezzaoucha. *Commande tolérante aux défauts de systemes non linéaires représentés par des modeles de Takagi-Sugeno*. PhD thesis, Université de Lorraine, 2013. (pages 4, 54).
- [BFN94] I Boldea, ZX Fu, and SA Nasar. Performance evaluation of axially-laminated anisotropic (ala) rotor reluctance synchronous motors. *IEEE transactions on industry applications*, 30(4):977–985, 1994. (page 25).

- [BLJ⁺93] Robert E Betz, Rolf Lagerquist, Milutin Jovanovic, Timothy JE Miller, and Richard H Middleton. Control of synchronous reluctance machines. *IEEE Transactions on Industry Applications*, 29(6):1110–1122, 1993. (page 23).
- [BMR99] Anass Boukhris, Gilles Mourot, and Jose Ragot. Non-linear dynamic system identification: a multi-model approach. *International Journal of Control*, 72(7-8):591–604, 1999. (page 4).
- [Bou09] Tahar Bouarar. *Contribution à la synthèse de lois de commande pour les descripteurs de type Takagi-Sugeno incertains et perturbés*. PhD thesis, Reims, 2009. (page 52).
- [BP00] Pontus Bergsten and Rainer Palm. Thau-luenberger observers for ts fuzzy systems. In *9th IEEE International Conference on Fuzzy Systems, FUZZ IEEE*, pages 7–10, 2000. (page 71).
- [BP08] Aldo Boglietti and Michele Pastorelli. Induction and synchronous reluctance motors comparison. In *2008 34th annual conference of IEEE industrial electronics*, pages 2041–2044. IEEE, 2008. (pages 15, 16).
- [BPB01] Yann Blanco, Wilfrid Perruquetti, and Pierre Borne. Stability and stabilization of nonlinear systems and takagi-sugeno’s fuzzy models. *Mathematical Problems in Engineering*, 7(3):221–240, 2001. (page 60).
- [BPD01] Pontus Bergsten, Rainer Palm, and Dimiter Driankov. Fuzzy observers. In *10th IEEE International Conference on Fuzzy Systems.(Cat. No. 01CH37297)*, volume 2, pages 700–703. IEEE, 2001. (pages 71, 72).
- [CB12] Mohammed Chadli and Pierre Borne. *Multiple models approach in automation: Takagi-Sugeno fuzzy systems*. John Wiley & Sons, 2012. (pages 4, 52, 53).
- [CGAL19] Abdelmadjid Cherifi, Kevin Guelton, Laurent Arcese, and Valter JS Leite. Global non-quadratic d-stabilization of takagi-sugeno systems with piecewise continuous membership functions. *Applied Mathematics and Computation*, 351:23–36, 2019. (page 61).

- [Cha02] Mohammed Chadli. *Stabilité et commande de systèmes décrits par des multimodèles*. PhD thesis, Vandoeuvre-les-Nancy, INPL, 2002. (pages [59](#), [60](#), [61](#), [64](#)).
- [CMR00] Mohammed Chadli, Didier Maquin, and José Ragot. Relaxed stability conditions for takagi-sugeno fuzzy systems. In *Smc 2000 conference proceedings. 2000 ieee international conference on systems, man and cybernetics.'cybernetics evolving to systems, humans, organizations, and their complex interactions'*(cat. no. 0, volume 5, pages 3514–3519. IEEE, 2000. (page [60](#)).
- [CT05] S.D. Chu and S. Torii. Torque-speed characteristics of superconducting synchronous reluctance motors with dybco bulk in the rotor. *IEEE Transactions on Applied Superconductivity*, 15(2):2178–2181, 2005. (page [29](#)).
- [Dav71] G David. An introduction to observers. *IEEE transactions on Automatic Control*, 16(6):596–602, 1971. (page [70](#)).
- [DIA19] Pierre-Marie Damon, Dalil Ichalal, and Hichem Arioui. Steering and lateral motorcycle dynamics estimation: validation of luenberger lpv observer approach. *IEEE Transactions on Intelligent Vehicles*, 4(2):277–286, 2019. (page [49](#)).
- [DLPT20] Hongkai Dai, Benoit Landry, Marco Pavone, and Russ Tedrake. Counterexample guided synthesis of neural network lyapunov functions for piecewise linear systems. In *2020 59th IEEE Conference on Decision and Control (CDC)*, pages 1274–1281. IEEE, 2020. (page [61](#)).
- [DTH20] Baocang Ding, Xiaoming Tang, and Jianchen Hu. A summary of dynamic output feedback robust mpc for linear polytopic uncertainty model with bounded disturbance. *Mathematical Problems in Engineering*, 2020, 2020. (page [49](#)).
- [EDBB10] Nesrine Elfelly, Jean-Yves Dieulot, Mohamed Benrejeb, and Pierre Borne. A new approach for multimodel identification of complex systems based on both neural and fuzzy clustering algorithms. *Engineering Applications of Artificial Intelligence*, 23(7):1064–1071, 2010. (pages [4](#), [53](#)).

- [FA03] Xingzhe Fan and Murat Arcaç. Observer design for systems with multivariable monotone nonlinearities. *Systems & Control Letters*, 50(4):319–330, 2003. (page 69).
- [Fil91] Dimiter Filev. Fuzzy modeling of complex systems. *International Journal of Approximate Reasoning*, 5(3):281–290, 1991. (pages 4, 49).
- [Gas00] Komi Gasso. *Identification des systèmes dynamiques non-linéaires: approche multi-modèle*. PhD thesis, 2000. (pages 4, 52).
- [Ham09] Mohand Ouramdane Hamiti. Réduction des ondulations de couple d’une machine synchrone à réductance variable. *p151, Thèse de Doctorat de l’université Henri Poincaré Nancy-I*, 2009. (pages 21, 33).
- [Ham12] Habib Hamdi. *Approche Multi-Modèle pour l’Observation d’état et le Diagnostic des Systèmes Singuliers Non Linéaires*. PhD thesis, Ecole Polytechnique de Tunis, 2012. (pages 44, 45, 49, 55).
- [Ham15] Mohamed Yacine Hammoudi. *Contribution à la commande et à l’observation dans l’association convertisseurs machine*. PhD thesis, Université Mohamed Khider-Biskra, 2015. (pages 41, 44, 49, 52, 53).
- [HAS98] Hiroaki Kikuchi, Akihiro Otake, and Shouhachirou Nakanishi. Functional completeness of hierarchical fuzzy modeling. *Information Sciences*, 110(1):51–60, 1998. Special issue: Modeling with Soft-Computing. (page 50).
- [HS00] Heath Hofmann and Seth R Sanders. High-speed synchronous reluctance machine with minimized rotor losses. *IEEE Transactions on Industry Applications*, 36(2):531–539, 2000. (page 27).
- [Ich09] Dalil Ichalal. *Estimation et diagnostic de systèmes non linéaires décrits par un modèle de Takagi-Sugeno*. PhD thesis, Institut National Polytechnique de Lorraine-INPL, 2009. (page 71).
- [IMR16] Dalil Ichalal, Said Mammar, and José Ragot. Auxiliary dynamics for observer design of nonlinear ts systems with unmeasurable premise variables. *IFAC-PapersOnLine*, 49(5):1–6, 2016. (pages 92, 96).

- [IMRM07] Dalil Ichalal, Benoît Marx, José Ragot, and Didier Maquin. Conception de multi-observateurs à variables de décision non mesurables. In *2èmes Journées Doctorales/Journées Nationales MACS, JD-JN-MACS*, page CDROM. GdR MACS, 2007. (pages [72](#), [74](#)).
- [IMRM09] D. Ichalal, B. Marx, J. Ragot, and D. Maquin. Simultaneous state and unknown inputs estimation with pi and pmi observers for takagi sugeno model with unmeasurable premise variables. pages 353–358, June 2009. (pages [5](#), [47](#), [71](#), [76](#), [77](#), [78](#), [82](#), [83](#)).
- [IMRM10] Dalil Ichalal, Benoît Marx, José Ragot, and Didier Maquin. State estimation of takagi–sugeno systems with unmeasurable premise variables. *IET Control Theory & Applications*, 4(5):897–908, 2010. (page [71](#)).
- [JS93] J-SR Jang and C-T Sun. Functional equivalence between radial basis function networks and fuzzy inference systems. *IEEE transactions on Neural Networks*, 4(1):156–159, 1993. (page [48](#)).
- [KI83] Arthur J Krener and Alberto Isidori. Linearization by output injection and nonlinear observers. *Systems & Control Letters*, 3(1):47–52, 1983. (page [69](#)).
- [Kou08] Katia Kouzi. *Contribution des techniques de la logique floue pour la commande d'une machine à induction sans transducteur rotatif*. PhD thesis, Université El Hadj Lakhdar de Batna, 2008. (page [38](#)).
- [KPS18] Patrick Kühne, Florian Pöschke, and Horst Schulte. Fault estimation and fault-tolerant control of the fast nrel 5-mw reference wind turbine using a proportional multi-integral observer. *International Journal of Adaptive Control and Signal Processing*, 32(4):568–585, 2018. (page [5](#)).
- [Kru07] Alexandre Kruszewski. *Lois de commande pour une classe de modèles non linéaires sous la forme Takagi-Sugeno: Mise sous forme LMI*. PhD thesis, Université de Valenciennes et du Hainaut-Cambresis, 2007. (pages [64](#), [71](#)).

- [Kso99] M Ksouri. *Contribution à la commande multimodèles des processus complexes*. PhD thesis, Thèse de Doctorat, Université des Sciences et Technologies de Lille, Lille, 1999. (page 43).
- [KTIT92] Shunji Kawamoto, Kensho Tada, Atsushi Ishigame, and Tsuneo Taniguchi. An approach to stability analysis of second order fuzzy systems. In *Fuzzy Systems, 1992., IEEE International Conference on*, pages 1427–1434. IEEE, 1992. (pages 4, 53).
- [LB01] Alan F Lynch and Scott A Bortoff. Nonlinear observers with approximately linear error dynamics: The multivariable case. *Automatic Control, IEEE Transactions on*, 46(6):927–932, 2001. (page 69).
- [LCC11] Wen-Bin Lin, Chien-An Chen, and Huann-Keng Chiang. Design and implementation of a sliding mode controller using a gaussian radial basis function neural network estimator for a synchronous reluctance motor speed drive. *Electric Power Components and Systems*, 39(6):548–562, 2011. (pages 5, 31).
- [Li-98] Li-Xin Wang. Universal approximation by hierarchical fuzzy systems. *Fuzzy Sets and Systems*, 93(2):223–230, 1998. (page 50).
- [LK22] Changhee Lee and Fuat Kucuk. Low-cost high-performance hybrid-pmsynrm for ev application. In *2022 IEEE 16th International Conference on Compatibility, Power Electronics, and Power Engineering (CPE-POWERENG)*, pages 1–6, 2022. (page 28).
- [LLYL19] En Lu, Wei Li, Xuefeng Yang, and Yufei Liu. Anti-disturbance speed control of low-speed high-torque pmsm based on second-order non-singular terminal sliding mode load observer. *ISA transactions*, 88:142–152, 2019. (page 5).
- [LS98] Winfried Lohmiller and Jean-Jacques E Slotine. On contraction analysis for non-linear systems. *Automatica*, 34(6):683–696, 1998. (page 69).
- [Lub03] Thierry Lubin. *Modélisation et commande de la machine synchrone à réluctance variable: prise en compte de la saturation magnétique*. PhD thesis, Université Henri Poincaré; Nancy I, 2003. (pages 17, 23).

- [Mar16] Guilherme Bueno Mariani. *Machine synchrone à réductance: modèles équivalents à réseau de réductances pour la simulation et l'optimisation*. PhD thesis, Université Grenoble Alpes, 2016. (pages 19, 20, 24, 26, 27, 28, 29).
- [MC17] Bwanga L Mbula and SP Daniel Chowdhury. Performance improvement of synchronous reluctance motors: A review. *2017 IEEE PES PowerAfrica*, pages 402–406, 2017. (page 12).
- [MHB⁺22] Imad eddine Meredef, Mohamed Yacine Hammoudi, Abir Betka, Madina Hamiane, and Khalida Mimoune. Stability and stabilization of ts fuzzy systems via line integral lyapunov fuzzy function. *Electronics*, 11(19):3136, 2022. (page 62).
- [MJC⁺21] Abdelkader Mahmoudi, Imed Jlassi, Antonio J Marques Cardoso, Khaled Yahia, and Mohamed Sahraoui. Inter-turn short-circuit faults diagnosis in synchronous reluctance machines, using the luenberger state observer and currents second-order harmonic. *IEEE Transactions on Industrial Electronics*, 2021. (pages 88, 92, 96).
- [Mor01] Yann Morère. *Mise en œuvre de loi de commandes pour les modèles flous de type Takagi-Sugeno*. PhD thesis, 2001. (page 64).
- [MSH98] Xiao-Jun Ma, Zeng-Qi Sun, and Yan-Yan He. Analysis and design of fuzzy controller and fuzzy observer. *Fuzzy Systems, IEEE Transactions on*, 6(1):41–51, 1998. (page 4).
- [MSJ] R Murray-Smith and TA Johansen. Multiple model approaches to modelling and control, 1997. (page 42).
- [MSJ97] R Murray-Smith and T Johansen. *Multiple Model Approaches To Nonlinear Modelling And Control*. CRC Press, 1997. (page 48).
- [MVB20] Zbynek Mynar, Pavel Vaclavek, and Petr Blaha. Synchronous reluctance motor parameter and state estimation using extended kalman filter and current derivative measurement. *IEEE Transactions on Industrial Electronics*, 68(3):1972–1981, 2020. (page 88).

- [Nag10] Anca Maria Nagy. *Analyse et synthèse de multimodèles pour le diagnostic. Application à une station d'épuration*. PhD thesis, Institut National Polytechnique de Lorraine-INPL, 2010. (pages [41](#), [45](#), [46](#), [48](#), [49](#), [50](#), [70](#), [71](#), [76](#)).
- [Ngu15] Duc-Quan Nguyen. *Modélisation, identification et commande sans capteur d'une machine synchrone à réluctance variable rapide*. PhD thesis, Nantes, 2015. (pages [32](#), [33](#), [35](#)).
- [NKMM⁺10] Anca Maria Nagy-Kiss, Benoît Marx, Gilles Mourot, Georges Schutz, and José Ragot. State estimation of two-time scale multiple models with unmeasurable premise variables. application to biological reactors. In *Decision and Control (CDC), 2010 49th IEEE Conference on*, pages 5689–5694. IEEE, 2010. (page [71](#)).
- [Orj08] Rodolfo Orjuela. *A contribution to state estimation and diagnosis of systems modelled by multiple models*. PhD thesis, Institut National Polytechnique de Lorraine-INPL, 2008. (pages [46](#), [48](#), [49](#)).
- [Oud08] Mohammed Oudghiri. *Commande multi-modèles tolérante aux défauts: Application au contrôle de la dynamique d'un véhicule automobile*. PhD thesis, Université de Picardie Jules Verne, 2008. (page [52](#)).
- [PCLT98] RJ Patton, J Chen, and CJ Lopez-Toribio. Fuzzy observers for nonlinear dynamic systems fault diagnosis. In *Decision and Control, 1998. Proceedings of the 37th IEEE Conference on*, volume 1, pages 84–89. IEEE, 1998. (page [71](#)).
- [Poo19] Hasan A Poonawala. Stability analysis via refinement of piece-wise linear lyapunov functions. In *2019 IEEE 58th Conference on Decision and Control (CDC)*, pages 1442–1447. IEEE, 2019. (page [61](#)).
- [Ram06] Tsaarafidy Raminosoa. *Optimisation des performances des machines synchro-réductantes par réseaux de perméances*. PhD thesis, Institut National Polytechnique de Lorraine-INPL, 2006. (pages [20](#), [27](#)).

- [RM11] Reza Rajabi Moghaddam. *Synchronous reluctance machine (SynRM) in variable speed drives (VSD) applications*. PhD thesis, KTH Royal Institute of Technology, 2011. (pages [19](#), [27](#)).
- [Rod15] Dany Prieto Rodriguez. *Modélisation et optimisation des machines synchro-réductantes à aimants permanents et de leur électronique*. PhD thesis, CentraleSupélec, 2015. (pages [11](#), [24](#), [26](#), [27](#)).
- [RW06] Bong-Jae Rhee and Sangchul Won. A new fuzzy lyapunov function approach for a takagi-sugeno fuzzy control system design. *Fuzzy sets and systems*, 157(9):1211–1228, 2006. (page [62](#)).
- [RZK91] GVS Raju, Jun Zhou, and Roger A Kisner. Hierarchical fuzzy control. *International journal of control*, 54(5):1201–1216, 1991. (page [50](#)).
- [SG92] Yongkyu Song and Jessy W Grizzle. The extended kalman filter as a local asymptotic observer for nonlinear discrete-time systems. In *American Control Conference, 1992*, pages 3365–3369. IEEE, 1992. (page [68](#)).
- [SMW93] DA Staton, TJE Miller, and SE Wood. Maximising the saliency ratio of the synchronous reluctance motor. In *IEE Proceedings B (Electric Power Applications)*, volume 140, pages 249–259. IET, 1993. (page [17](#)).
- [SOK⁺20] Filipe Scalcon, Caio Osorio, Gustavo Koch, Thieli Smidt Gabbi, Rodrigo Padilha Vieira, Hilton Grundling, Ricardo Oliveira, and Vinicius Montagner. Robust control of synchronous reluctance motors by means of linear matrix inequalities. *IEEE Transactions on Energy Conversion*, 2020. (pages [31](#), [36](#)).
- [Son81] Eduardo D Sontag. Nonlinear regulation: The piecewise linear approach. *Automatic Control, IEEE Transactions on*, 26(2):346–358, 1981. (page [48](#)).
- [SSPP23] Bernard Steyaert, Ethan Swint, W Wesley Pennington, and Matthias Preindl. Piecewise affine maximum torque per ampere for the wound rotor synchronous machine. *IEEE Transactions on Transportation Electrification*, 2023. (page [44](#)).

- [Tag15] Seyedmorteza Taghavi. *Design of Synchronous Reluctance Machines for Automotive Applications*. PhD thesis, Université Concordia Canada, 2015. (pages [iv](#), [11](#), [12](#), [13](#), [14](#), [19](#), [20](#), [26](#)).
- [Tha73] FE Thau. Observing the state of non-linear dynamic systems. *International Journal of Control*, 17(3):471–479, 1973. (page [69](#)).
- [THW03] Kazuo Tanaka, Tsuyoshi Hori, and Hua O Wang. A multiple lyapunov function approach to stabilization of fuzzy control systems. *Fuzzy Systems, IEEE Transactions on*, 11(4):582–589, 2003. (page [71](#)).
- [TP15] Seyed Morteza Taghavi and Pragasen Pillay. A mechanically robust rotor with transverse laminations for a wide-speed-range synchronous reluctance traction motor. *IEEE Transactions on Industry Applications*, 51(6):4404–4414, 2015. (page [18](#)).
- [TRU16] Phuoc Hoa TRUONG. *Optimisation des performances de la machine synchrone à réluctance variable: approches par la conception et par la commande*. PhD thesis, Université de Haute-Alsace, 2016. (pages [iv](#), [15](#), [18](#)).
- [TS85] Tomohiro Takagi and Michio Sugeno. Fuzzy identification of systems and its applications to modeling and control. *IEEE transactions on systems, man, and cybernetics*, (1):116–132, 1985. (pages [42](#), [46](#)).
- [TW04] Kazuo Tanaka and Hua O Wang. *Fuzzy control systems design and analysis: a linear matrix inequality approach*. John Wiley & Sons, 2004. (pages [4](#), [41](#), [51](#), [53](#), [60](#)).
- [VDS92] Arjan J Van Der Schaft. \mathcal{L}_2 -gain analysis of nonlinear systems and nonlinear state feedback h_∞ control. *IEEE transactions on automatic control*, 37(6):770–784, 1992. (page [76](#)).
- [VL18] Lukas Veg and Jan Laksar. Overview of technology, problems and comparison of high speed synchronous reluctance machines. In *2018 ELEKTRO*, pages 1–4. IEEE, 2018. (page [16](#)).
- [Wei12] Alexander Weinmann. *Uncertain models and robust control*. Springer Science & Business Media, 2012. (page [76](#)).

- [Yam15] Samer Yammine. *Contribution to the synchronous reluctance machine performance improvement by design optimization and current harmonics injection*. PhD thesis, 2015. (pages [12](#), [13](#), [14](#), [15](#), [16](#), [26](#)).
- [YCKW17] T Youssef, Mohammed Chadli, Hamid Reza Karimi, and Rongrong Wang. Actuator and sensor faults estimation based on proportional integral observer for ts fuzzy model. *Journal of the Franklin Institute*, 354(6):2524–2542, 2017. (page [5](#)).
- [YIO⁺14] Zedjiga Yacine, Dalil Ichalal, Naima Ait Oufroukh, Said Mammar, and Said Djennoune. New nonlinear takagi–sugeno vehicle model for state and road curvature estimation via a nonlinear pmi observer. *Journal of Intelligent Systems*, 23(2):155–170, 2014. (page [5](#)).
- [YM22] Dharmendra Singh Yadav and Manisha Manisha. Electric propulsion motors: A comparative review for electric and hybrid electric vehicles. In *2022 IEEE International Conference on Distributed Computing and Electrical Circuits and Electronics (ICDCECE)*, pages 1–6. IEEE, 2022. (page [13](#)).
- [YMEC14] Khaled Yahia, Diogo Matos, Jorge O Estima, and AJ Marques Cardoso. Modeling synchronous reluctance motors including saturation, iron losses and mechanical losses. In *2014 International Symposium on Power Electronics, Electrical Drives, Automation and Motion*, pages 601–606. IEEE, 2014. (page [90](#)).
- [Zem07] Ali Zemouche. *Sur l’observation de l’état des systèmes dynamiques non linéaires*. PhD thesis, Université Louis Pasteur-Strasbourg I, 2007. (page [69](#)).
- [Zer11] Mohamed Zerrougui. *Observation et commande des systemes singuliers non linéaires*. PhD thesis, Université Henri Poincaré-Nancy I, 2011. (pages [57](#), [59](#), [68](#)).
- [ZZOL19] Lei Zhang, Hui Zhang, Hussein Obeid, and Salah Laghrouche. Time-varying state observer based twisting control of linear induction motor considering

dynamic end effects with unknown load torque. *ISA transactions*, 93:290–301, 2019. (pages [5](#), [98](#)).